

Layered Compounds

2D = Two-dimensional layers

Graphite and Graphene

Clay Minerals, Mica

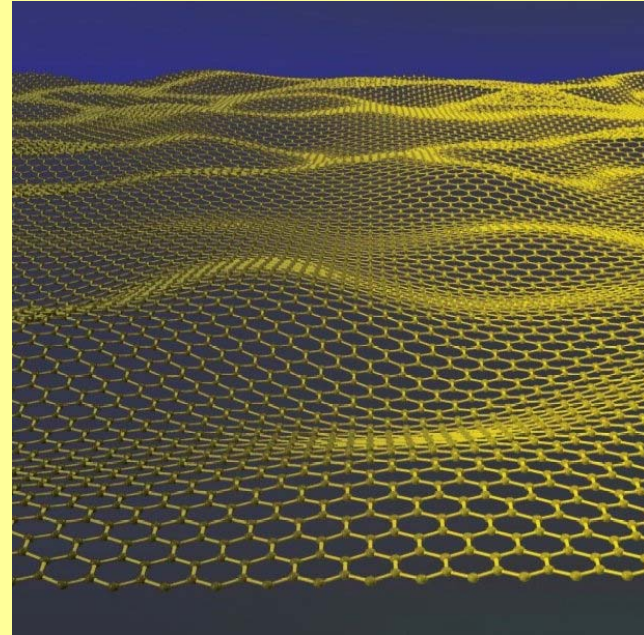
Layered Double Hydroxides (LDHs)

Layered Zirconium Phosphates and Phosphonates

Layered Metal Oxides

Layered Metal Chalcogenides - TiS_2 , MoS_2 , WS_2 , MPS_3 (M = Ti, V, Mo, W, Mn, Fe, Co, Ni, Zn)

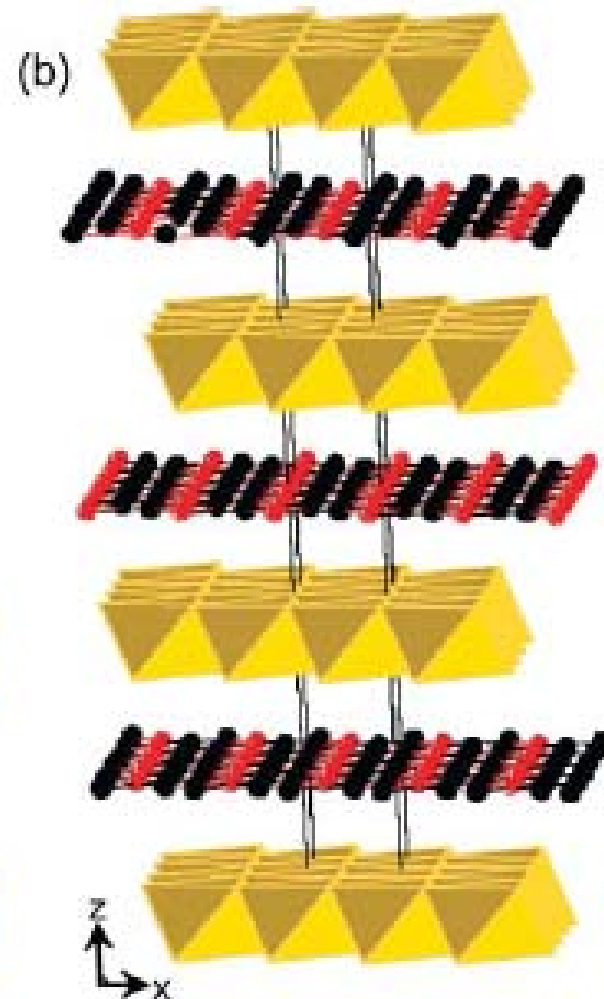
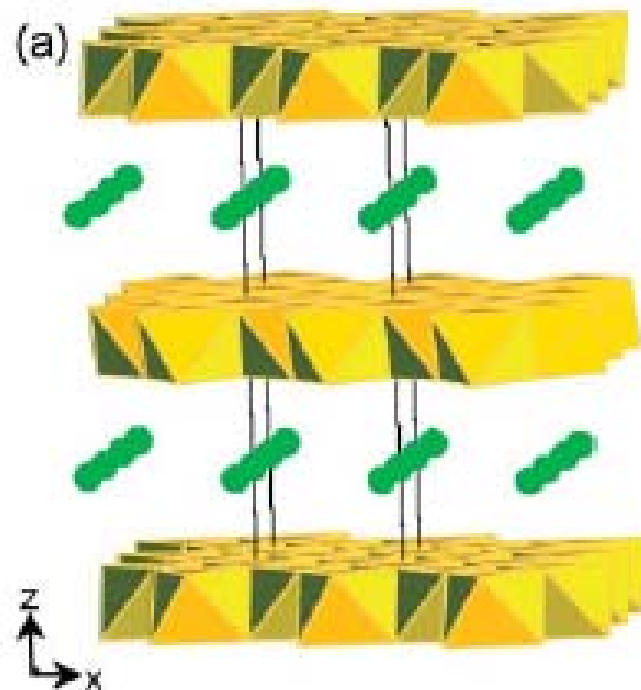
Alkali Silicates and Crystalline Silicic Acids



Layered Compounds

**Intralayer bonding - strong
(covalent, ionic)**

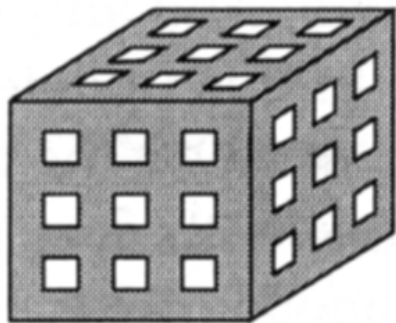
**Interlayer bonding - weak
(H-bonding, vdWaals)**



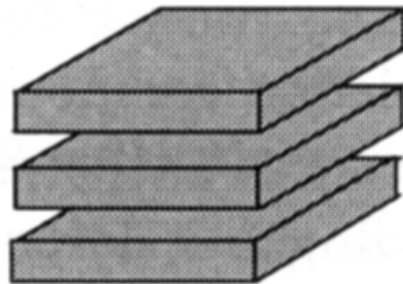
Host-Guest Structures

Host dimensionality

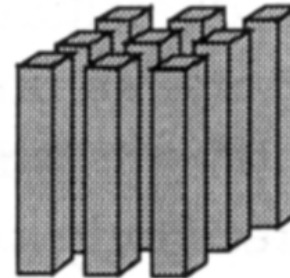
3D



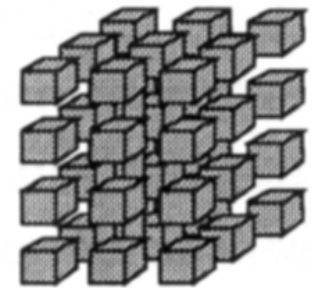
2D



1D



0D

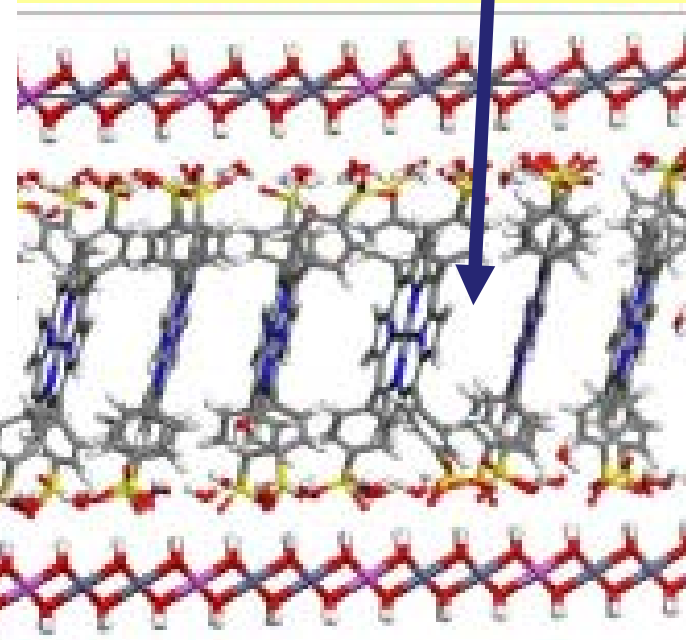
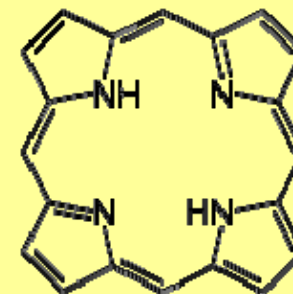
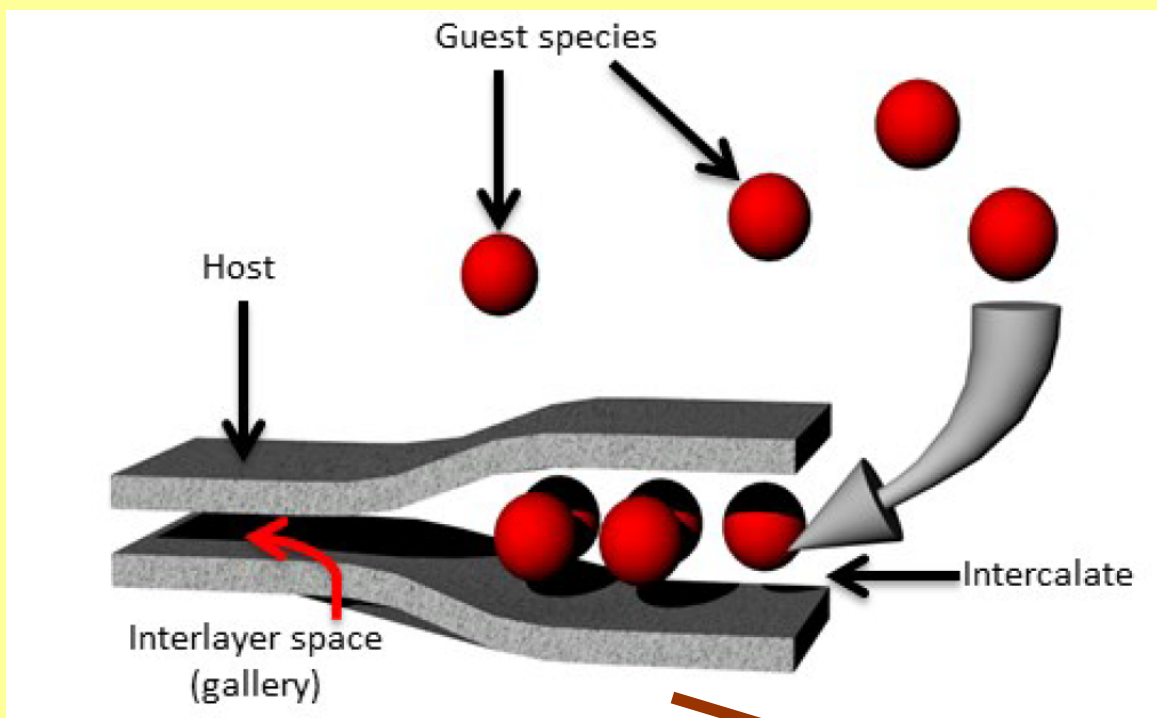


TOPOTACTIC SOLID-STATE REACTIONS = modifying existing solid state structures while maintaining the integrity of the overall structure

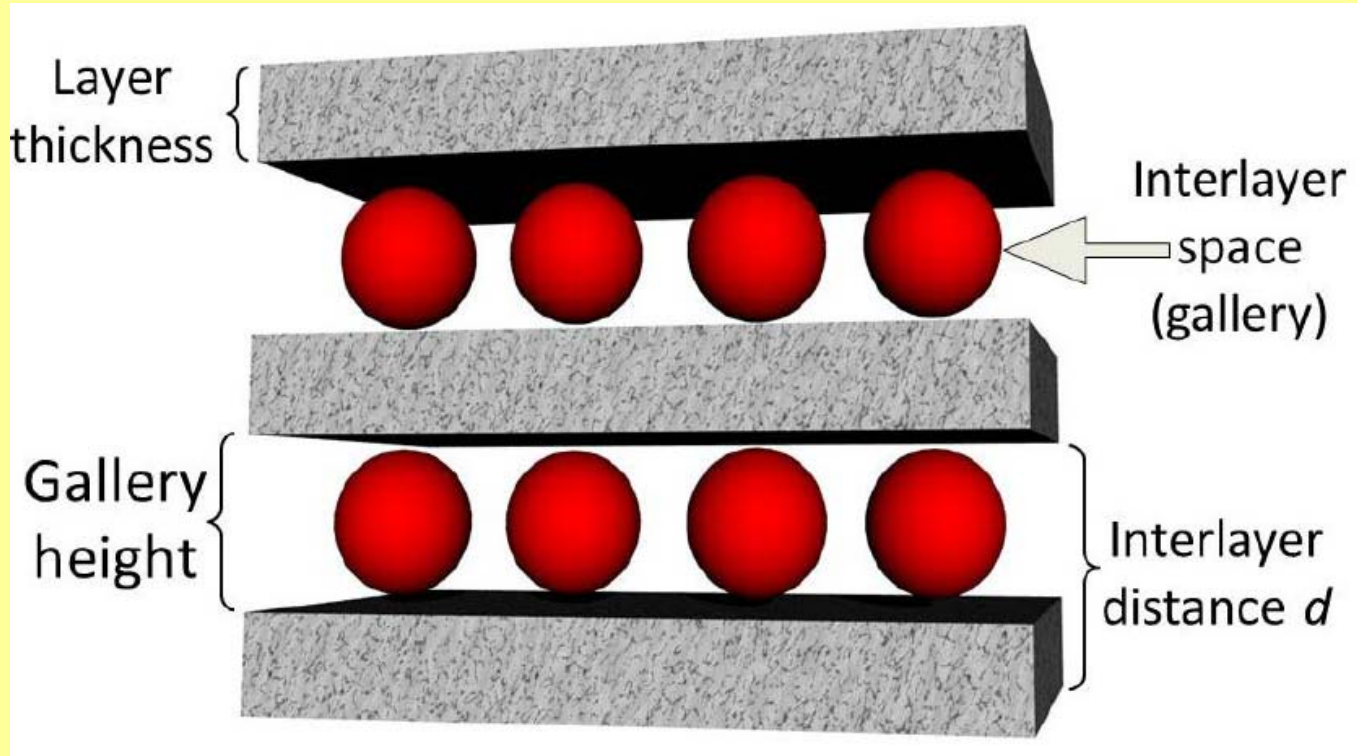
Intercalation

Intercalation

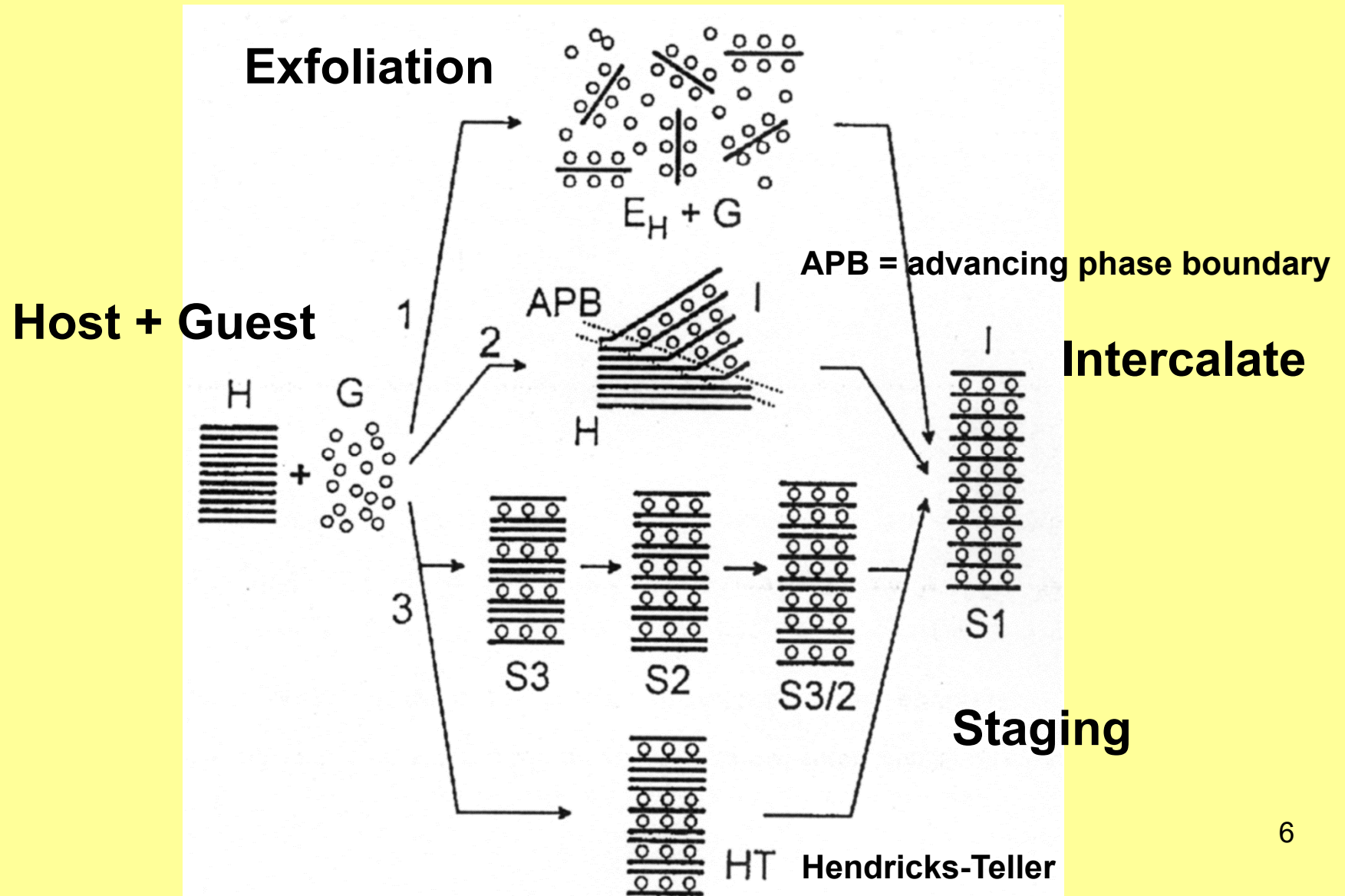
Insertion of molecules between layers



Intercalation

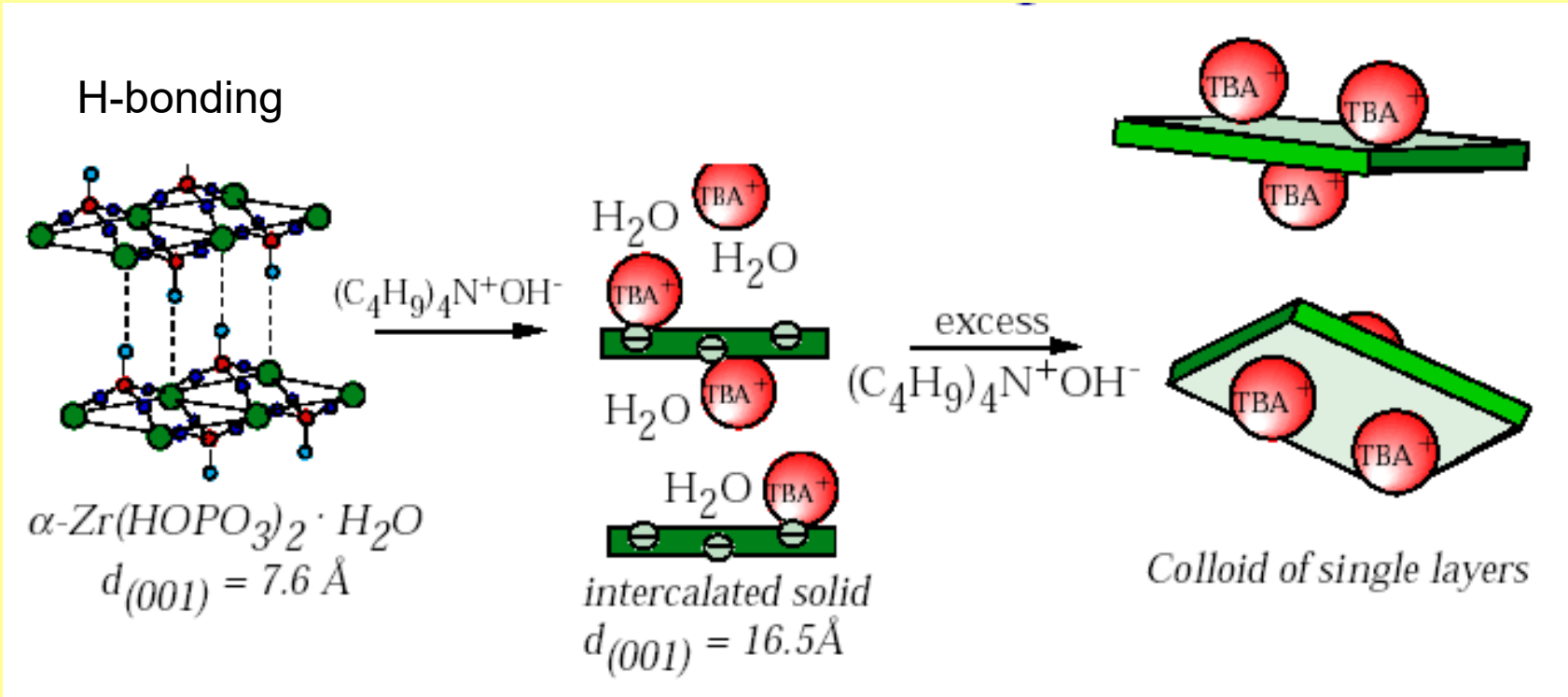


Intercalation



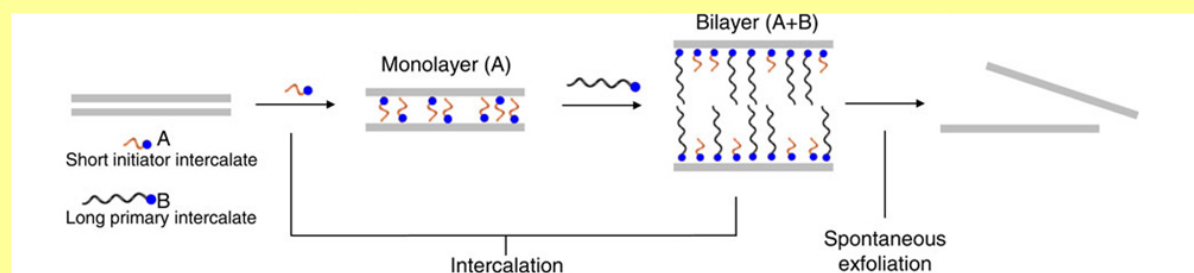
Exfoliation

Decrease attractive forces between layers
Separate layers

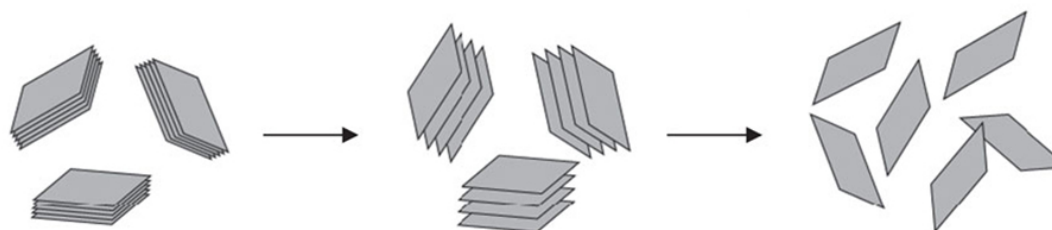


Tandem Molecular Intercalation

Lewis base short initiator first intercalates to open up the interlayer gap, and the long molecules then bring the gap to full width and overcome the interlayer attractive force resulting in spontaneous exfoliation

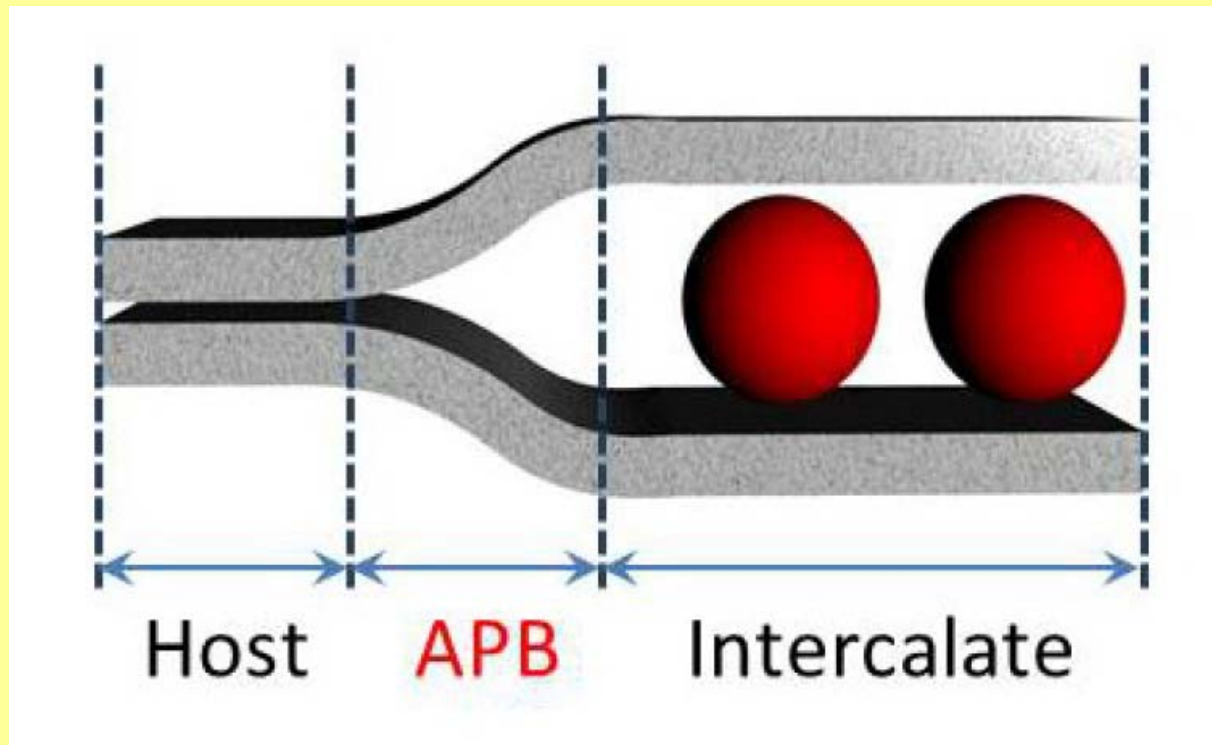


Transition-Metal Chalcogenides



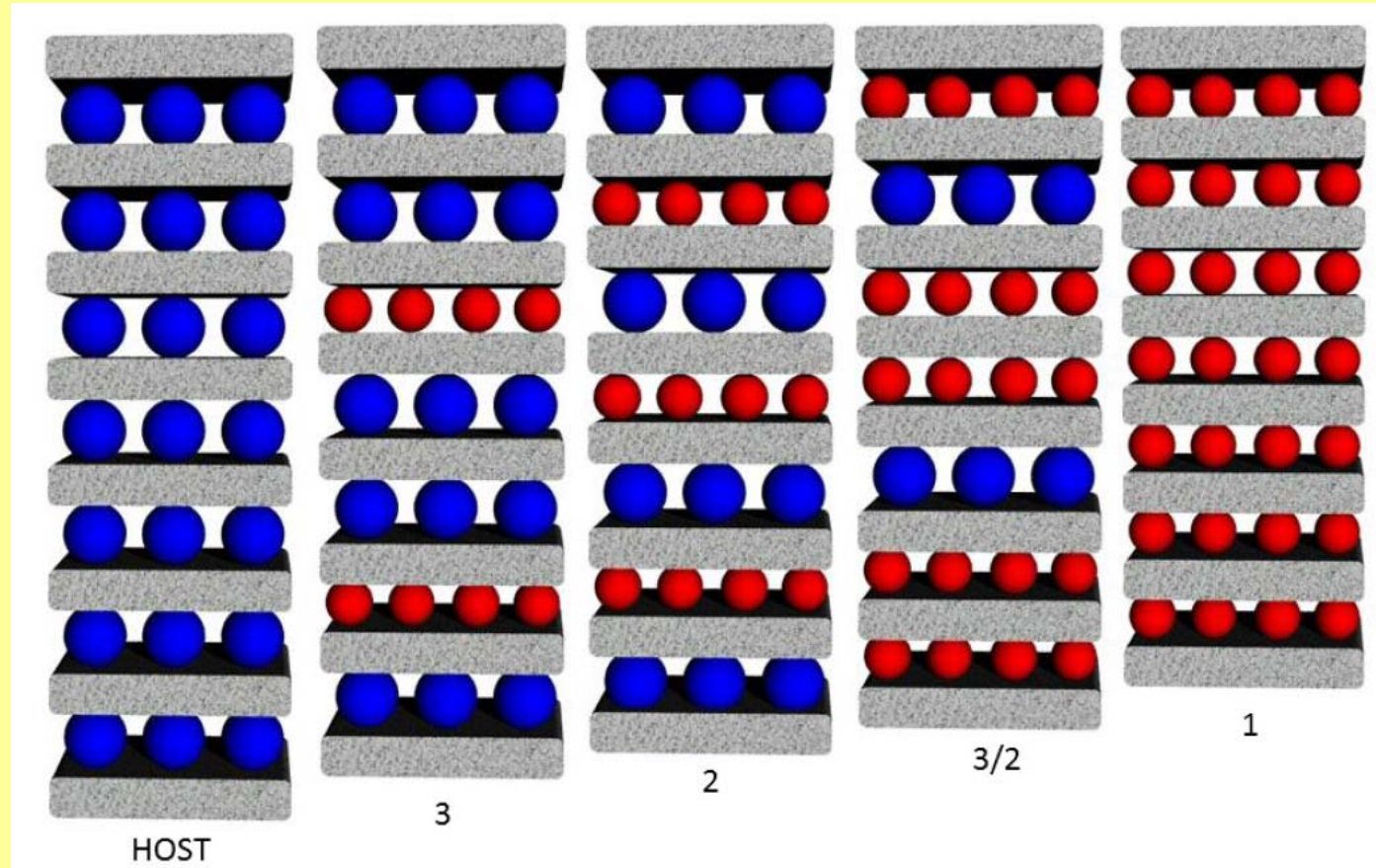
Nat. Commun. 2015,6, 5763, Jan. 9, 2015

APB = Advancing Phase Boundary

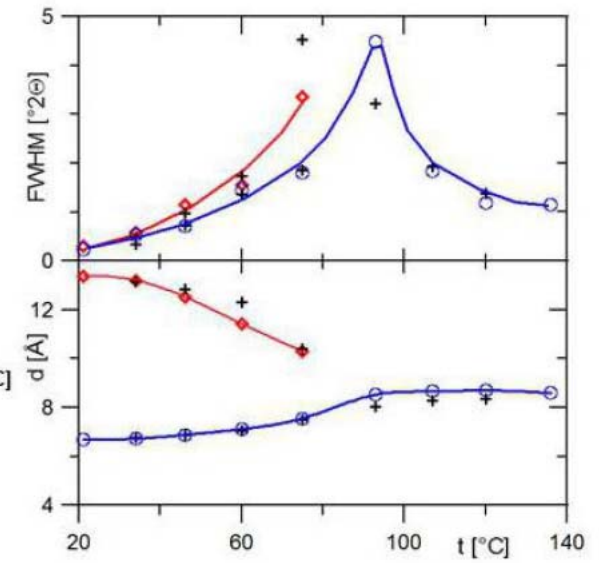
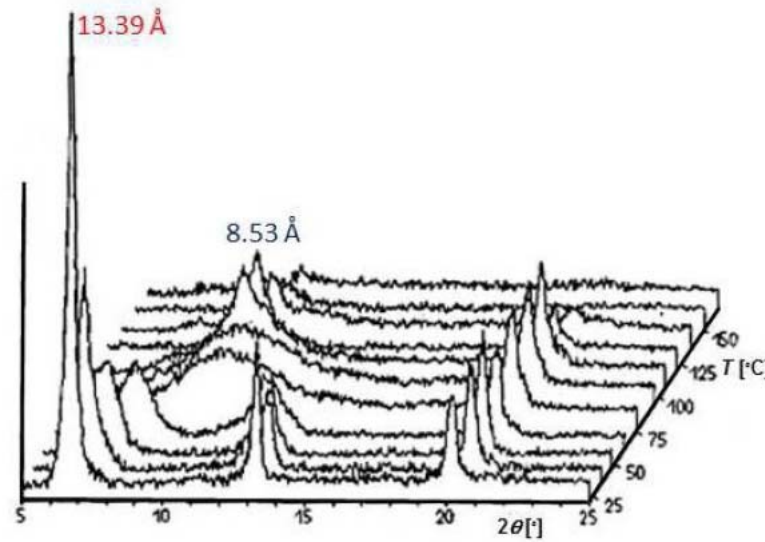
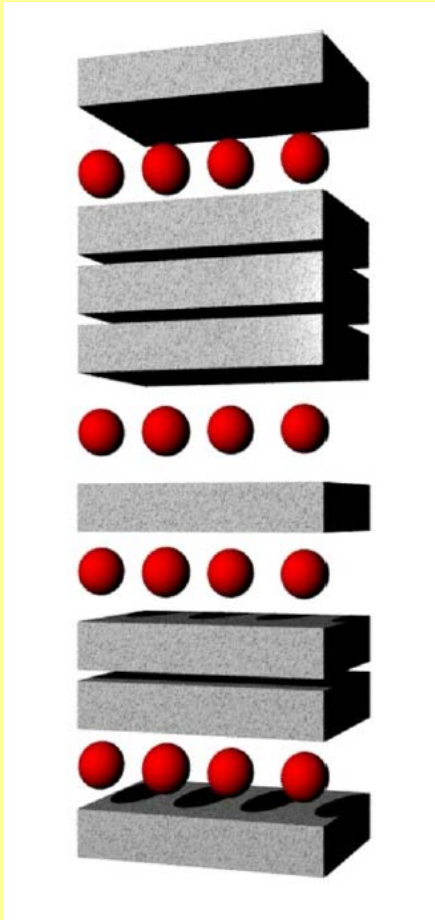


APB = advancing phase boundary

Staging

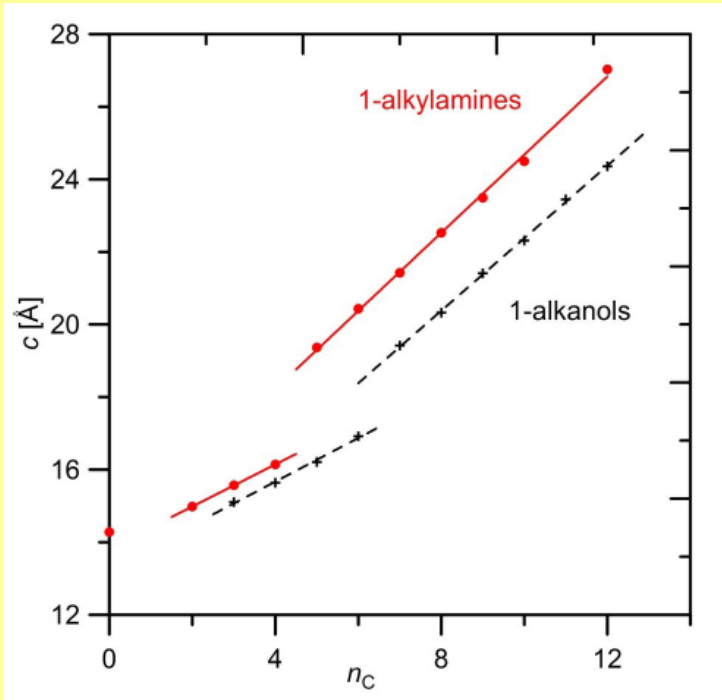


Hendricks-Teller Effect

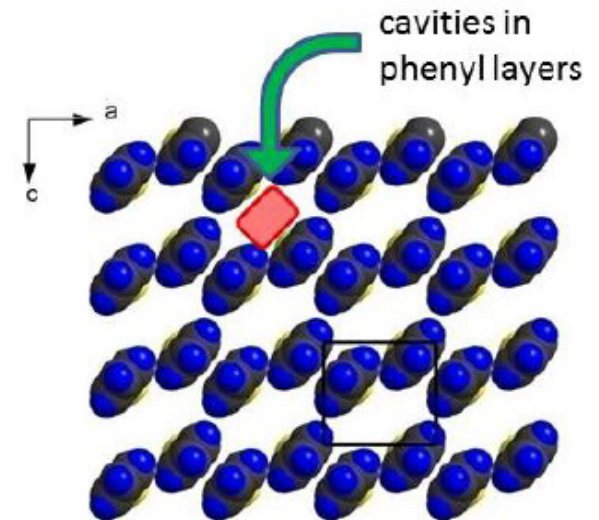
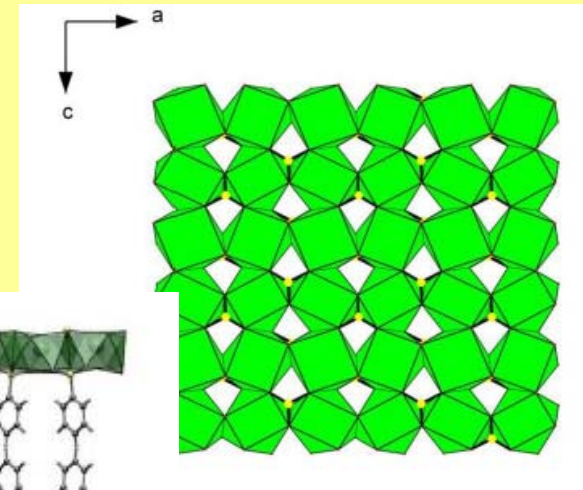
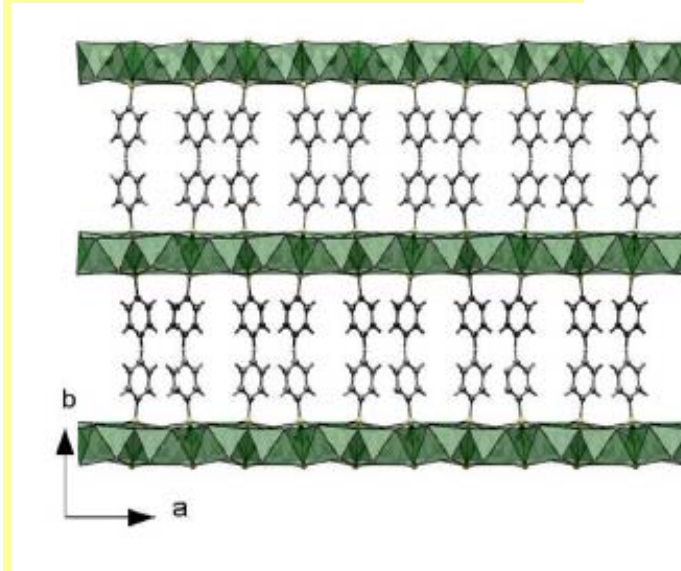


HT = galleries are filled randomly

Intercalation

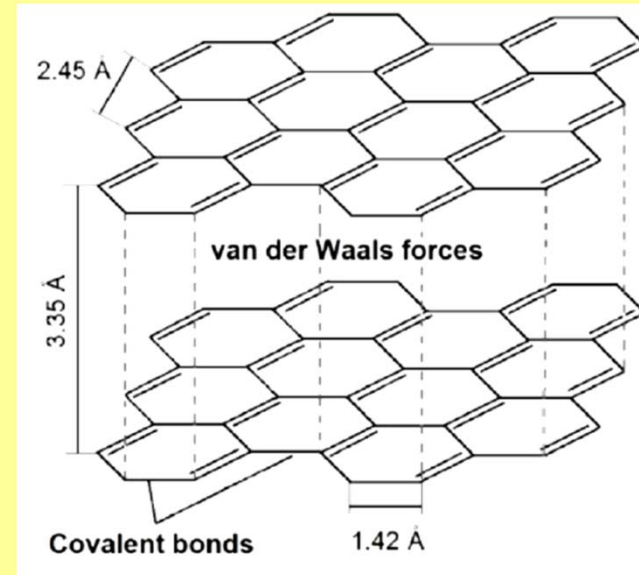
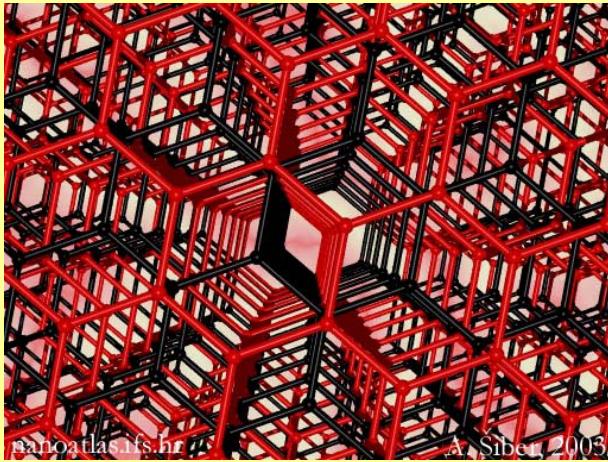


Dependence of the basal spacing of the intercalates of the alkylamines (circles) and alkanols (crosses) on the number of carbon atoms n_C in $\text{SrC}_6\text{H}_5\text{PO}_3 \cdot 2\text{H}_2\text{O}$



Graphite

Stacking of layers
ABABAB

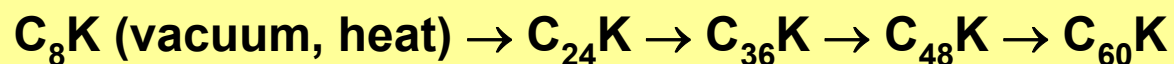


Graphite sp^2 sigma-bonding in-plane p-p-bonding out of plane
Hexagonal graphite = two-layer ABAB stacking sequence

SALCAOs of the p-p-type create the valence and conduction bands of graphite, very small band gap, metallic conductivity properties in-plane, 10^4 times that of out-of plane conductivity

Graphite

GRAPHITE INTERCALATION



C₈K potassium graphite ordered structure

Ordered K guests between the sheets, K to G charge transfer

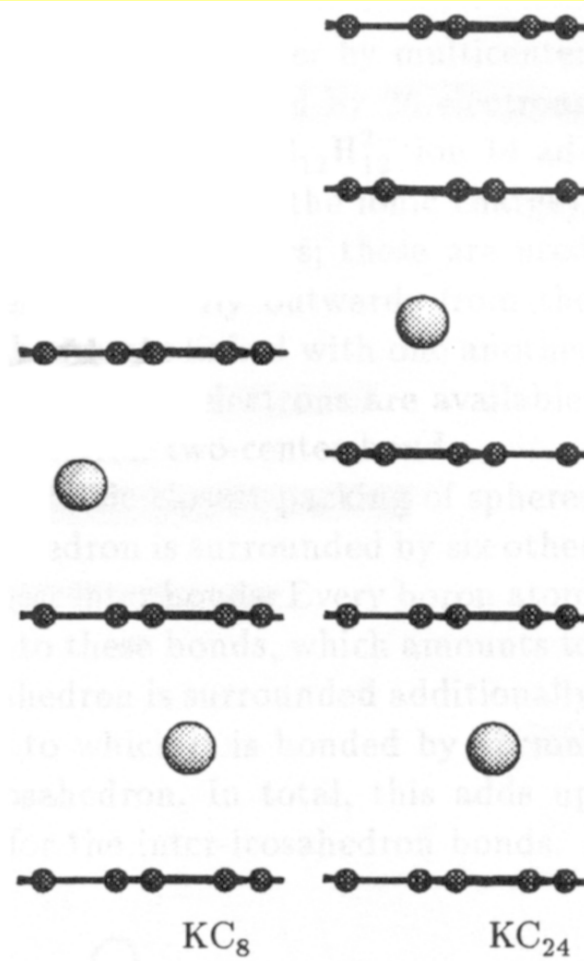
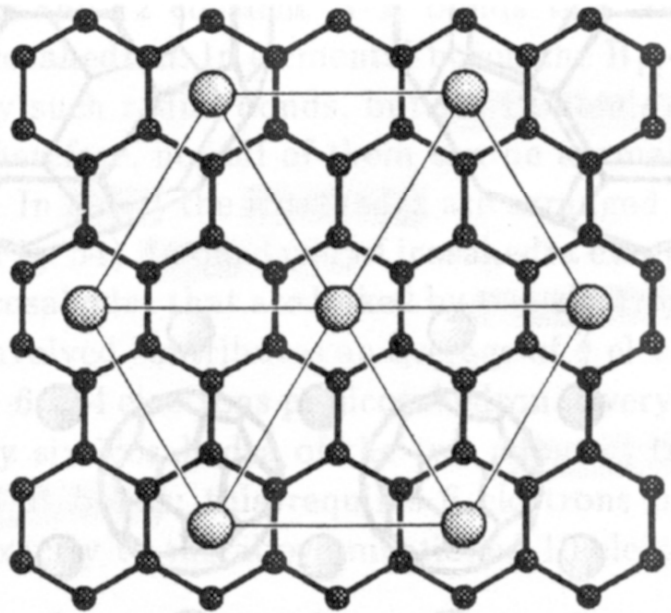
AAAA stacking sequence

reduction of graphite sheets, electrons enter CB

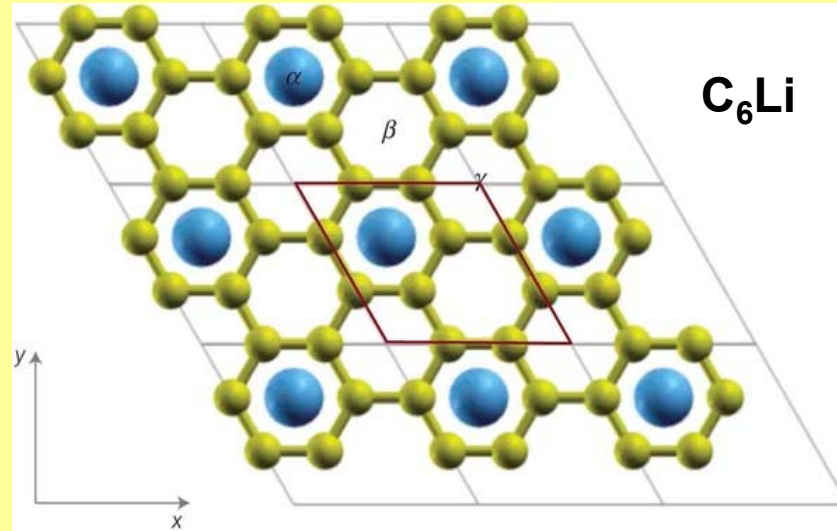
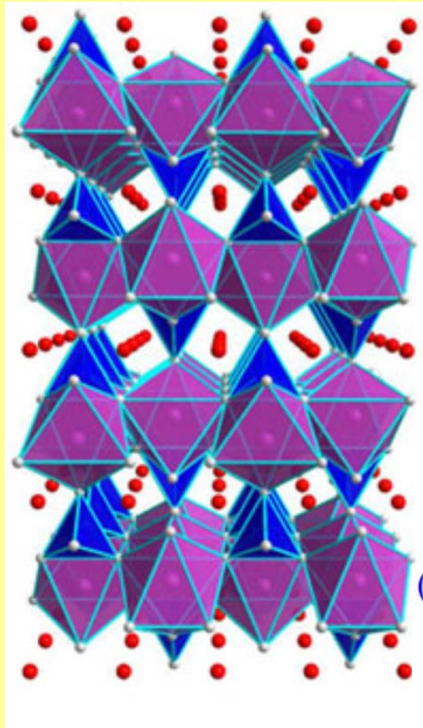
K⁺ nesting between parallel eclipsed hexagonal planar carbon six-rings

Graphite

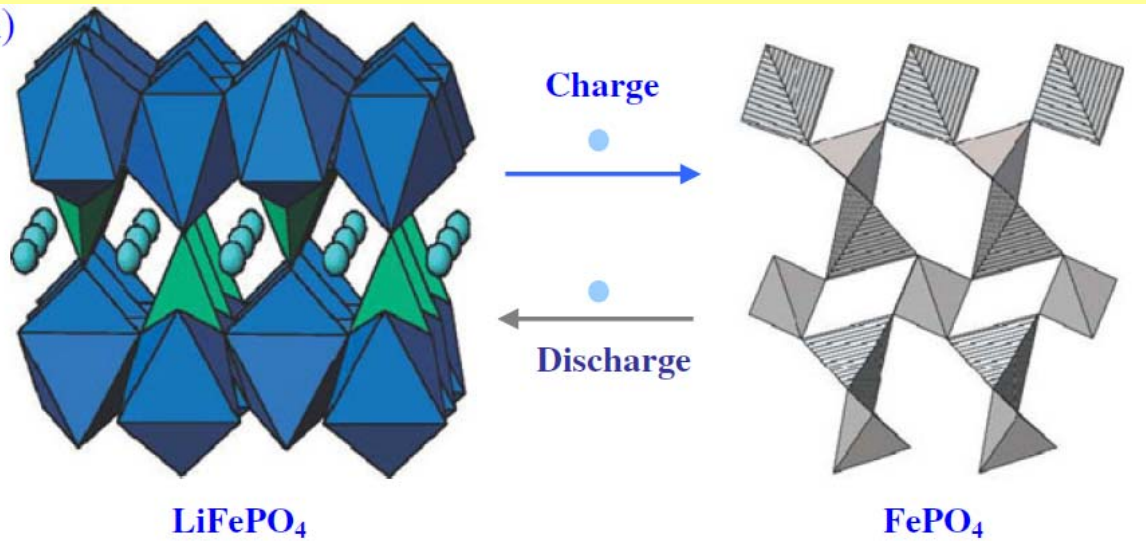
Intercalates



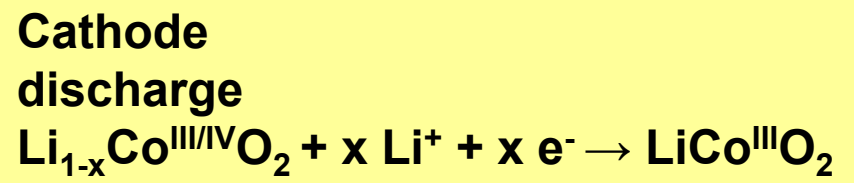
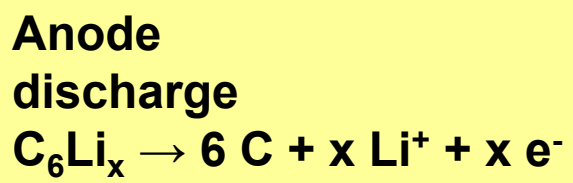
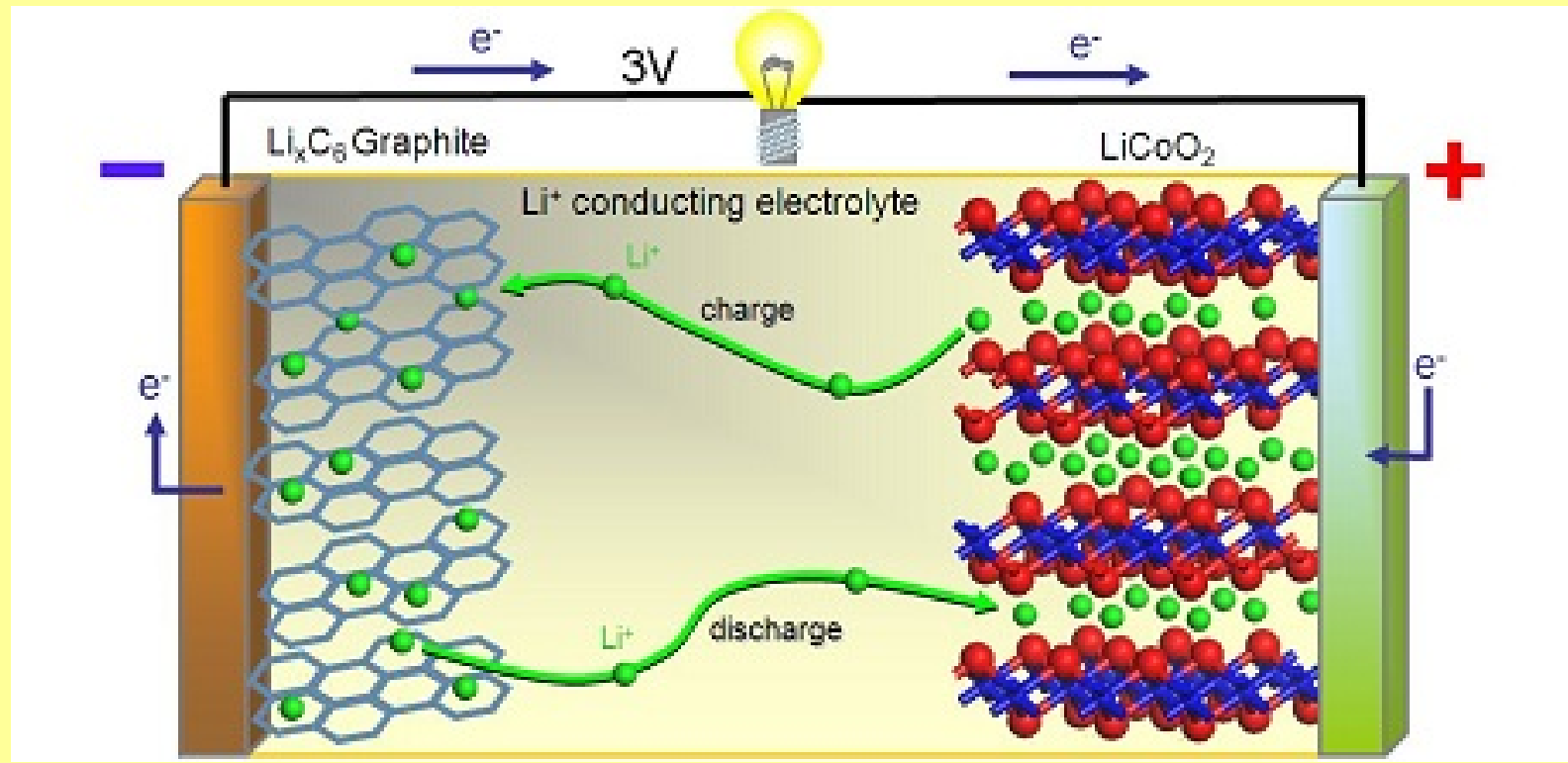
Intercalation in Li-ion Cells



(a)



Intercalation in Li-ion Cells



Graphene Family

Graphene

Graphene oxide

h-BN

BCN

Fluorographene

C_3N_4

Graphene

- 1962 H.-P. Boehm monolayer flakes of reduced graphene oxide
- 2004 Andre Geim and Konstantin Novoselov - Graphene produced and identified
- Exotic properties:
 - Firm structure
 - Inert material
 - Hydrofobic character
 - Electric and thermal conductivity
 - High mobility of electrons
 - Specific surface area (theoretically): $2630 \text{ m}^2\text{g}^{-1}$

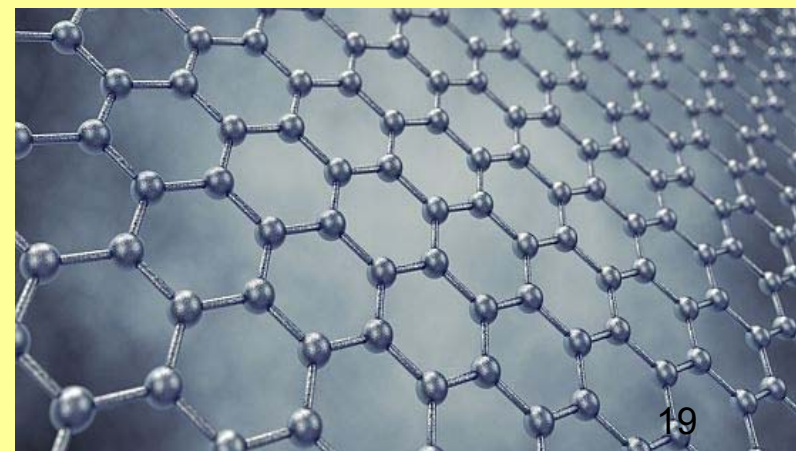


K. Novoselov

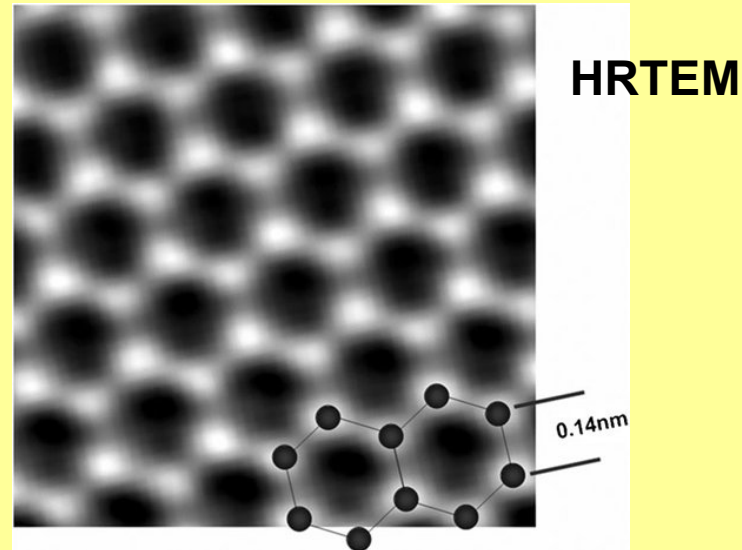
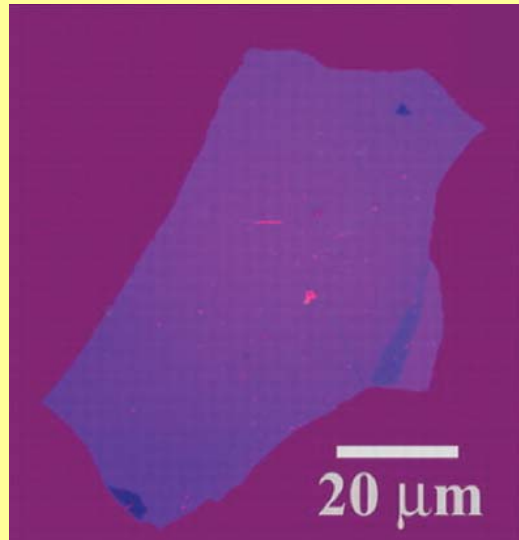


A. Geim

2010 Nobel Prize in Physics



Graphene



High electric conductivity (metallic, $\sim 20,000$ S/cm)

High mobility at low temperature ($2 \cdot 10^5$ cm² V⁻¹ s⁻¹, Si ~ 800 cm² V⁻¹ s⁻¹ at r.t.)

Optically transparent ($\sim 97.7\%$) – 1 layer absorbs 2.3% of photons

Low reflectiveness ($< 0.1\%$)

High mechanical strength ($E \sim 1$ TPa)

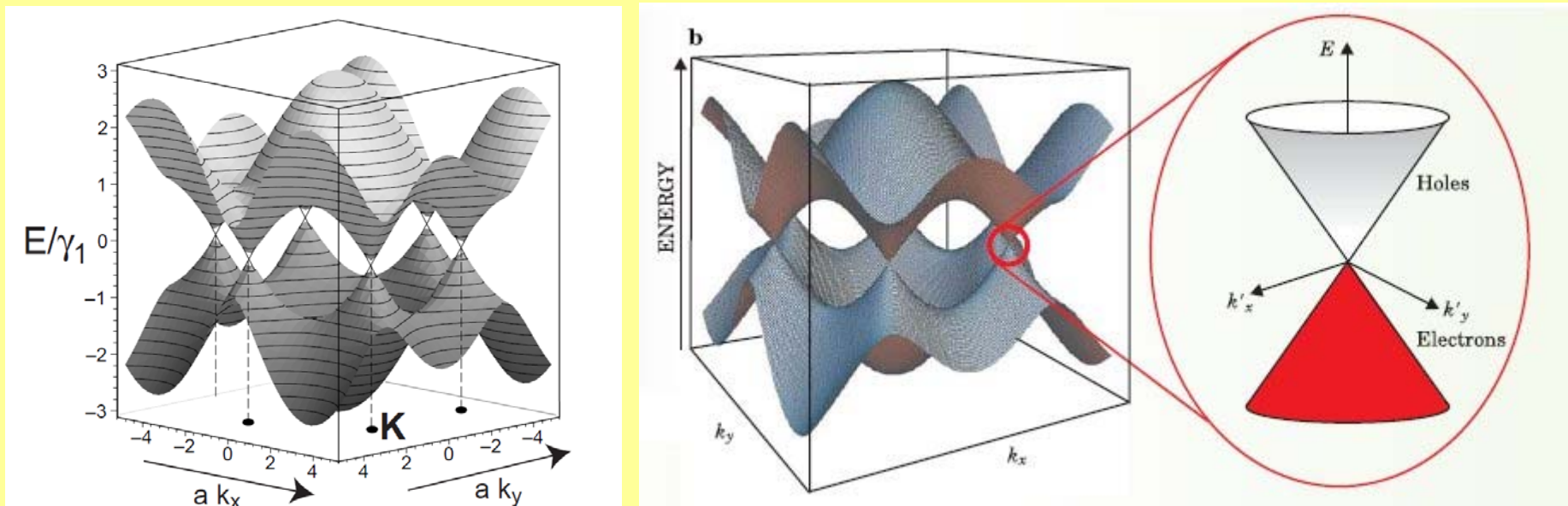
High thermal conductivity ($K \sim 5 \cdot 10^3$ W m⁻¹ K⁻¹)

Low anisotropic thermal expansion coefficient

High stability in air atmosphere up to 400 °C

Graphene

LCAO-band structure of graphene



Synthesis of Graphene

Top down

Mechanical exfoliation

Chemical exfoliation (oxidation/reduction)

Dry and/or liquid-phase exfoliation

Unzipping of nanotubes

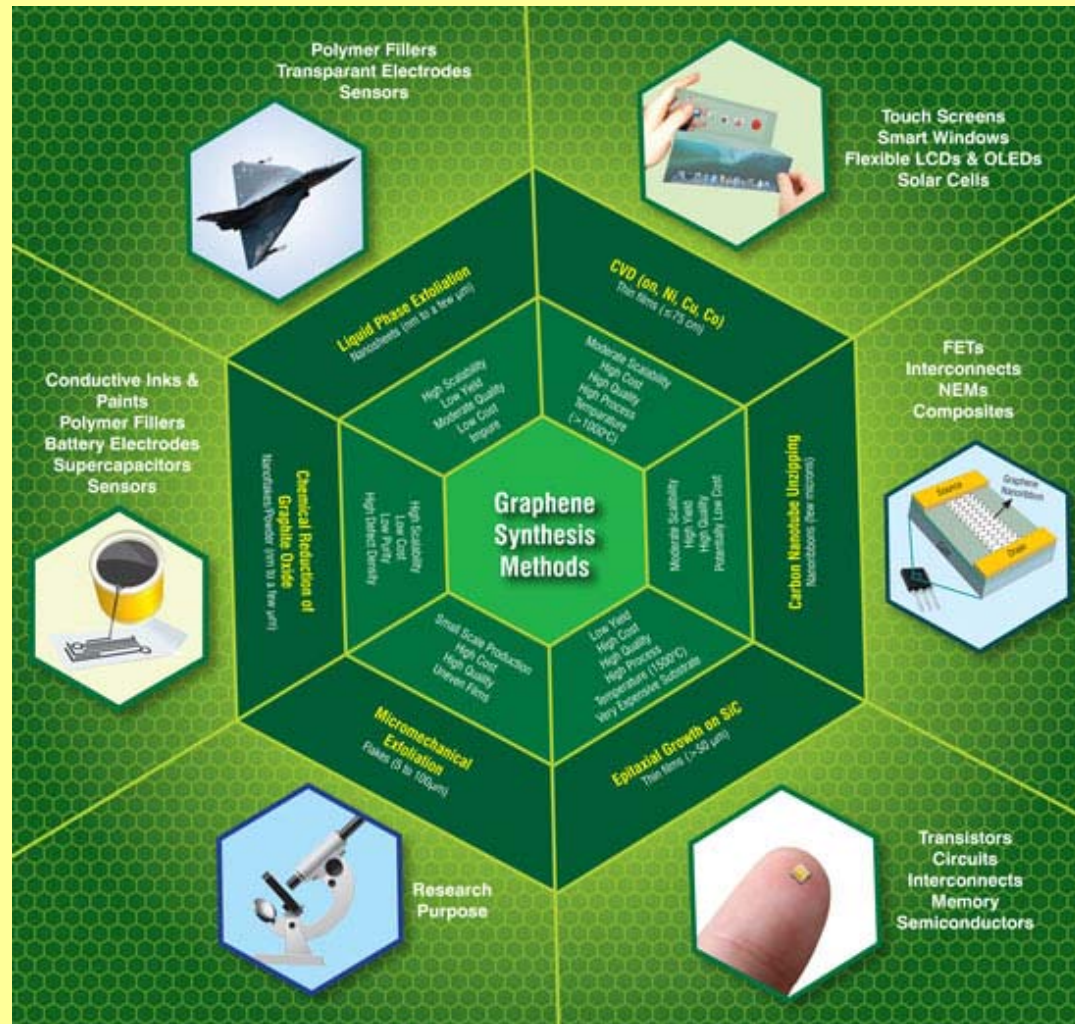
Bottom up

CVD, epitaxial growth, (on SiC and on metals)

Precipitation

Molecular beam epitaxy

Synthesis of Graphene

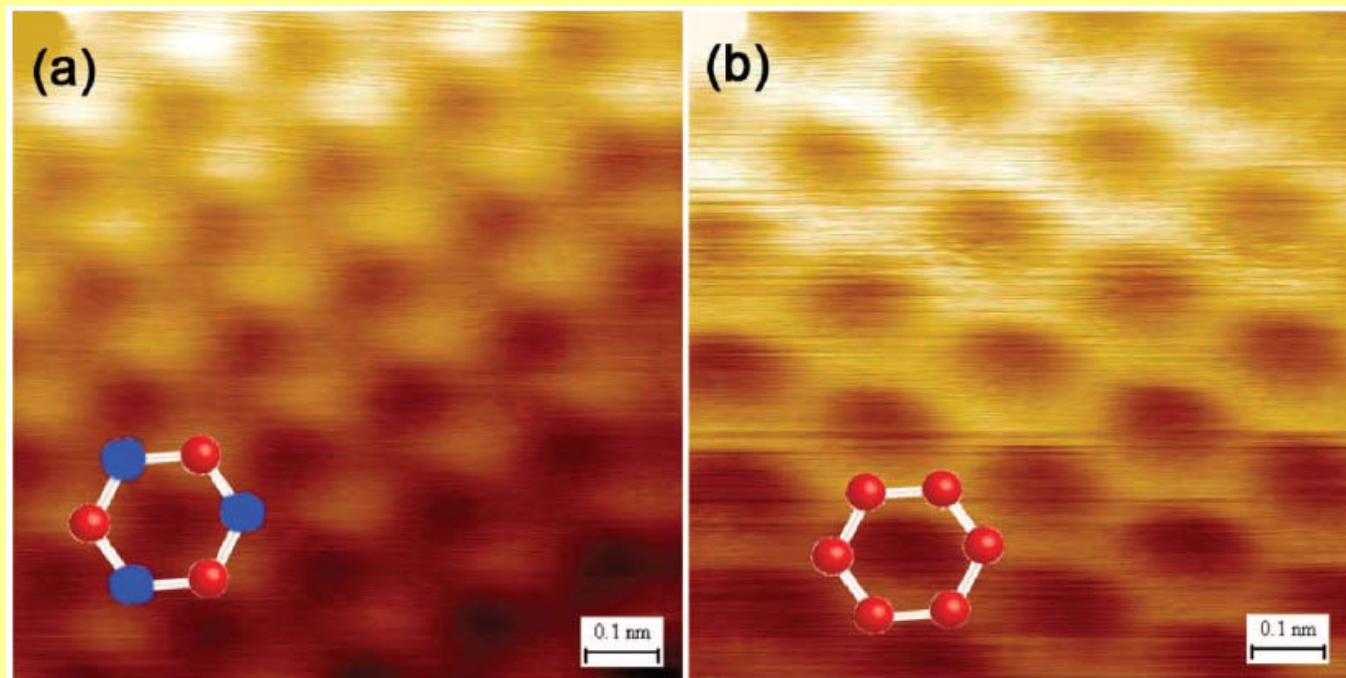


http://www.nanowerk.com/what_is_graphene.php

Graphene

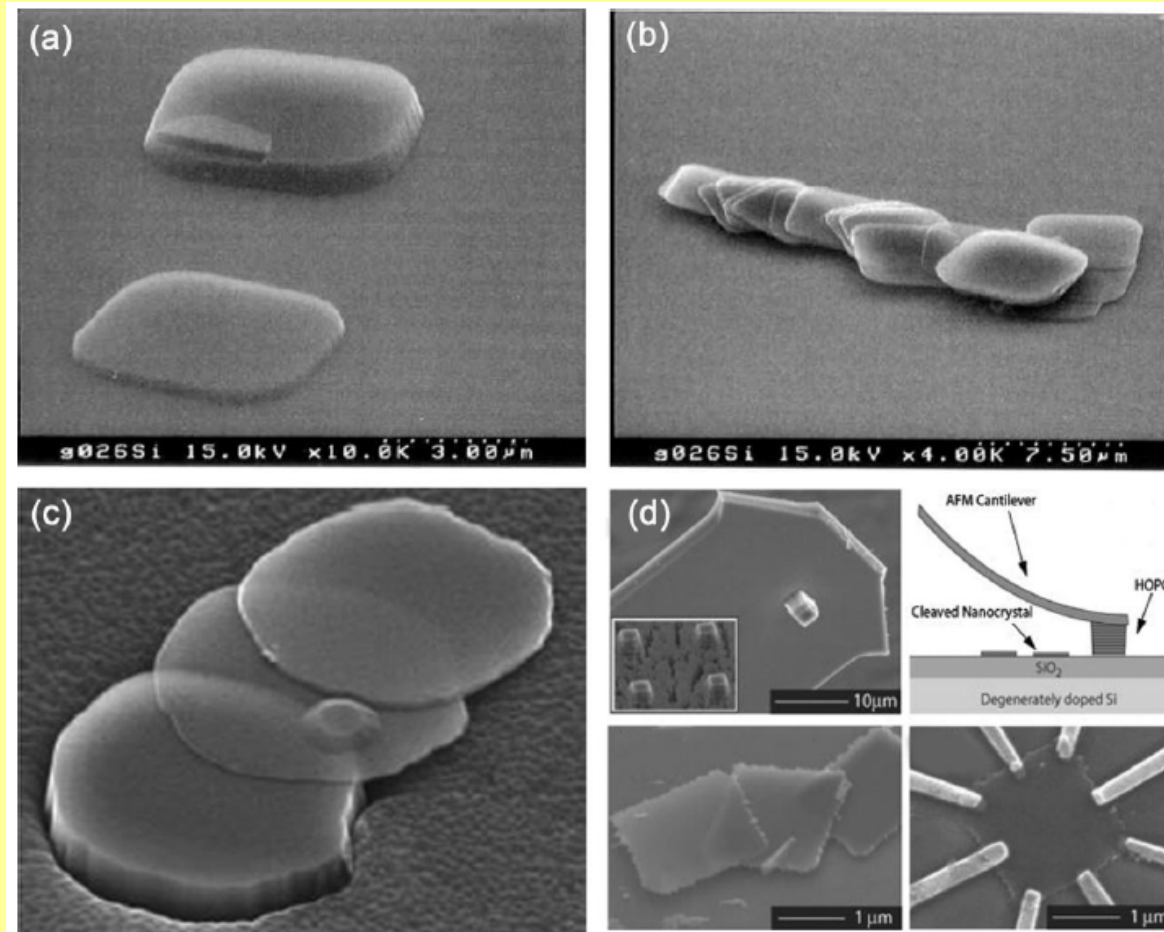
Preparation:

- Scotch tape – layer peeling, flaking
- SiC pyrolysis – epitaxial graphene layer on a SiC crystal
- Exfoliation of graphite (chemical, sonochemical)
- CVD from CH_4 , CH_2CH_2 , or CH_3CH_3 on Ni (111), Cu, Pt surfaces

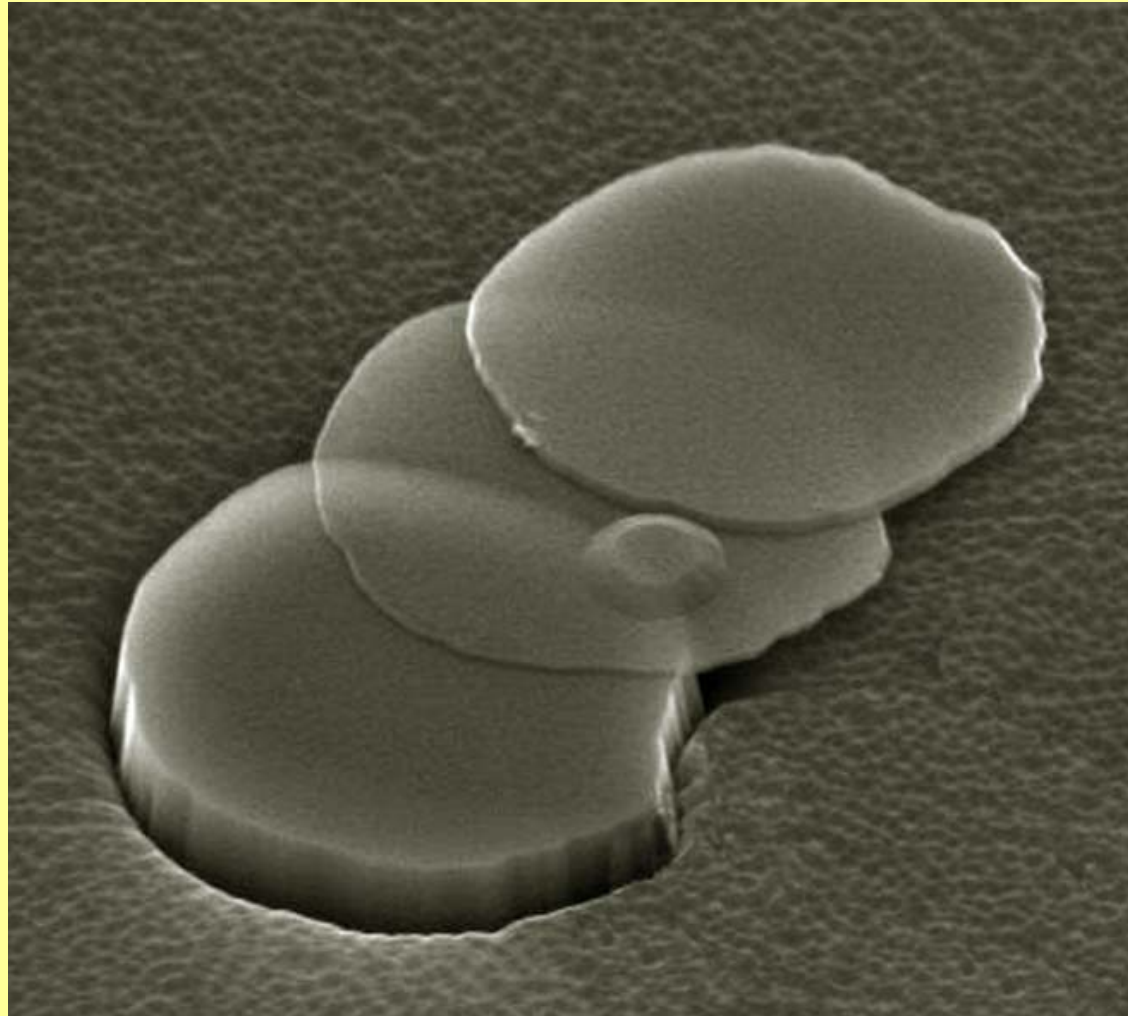


Scotch Tape – Layer Peeling

Mechanical exfoliation

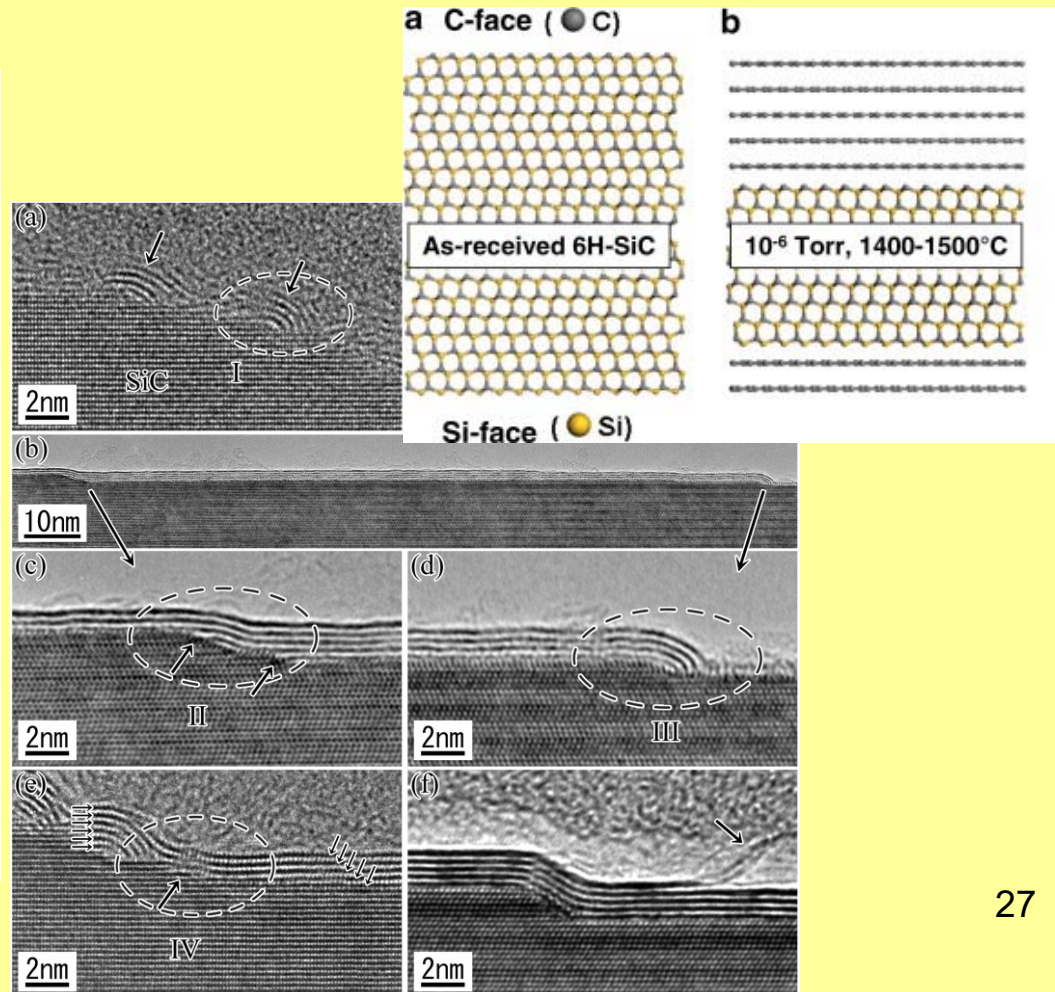
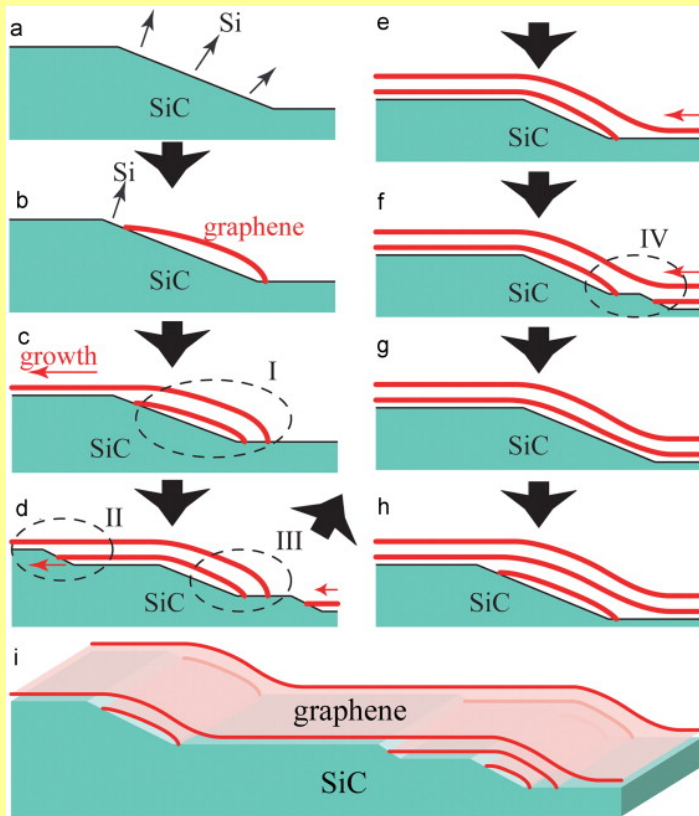


Scotch Tape – Layer Peeling



SiC Pyrolysis

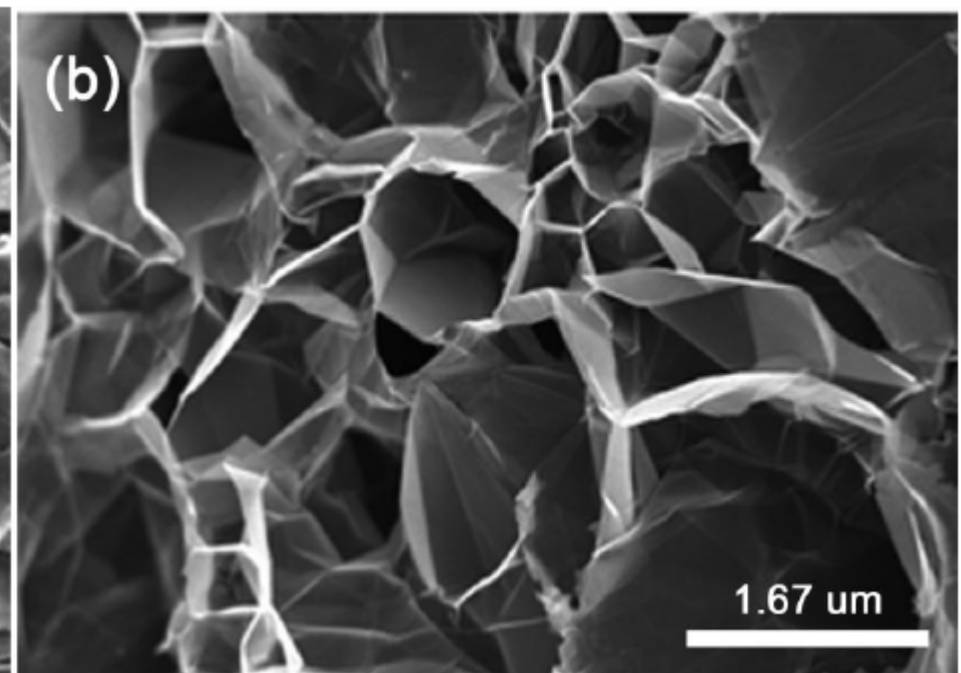
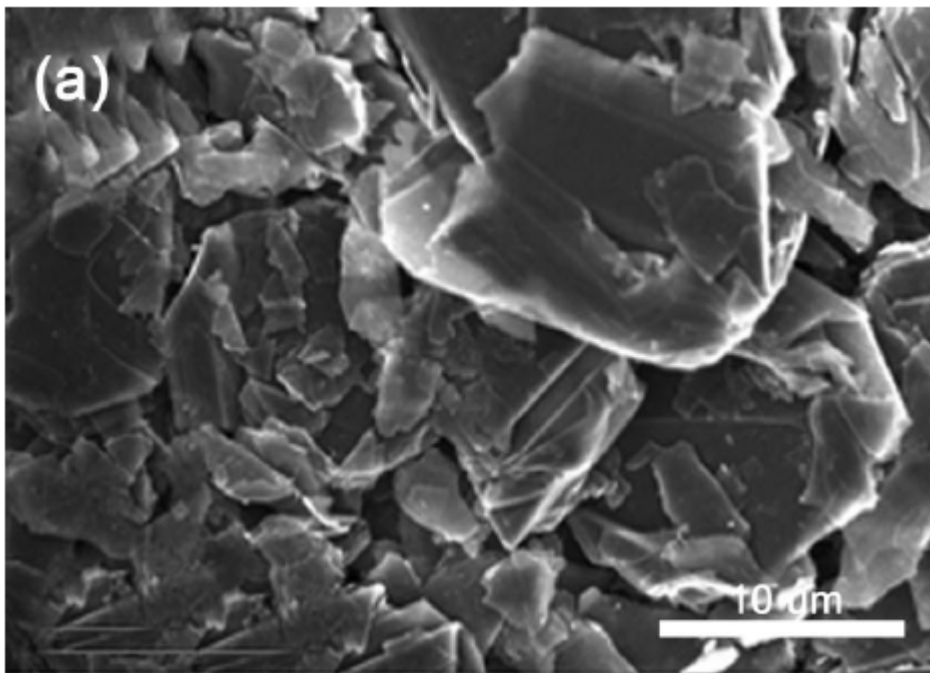
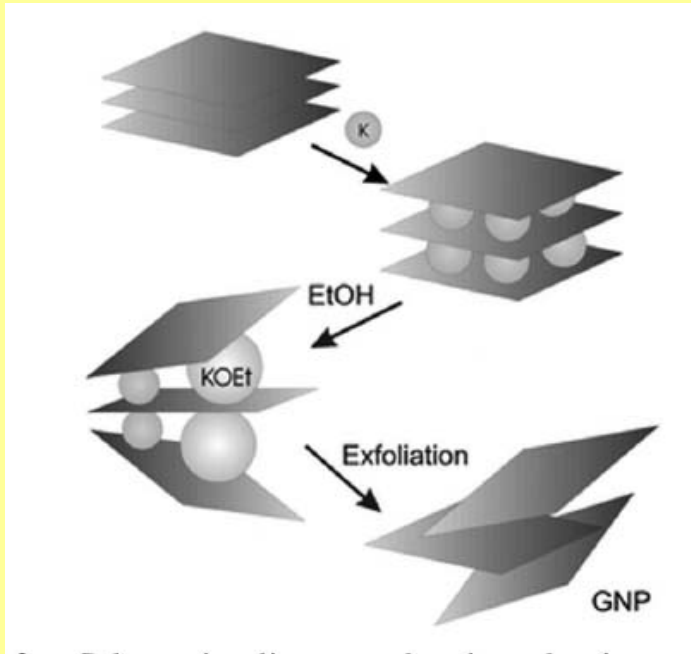
- Annealing of the SiC crystal in a vacuum furnace (UHV 10^{-10} Torr)
- Sublimation of Si from the surface at 1250 - 1450 °C
- The formation of graphene layers by the remaining carbon atoms



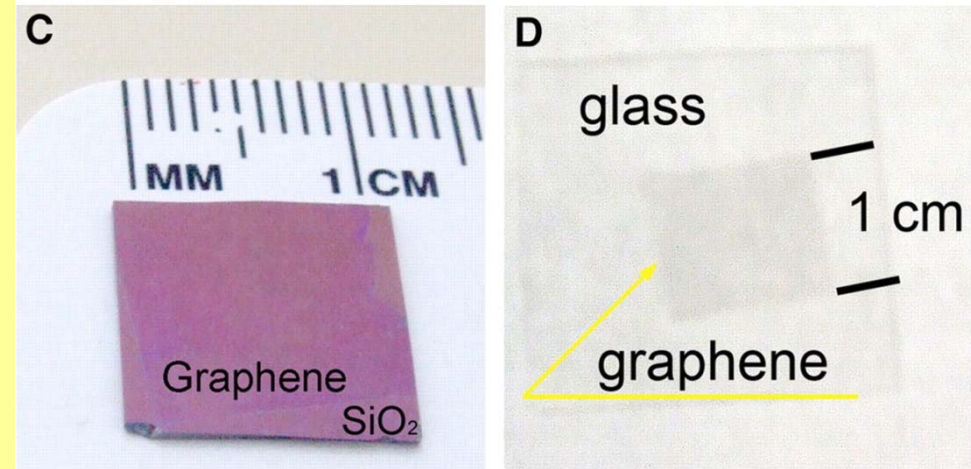
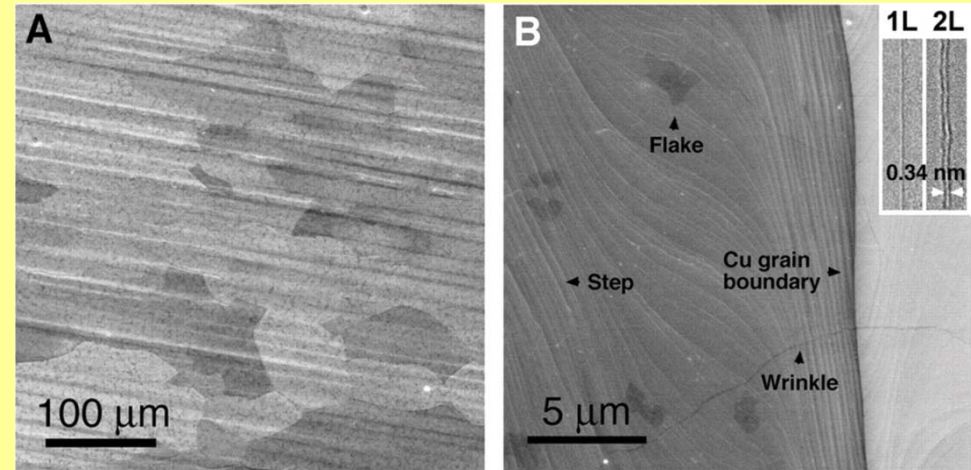
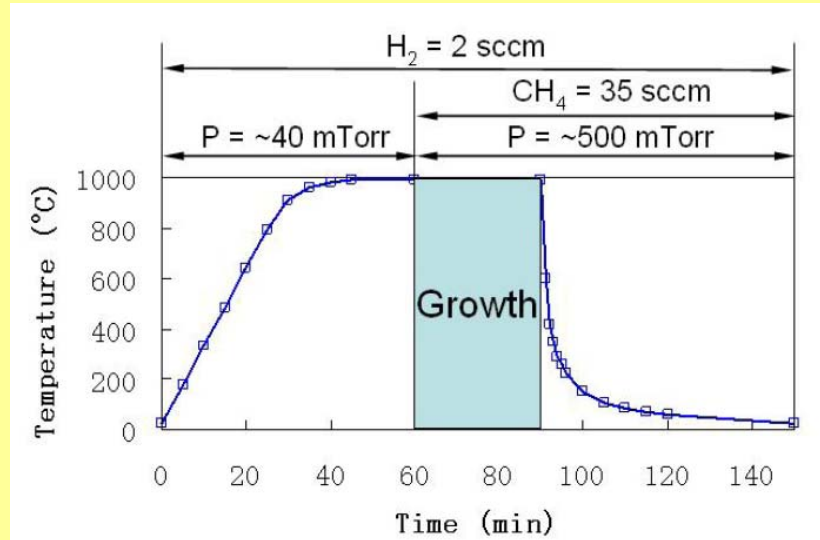
Exfoliation

Chemical exfoliation (surfactant)

Sonochemical exfoliation



CVD from CH₄ / H₂ on Metal Surfaces



(A) SEM - graphene on a copper foil

(B) High-resolution SEM - Cu grain boundary and steps, two- and three-layer graphene flakes, and graphene wrinkles. Inset (B) TEM images of folded graphene edges. 1L, one layer; 2L, two layers.

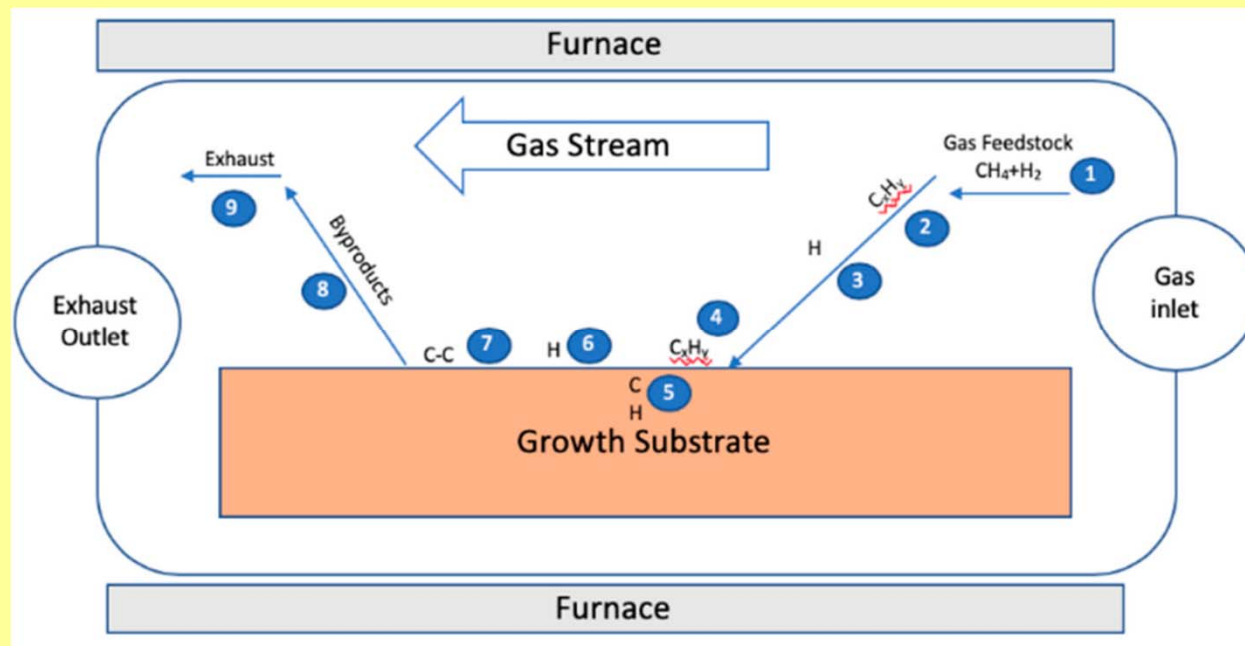
Graphene transferred onto
(C) a SiO₂/Si substrate
(D) a glass plate

CVD from Hydrocarbons on Metal Surfaces

The first graphene synthesis by CVD
2006 Somani - camphor and nickel substrate

Carbon cannot diffuse into Cu = monolayer graphene

Carbon diffuses into Ni = formation of multi-layered graphene



Graphene on SiO₂



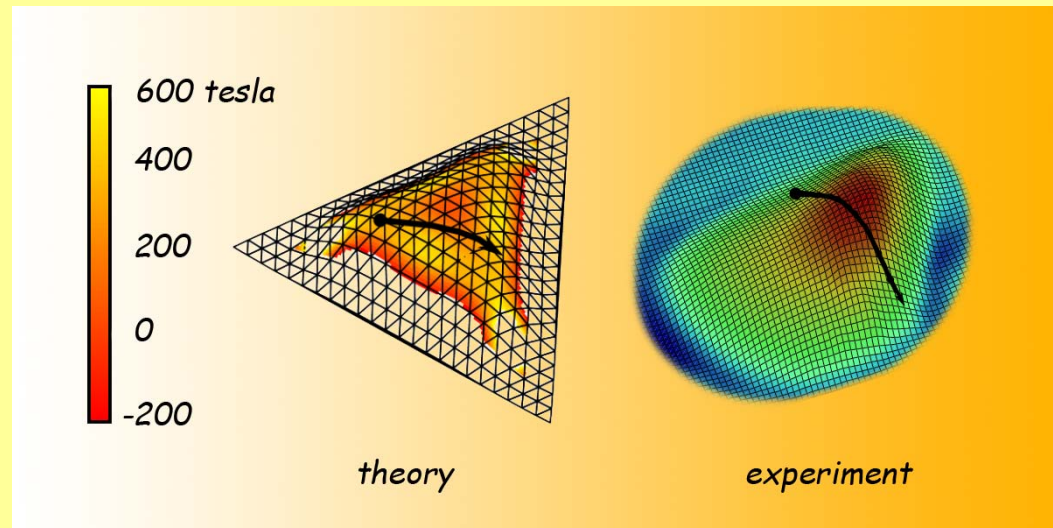
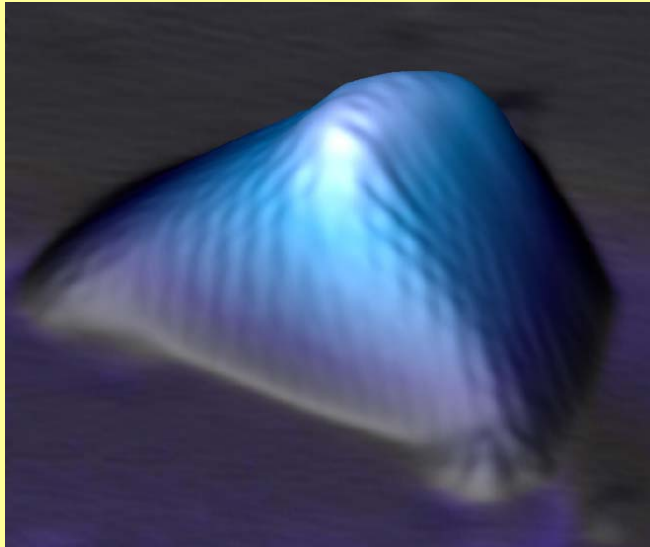
Pseudo-Magnetism

Graphene on platinum grown from ethylene at high temperatures
Cooled to low temperature to measure STM to a few degrees above absolute zero

Both the graphene and the platinum contracted – but Pt shrank more, excess graphene pushed up into bubbles, size 4-10 nm x 2-3 nm

The stress causes electrons to behave as if they were subject to huge magnetic fields around 300 T

(record high in a lab, max 85 T for a few ms)



Magic-Angle Twisted Bilayer Graphene

MAGIC ANGLE
Stacking one sheet of graphene on top of another can have a range of effects. If the sheets are rotated with respect to one another at just the right angle, the interaction of electrons in the two layers can give rise to new electronic properties.

SIMPLE STRUCTURE
The crystal structure of a single layer of graphene can be described as a simple repetition of two atoms — its 'unit cell'.

Unit cell of graphene

Enlarged unit cell

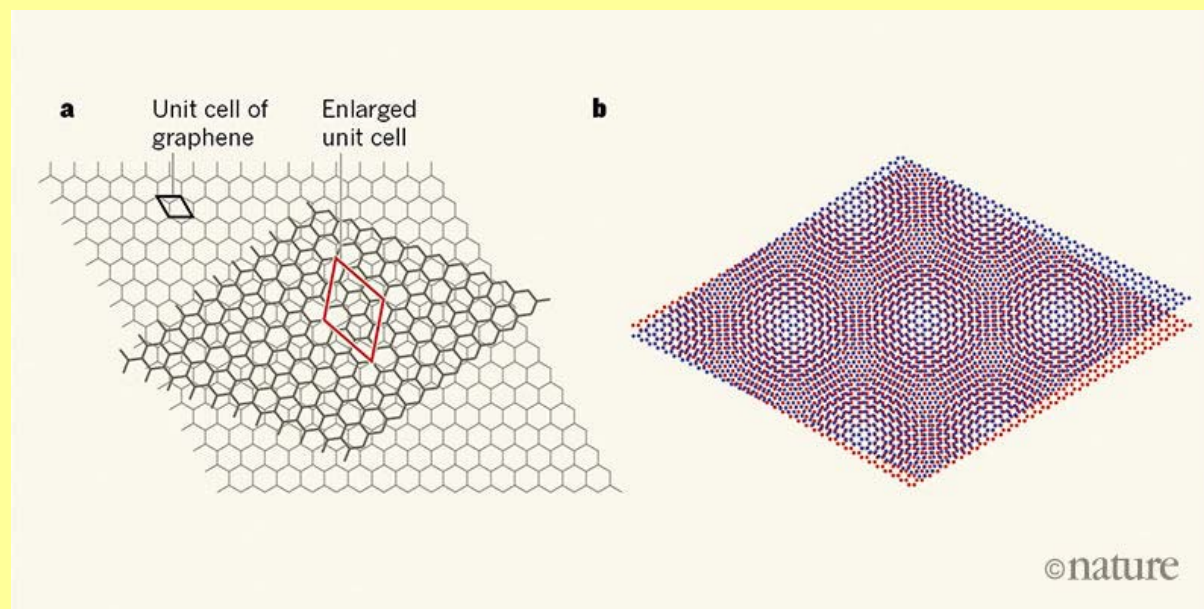
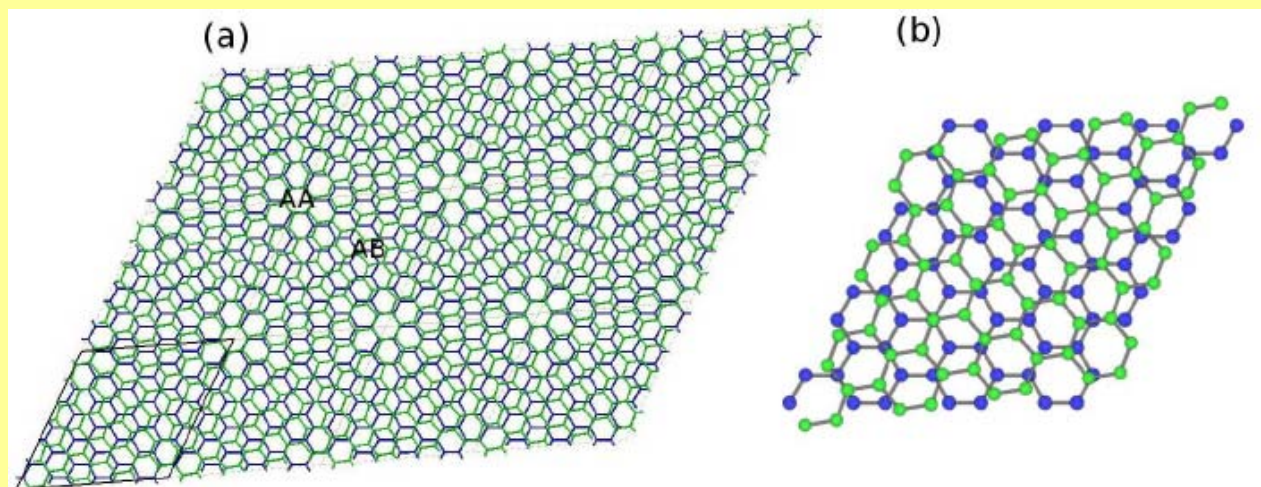
Visible interference pattern

SUPERLATTICE
With some rotations, a two-layer stack forms a more complex repeating structure called a superlattice, with a larger unit cell. Electrons can move between the two layers.

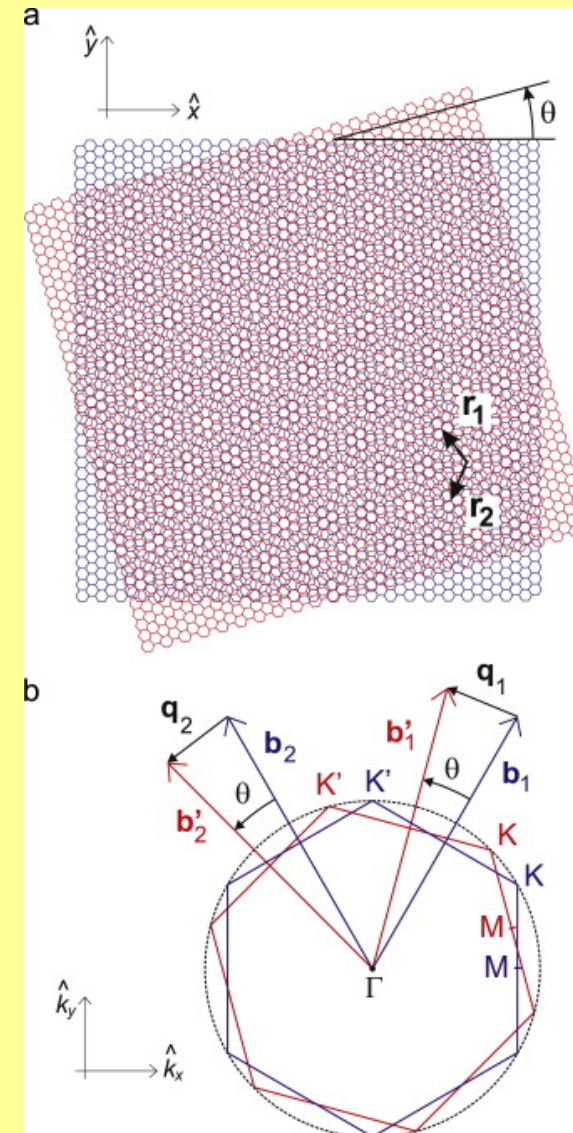
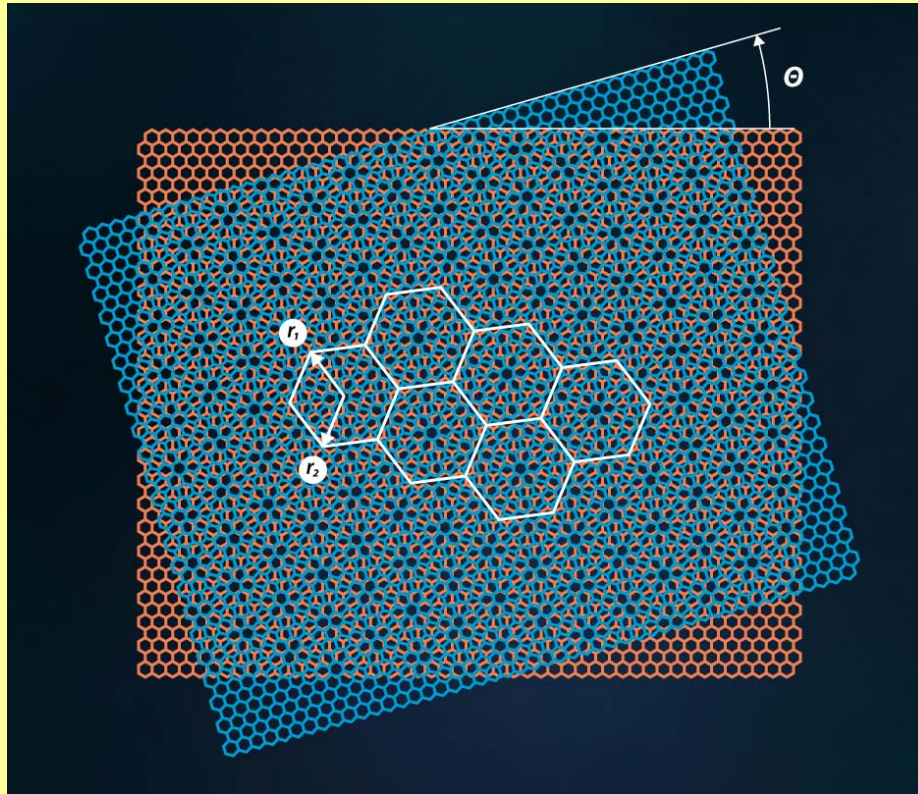
1.1° rotation

When twisted to a specific 'magic angle', the stack seems to exhibit behaviour not seen in ordinary graphene, such as superconductivity.

©nature

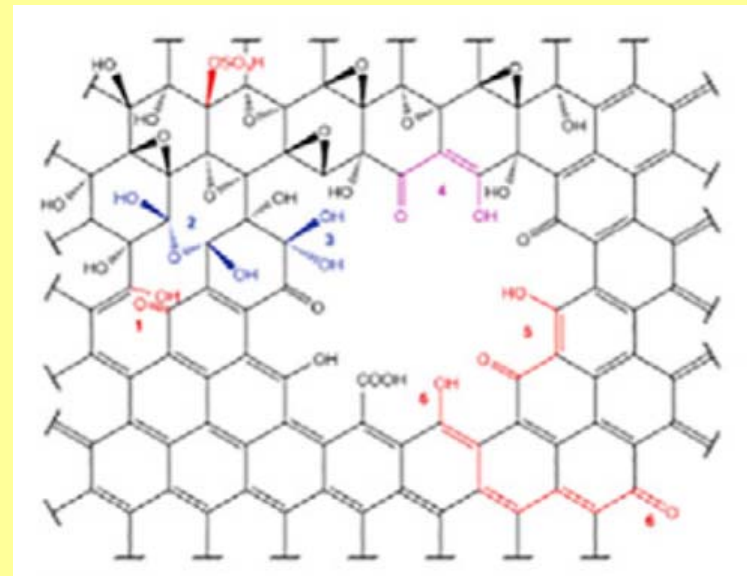
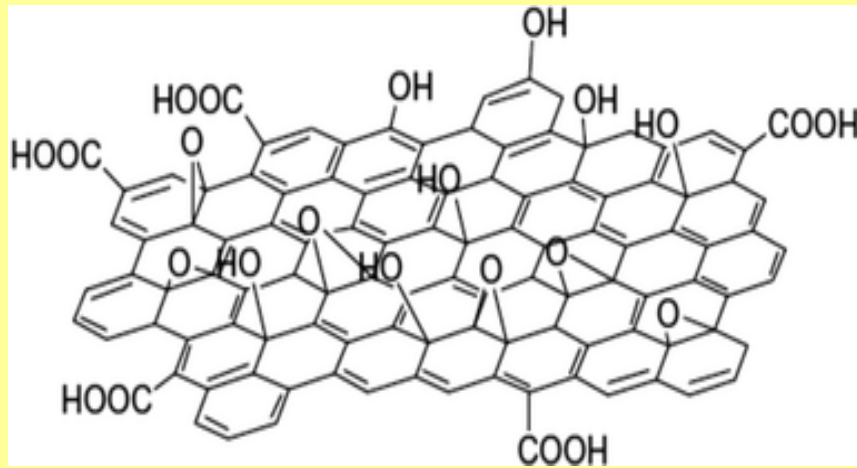


Twisted Bilayer Graphene



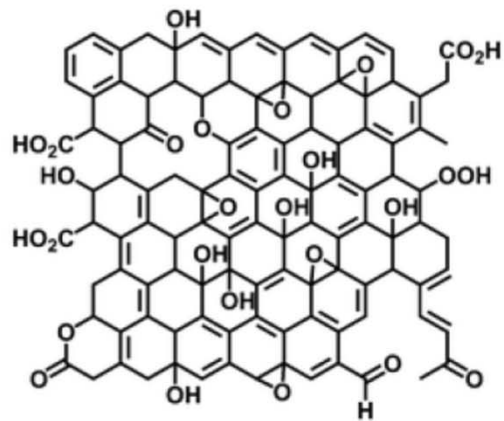
Graphene Oxide

- More reactive than graphene
- Presence of oxygen groups: -OH, -COOH, =O, -O-
- Hydrophilic character
- Electric insulator, sheet resistance $R_s \sim 10^{12} \Omega/\text{sq}$
- Specific SA (theoretical): $\sim 890 \text{ m}^2\text{g}^{-1}$ (1700-1800 m^2g^{-1})
- Photoluminescence properties
- Bandgap from 1.7 to 2.1 eV

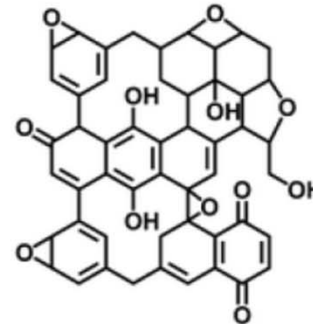


Graphene Oxide

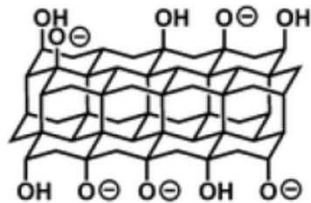
LERF-KLINOWSKI



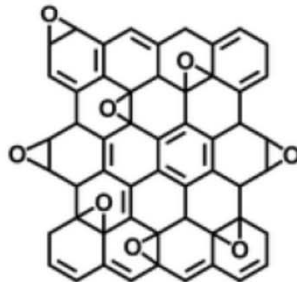
DÉKÁNY



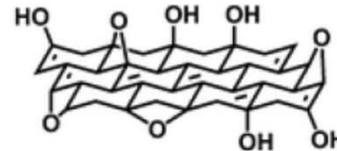
NAKAJIMA-MATSUO



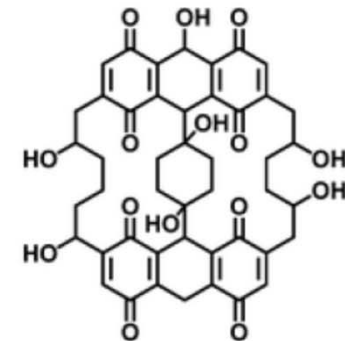
HOFMANN



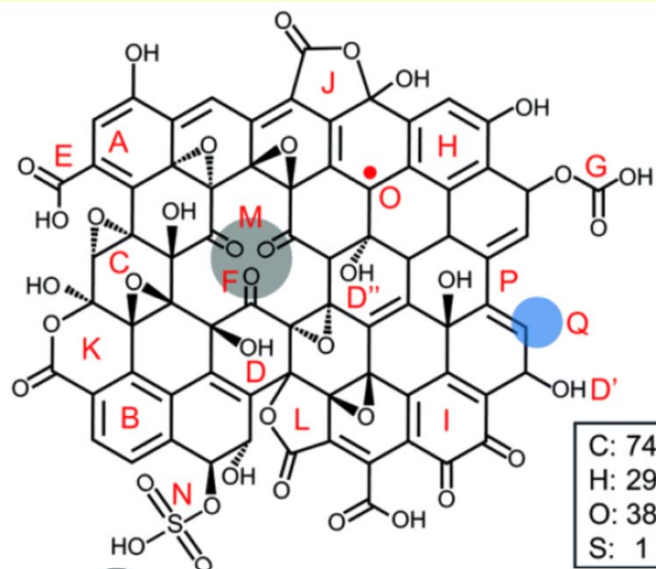
RUESS



SCHOLZ-BOEHM



Graphene Oxide

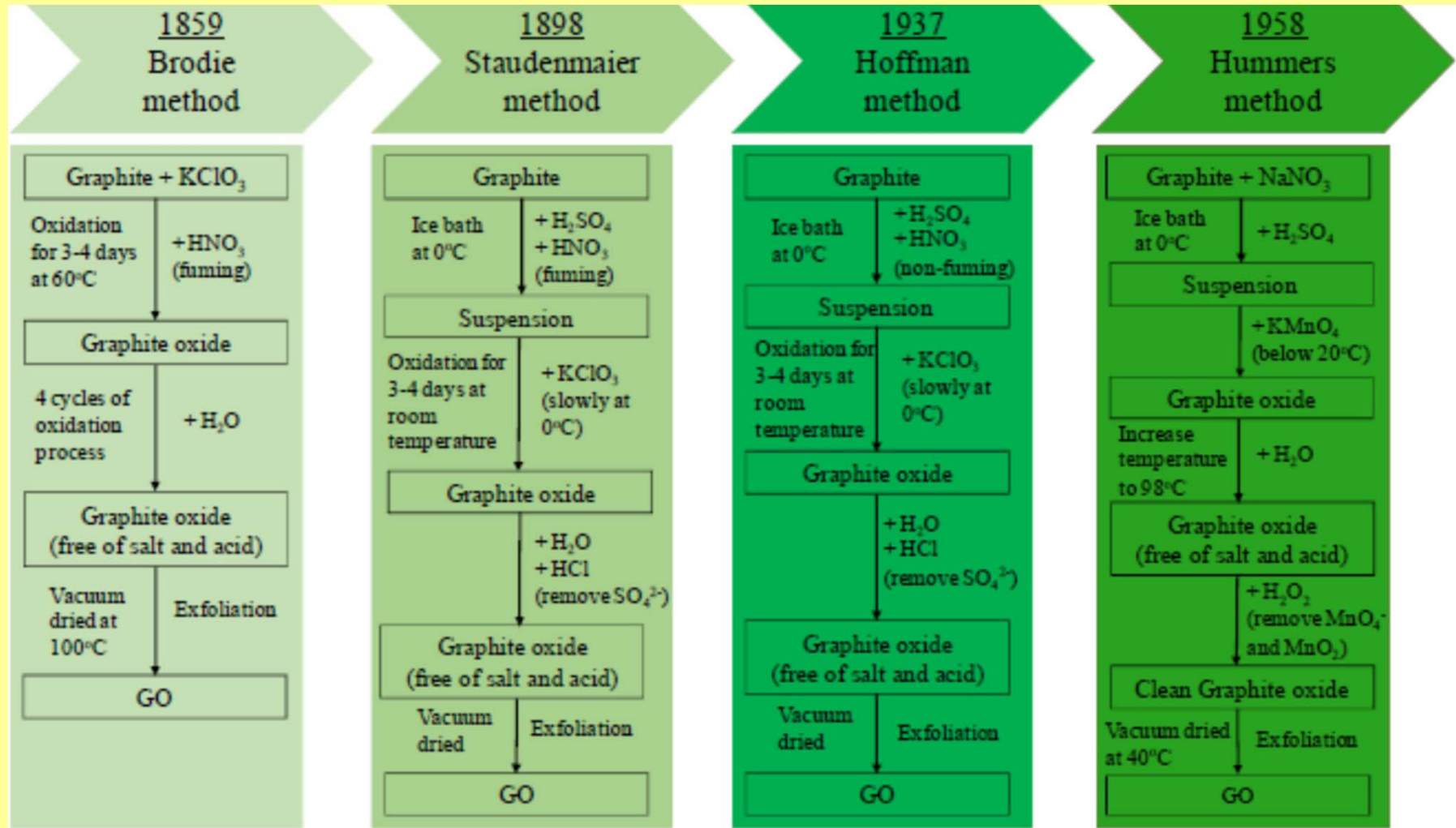


C: 74
H: 29
O: 38
S: 1

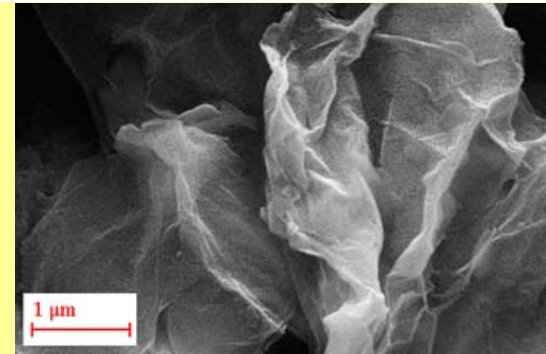
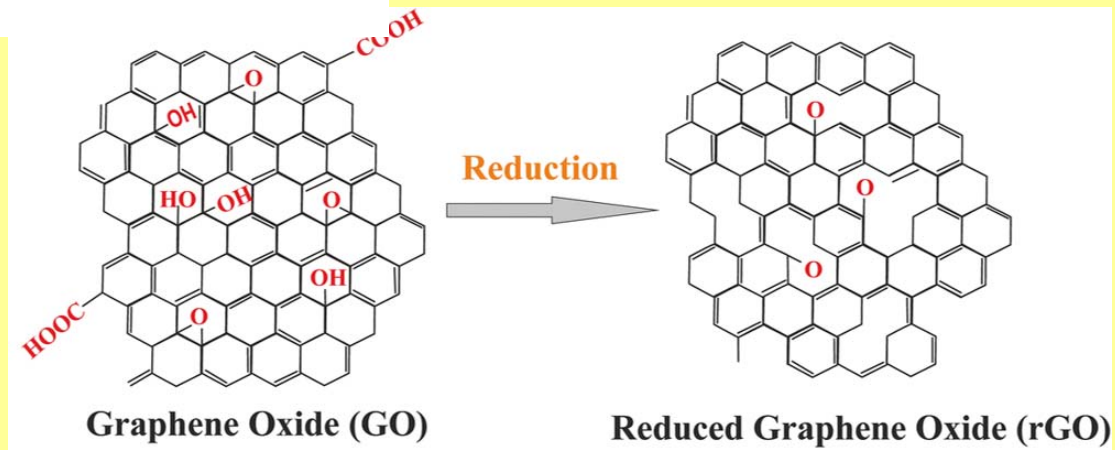
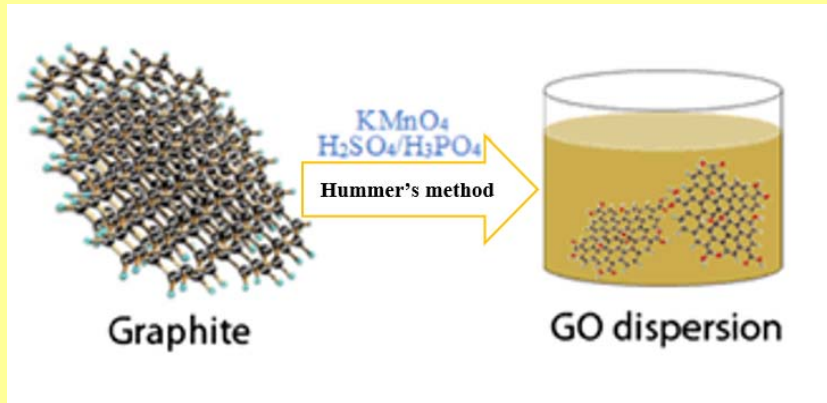
C/O = 1.95

- 1996-1998 LK
- A Double bond (C=C) ← 2008
 - B Aromatic entity
 - C Epoxy (C-O-C: 1,2-ether) ← 2D Connectivities
 - D Hydroxy (C-OH: >2 types) ← Keto-enol Tautomerism
 - E Carboxylic acid (HO-C=O or salt) ←
- 2005-2006
- F Ketone (C=O) ←
 - G Organic carbonate (C-O-CO H)
 - H Phenol
 - I Quinone
- 2009
- J Lactol (5)
 - K Lactol (6)
 - L Ester carbonyl
- 2010 ● M Carbon vacancy (hole)
- 2012 N Sulfate ester (C-O-SO₃H)
- 2014 ● O π-Conjugated carbon radical
- 2016
- P 1,3-Butadiene
 - Q Implicit carbon-hydrogen bond (C-H)

Graphene Oxide



Hummers Method



Graphene Oxide Characterization

Well oxidized GO: C/O = 2.1 - 2.9

UV-vis:

~227-231 nm (arom. C=C, $\pi \rightarrow \pi^*$)

~300 nm (C=O, $n \rightarrow \pi^*$)

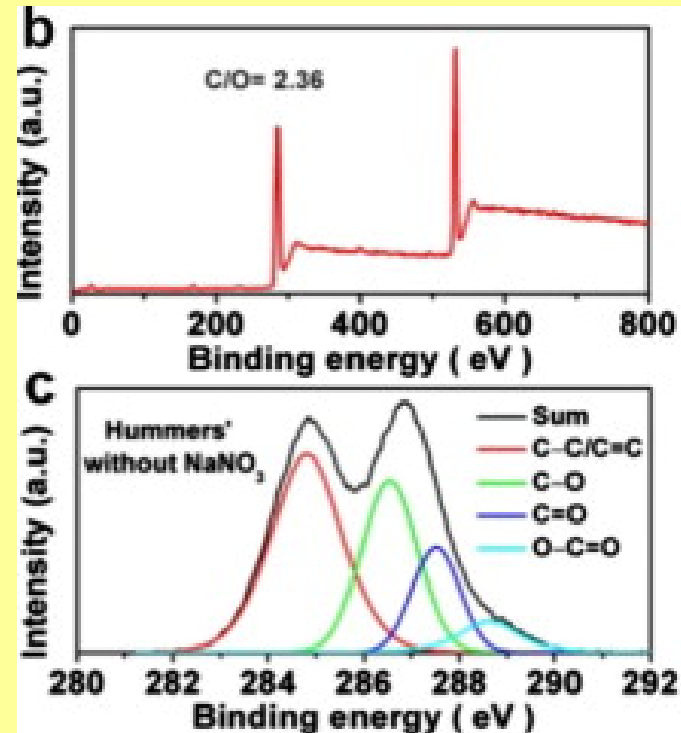
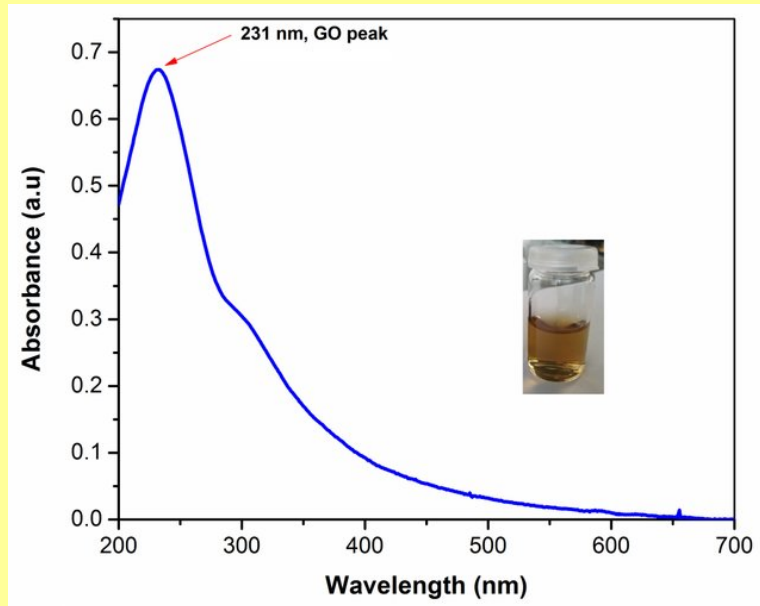
C 1s XPS spectrum (eV)

C-C/C=C 284.6

C-O 286.6

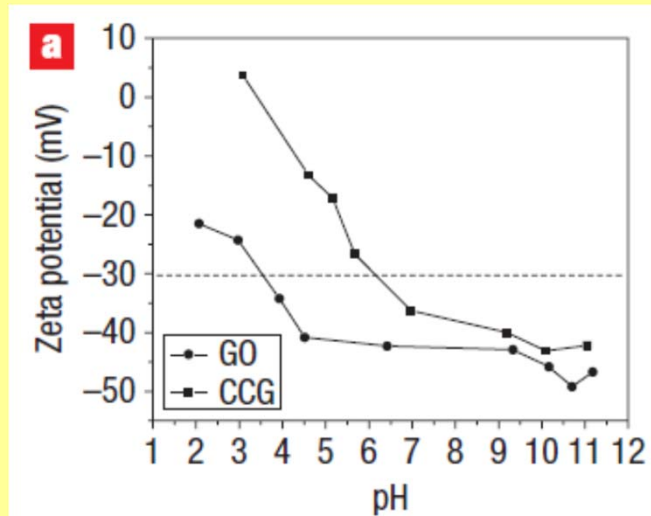
C=O 287.8

O-C=O 289.0

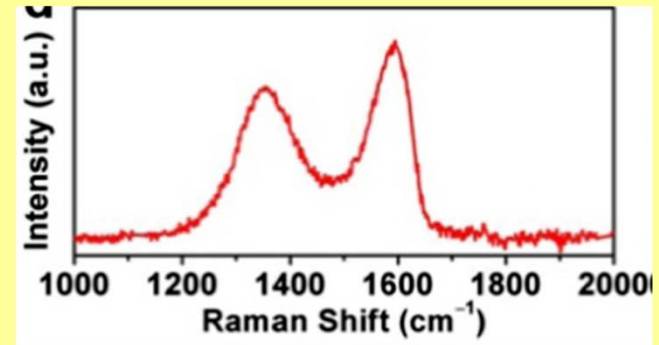


Graphene Oxide Characterization

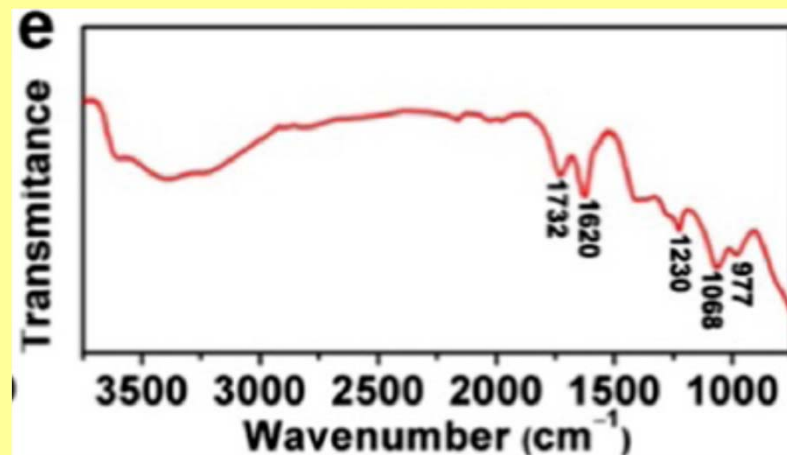
Zeta potential: -44 mV
aqueous dispersions
0.05 mg/ml



Raman, cm^{-1}
G-band 1590
D-band 1350



FTIR ATR spectra, cm^{-1}
C-O-C 1000, C-O 1230, C=C 1590-1620,
C=O 1740-1720, O-H stretching 3600-
3300



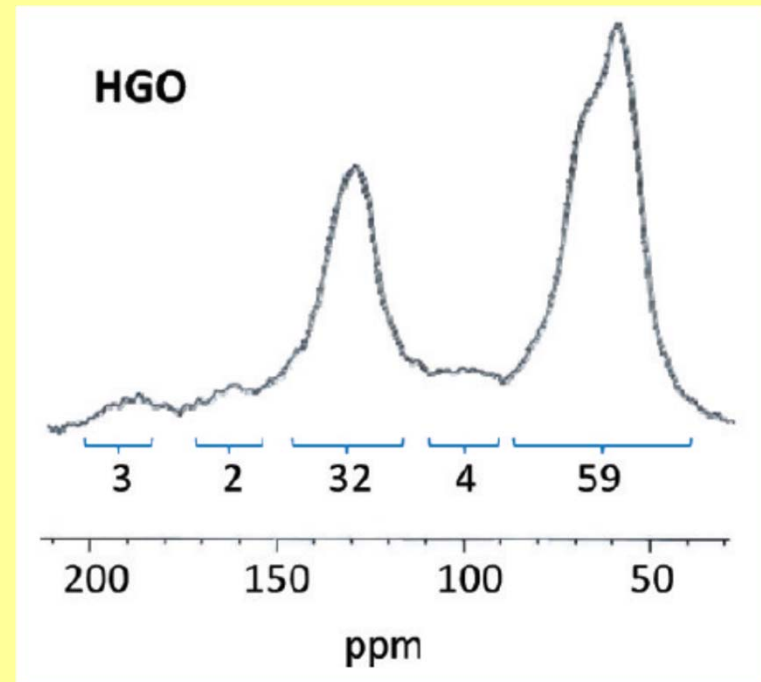
Graphene Oxide Characterization

Solid-state ^{13}C NMR, ppm

Ketone carbonyls	190
Ester and lactol carbonyls	164
Graphitic sp^2 carbons	131
Lactols $\text{O}-\text{C}(\text{sp}^3)-\text{O}$	101
Alcohols	70
Epoxides	61

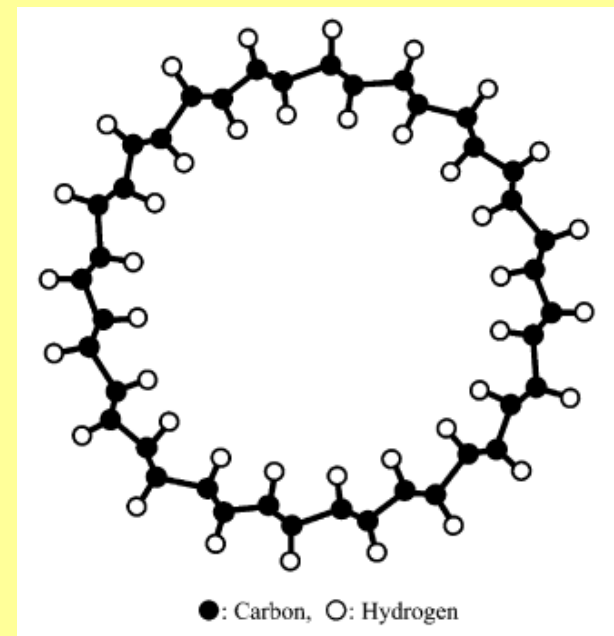
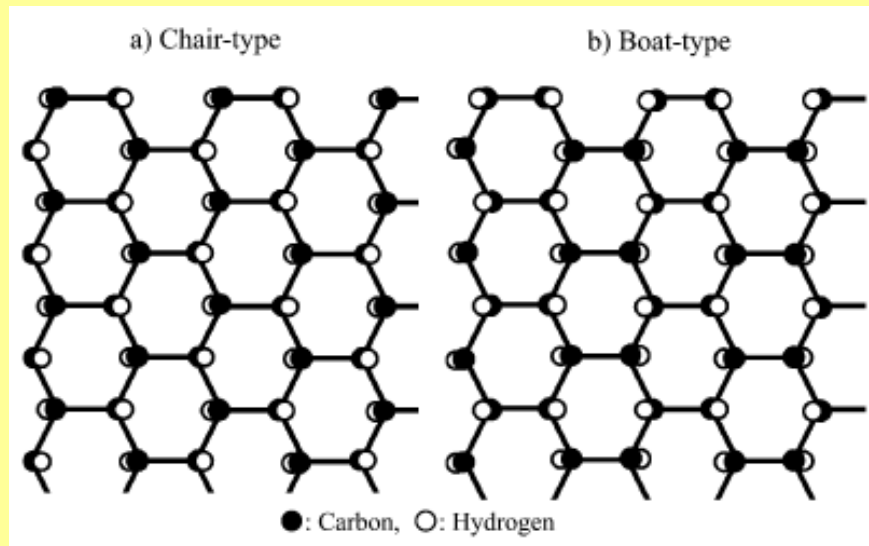
The measure of oxidation

The ratio between the alcohol/epoxide signal and graphitic sp^2 carbon signal

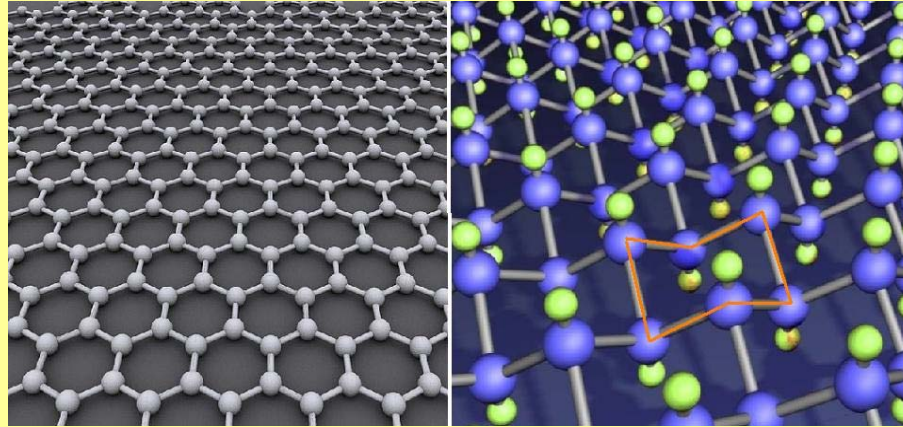


Graphane – Hydrogenated Graphene

- 2009 (graphene + cold hydrogen plasma)
- Two conformations: chair x boat
- Calculated binding energy = most stable compound with stoichiometric formula CH
- Chair type graphane insulating nanotubes

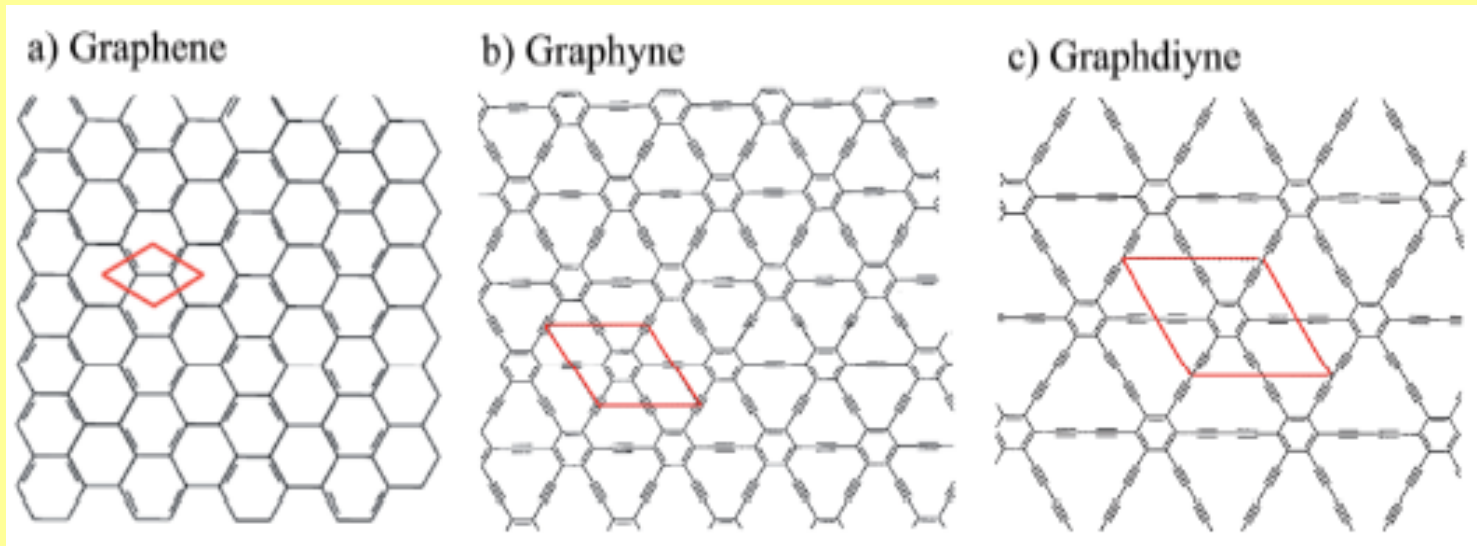


Fluorographene



- **Monolayer of graphite fluoride**
- **Chair type x boat type-strong repulsion**
- **Synthesis:**
 - Graphene + XeF_2/CF_4 (room temperature)
 - Mechanical or chemical exfoliation of graphite fluoride
 - By heating graphene in XeF_2 gas at 250 °C
- **Graphene + XeF_2 at 70 °C – high-quality insulator, stable up to 400 °C (resemblance with teflon)**

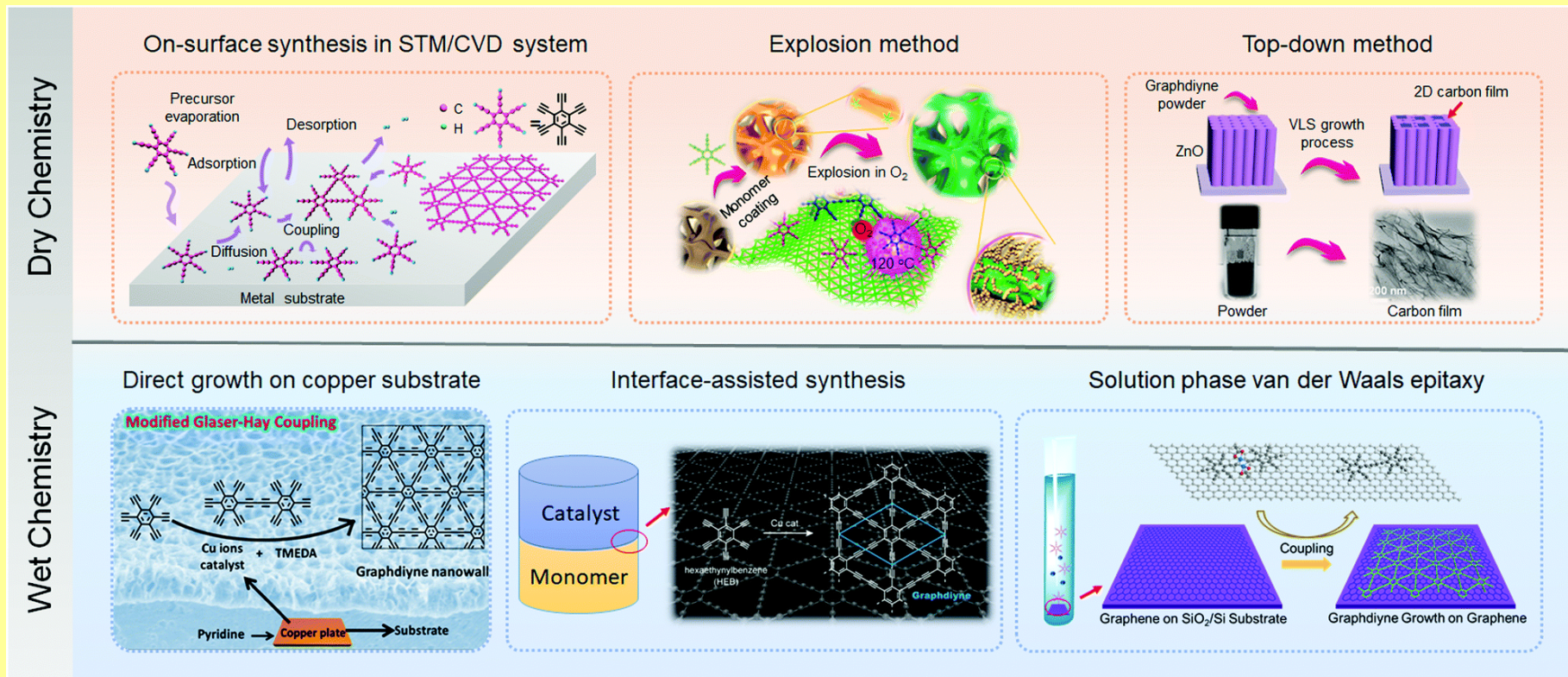
Graphyn, Graphydiyn



- **Predicted**
- **“Non-derivatives“ of graphene**
- **Semiconductors**
- **Movement of electrons as in graphene but only in one direction**

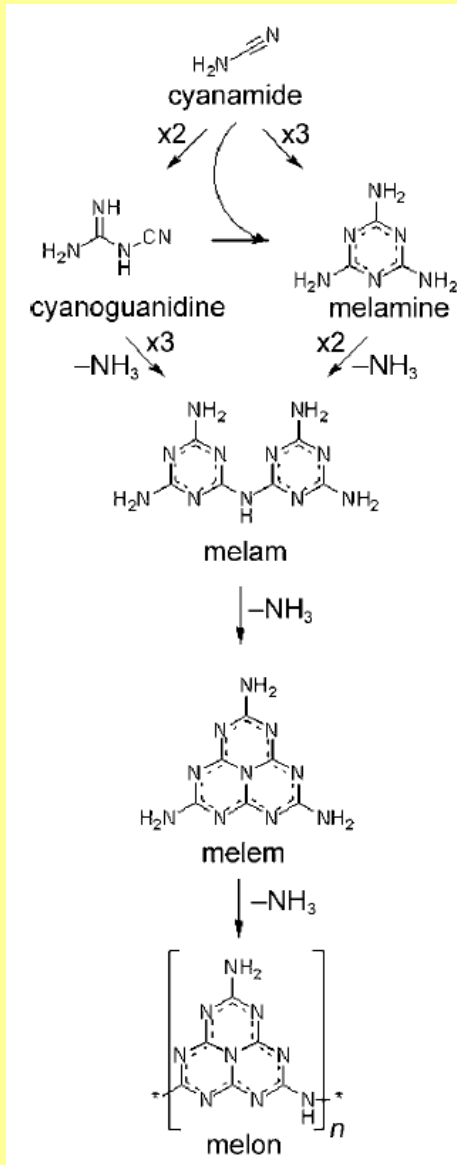
Graphdiyn

Synthesis



Graphitic Carbon Nitride

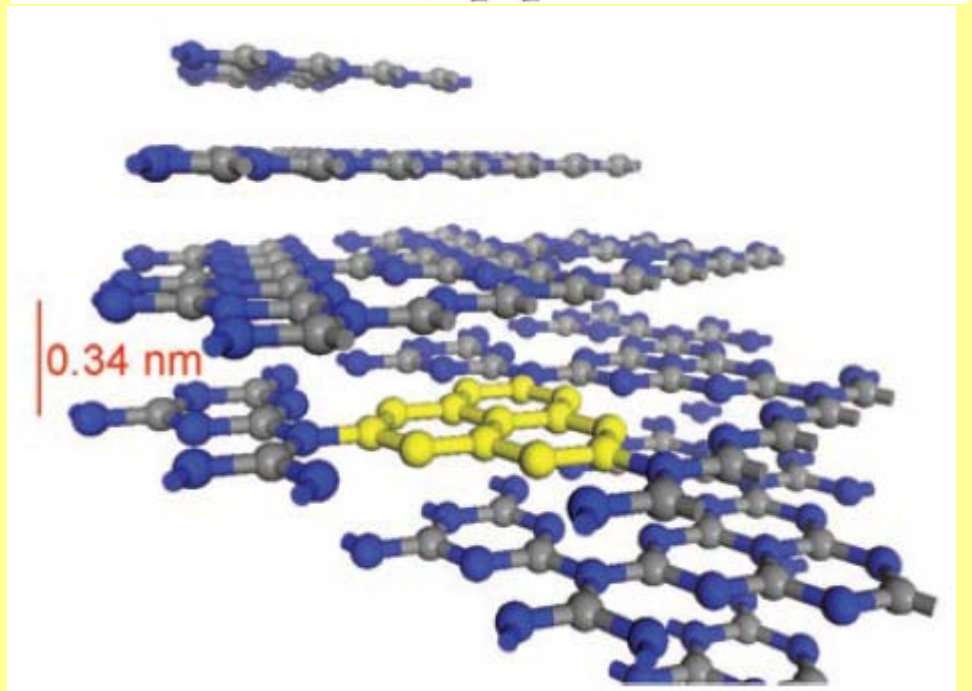
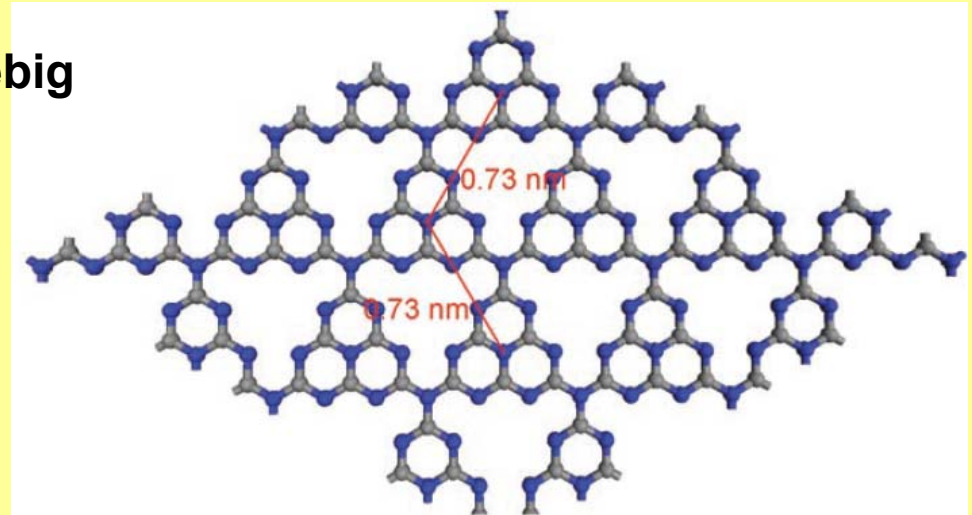
1834 Berzelius, Liebig



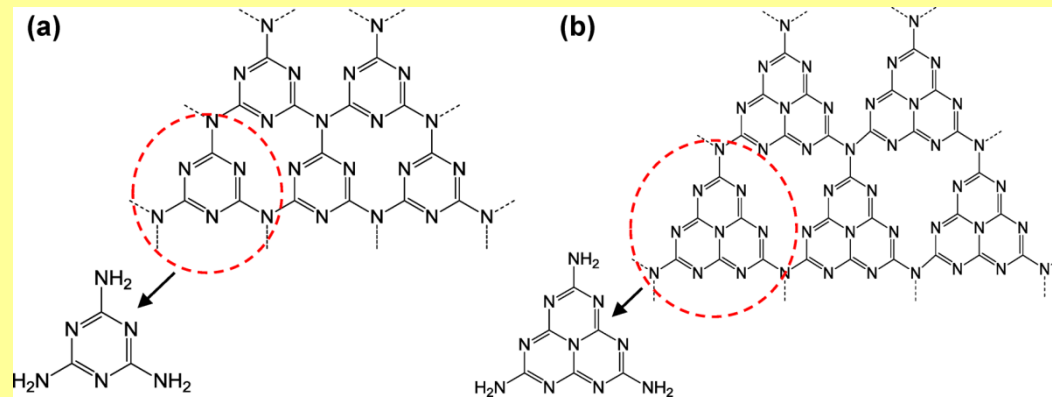
Temperature-induced condensation

dicyandiamide
 $\text{NH}_2\text{C}(\text{=NH})\text{NHCN}$

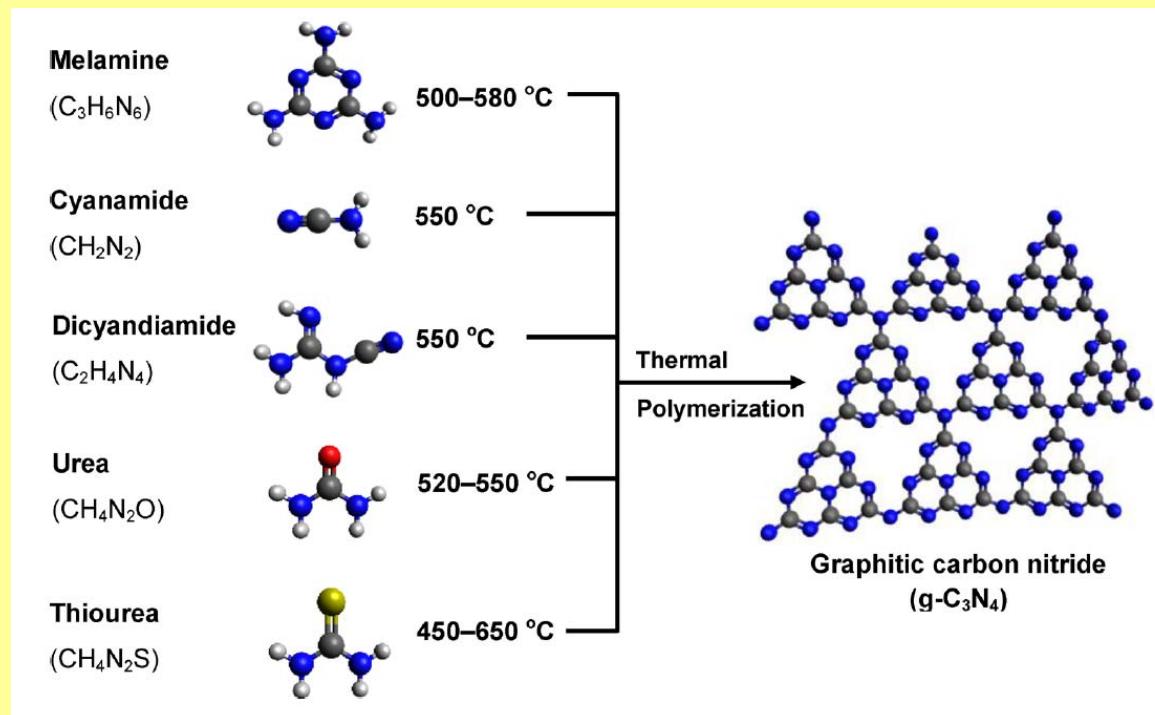
In a LiCl/KCl melt



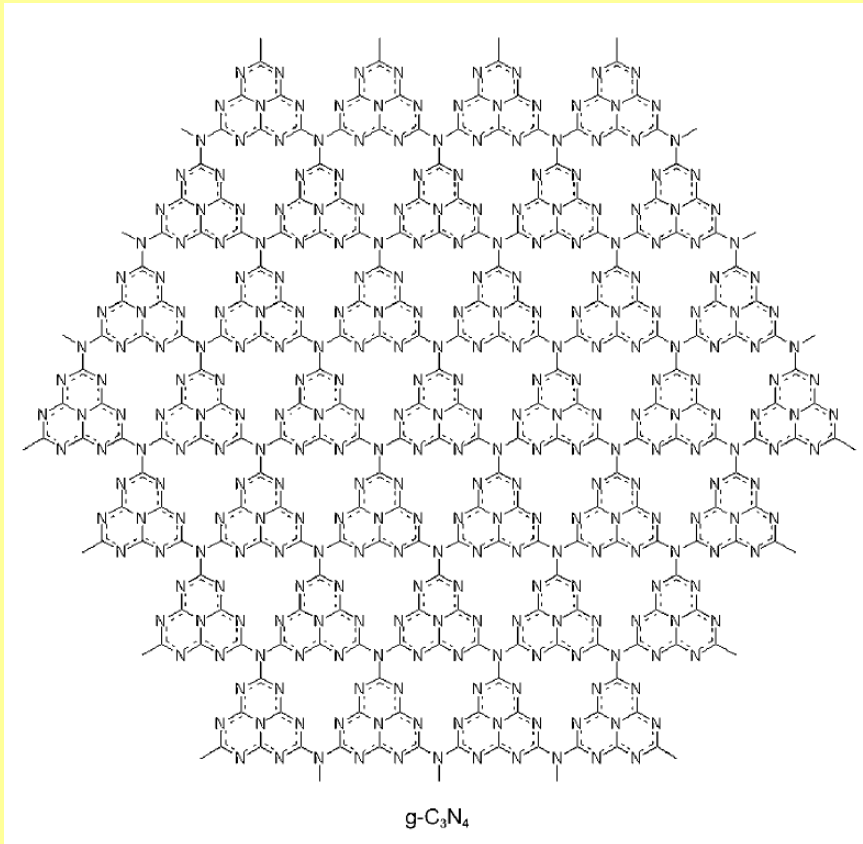
Graphitic Carbon Nitride



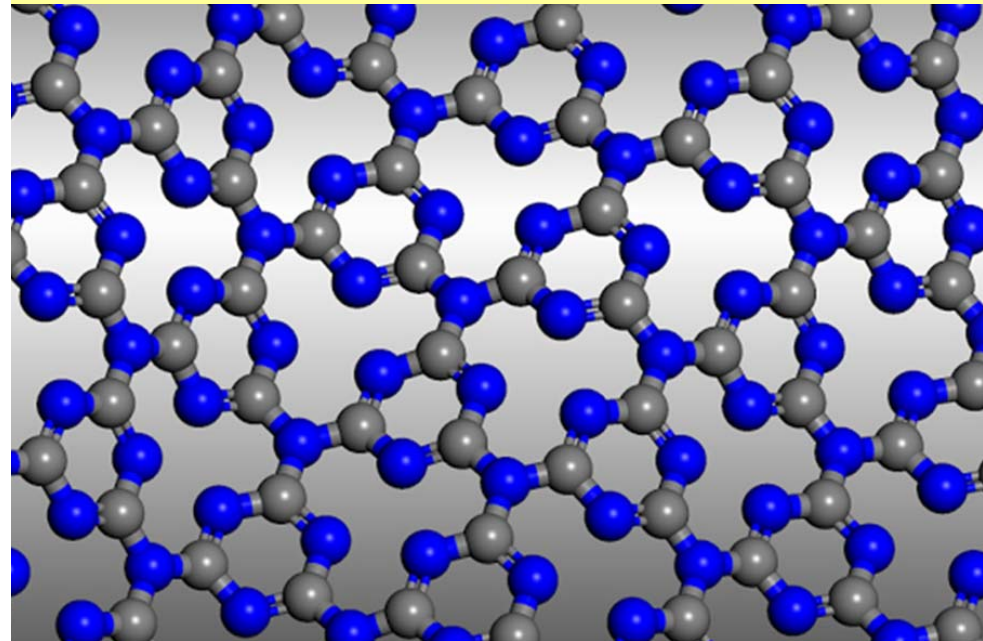
(a) triazine and (b) tri-s-triazine (heptazine)



Graphitic Carbon Nitride



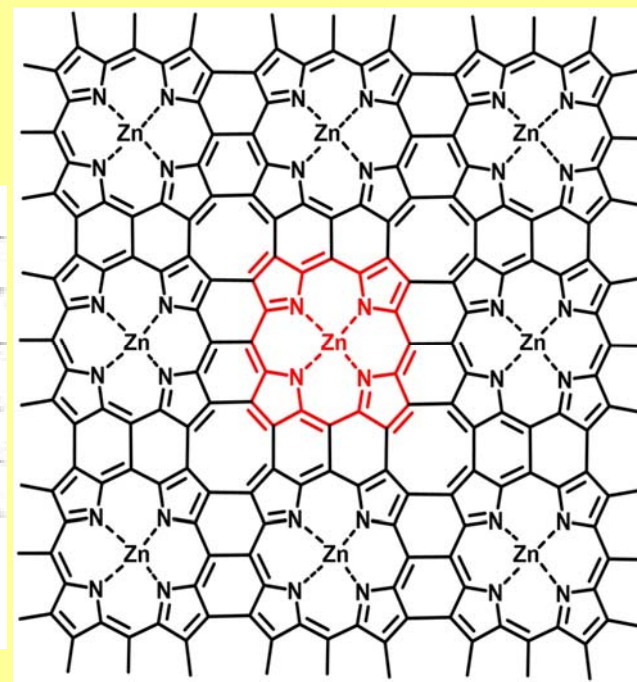
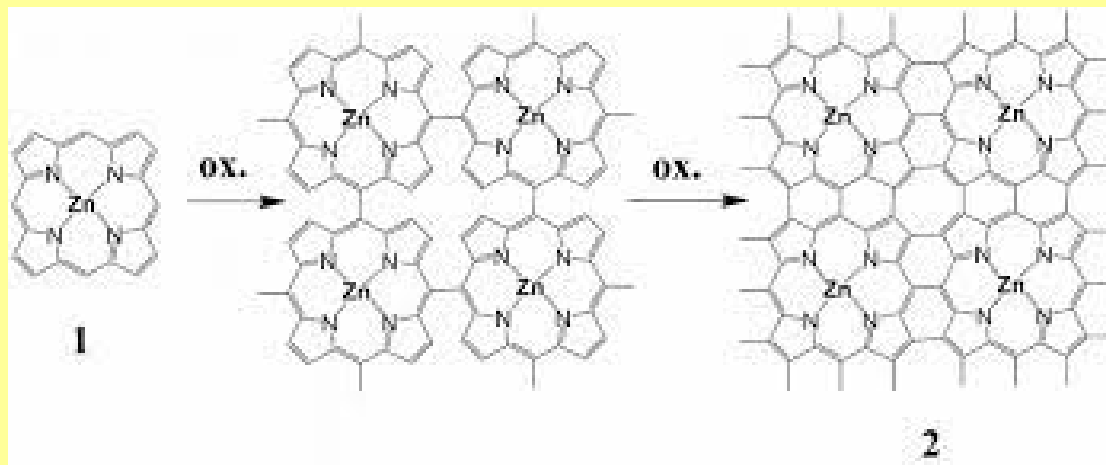
(“g-C₃N₄”)



Band gap 1.6 - 2.0 eV
Small band gap semiconductors
Si (1.11 eV), GaAs (1.43 eV), and GaP (2.26 eV)

Porphene

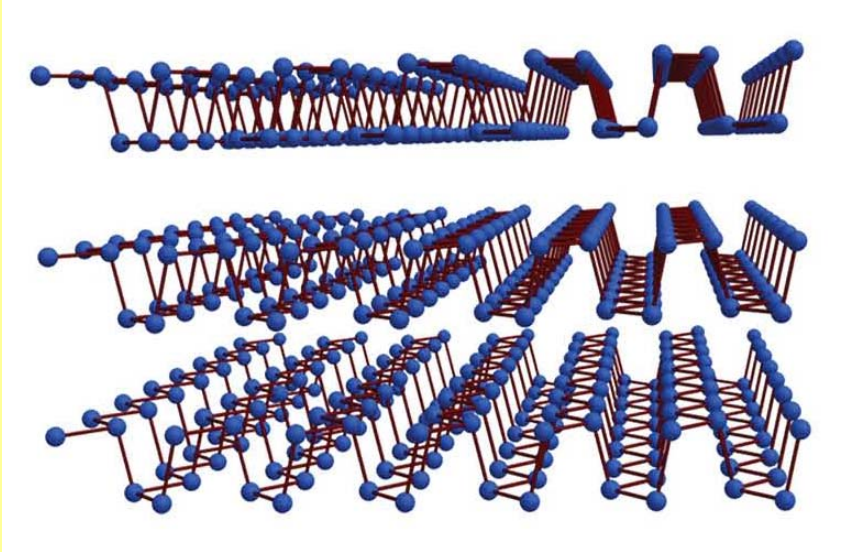
**Surface-constrained oxidative coupling of metalloporphyrins (zinc porphyrin) at the air/water interface
A bilayer is formed**



**Fully conjugated
Antiaromatic
Semiconductor
Rectangular unit cell P2mm
Family of 2-dimensional polymers
Changing metal, up to two substituents**



Phosphorene



Black phosphorus

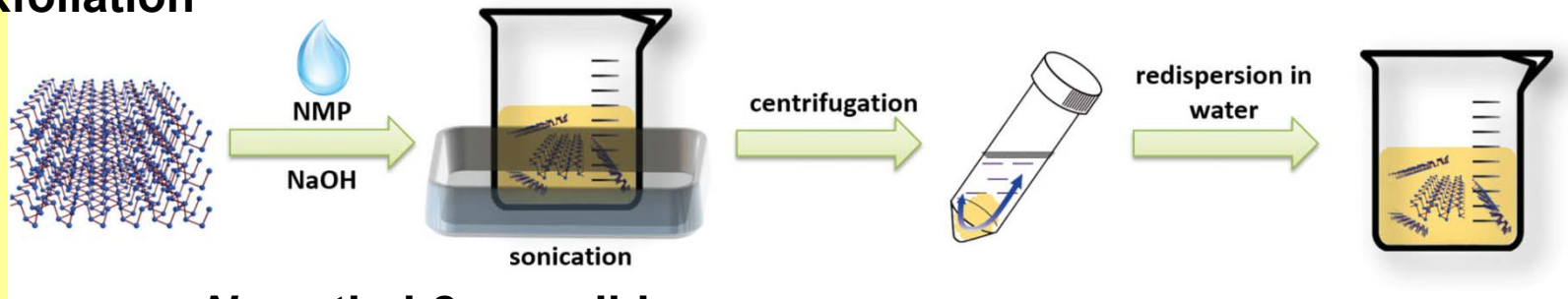
Orthorhombic

$a = 3.31 \text{ \AA}$, $b = 4.38 \text{ \AA}$, $c = 10.50 \text{ \AA}$

$\alpha = \beta = \gamma = 90^\circ$

Space group *Bmab*

Exfoliation



N-methyl-2-pyrrolidone

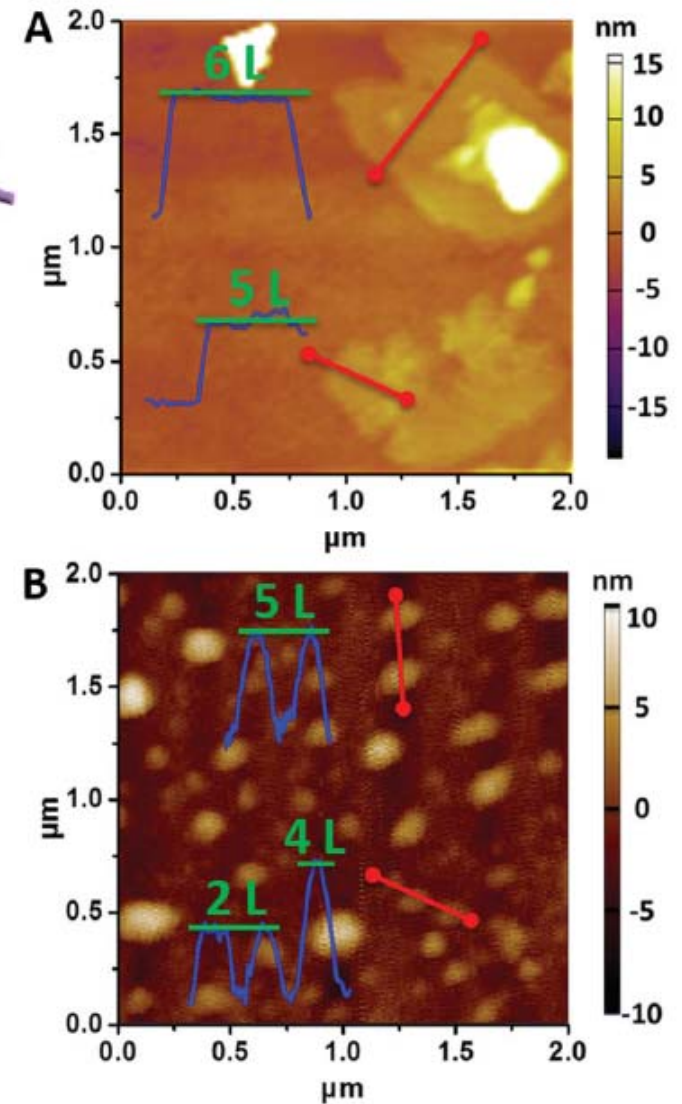
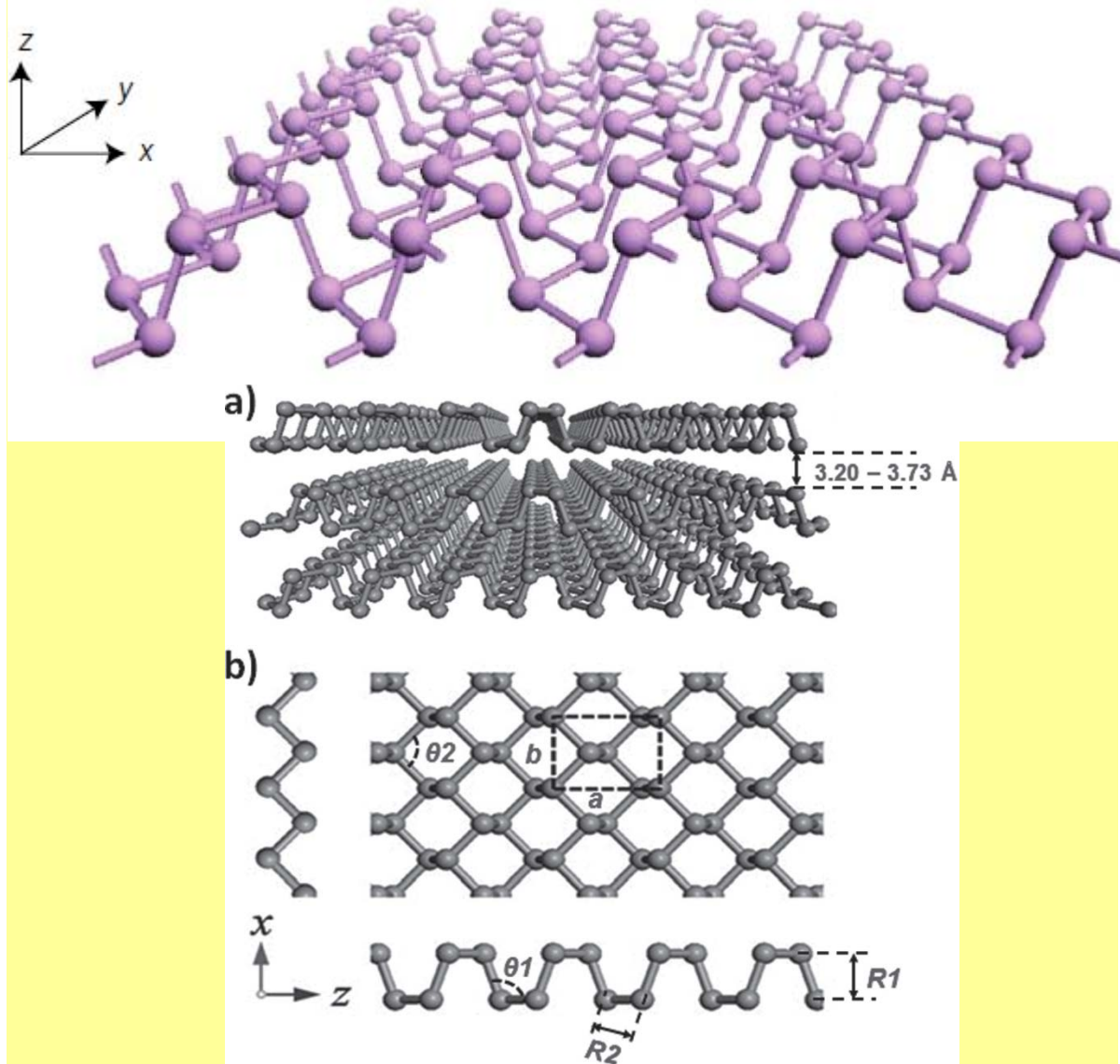
Semiconductor - direct band gap

bulk BP 0.3 eV

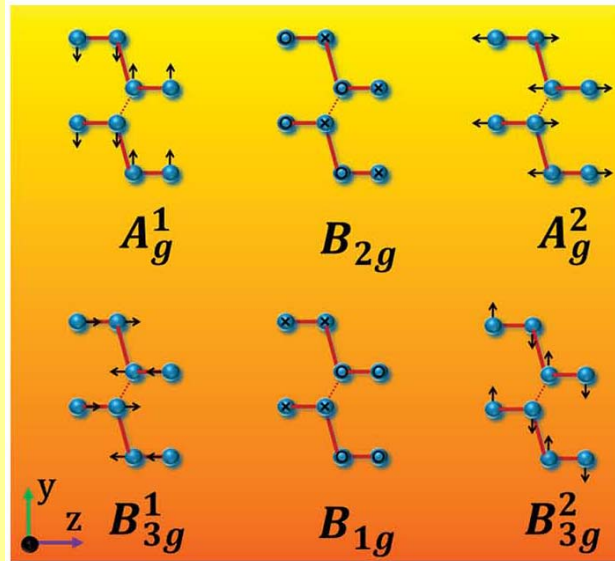
monolayer phosphorene 1.5 eV

Phosphorene

Height-mode AFM images
single-layer phosphorene
ca. 0.9 nm



Phosphorene



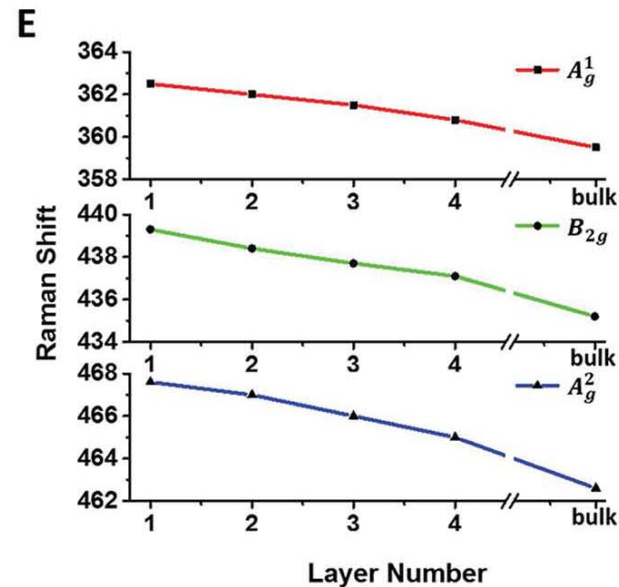
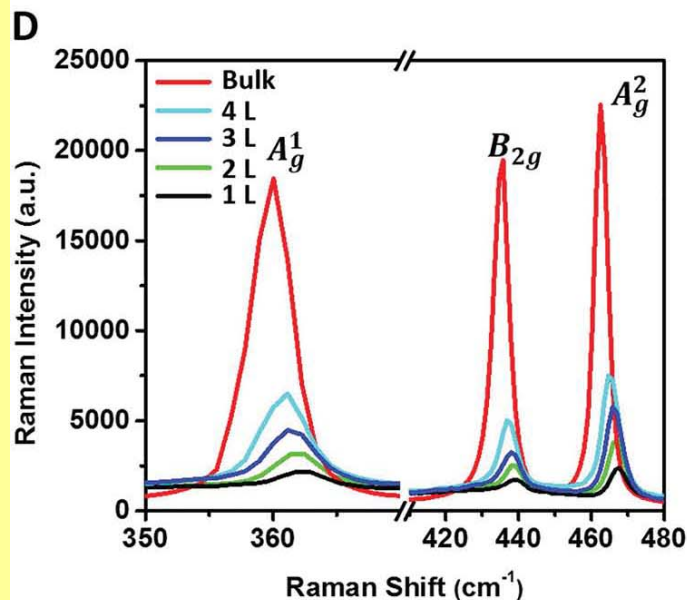
Black phosphorus

12 lattice vibrational modes

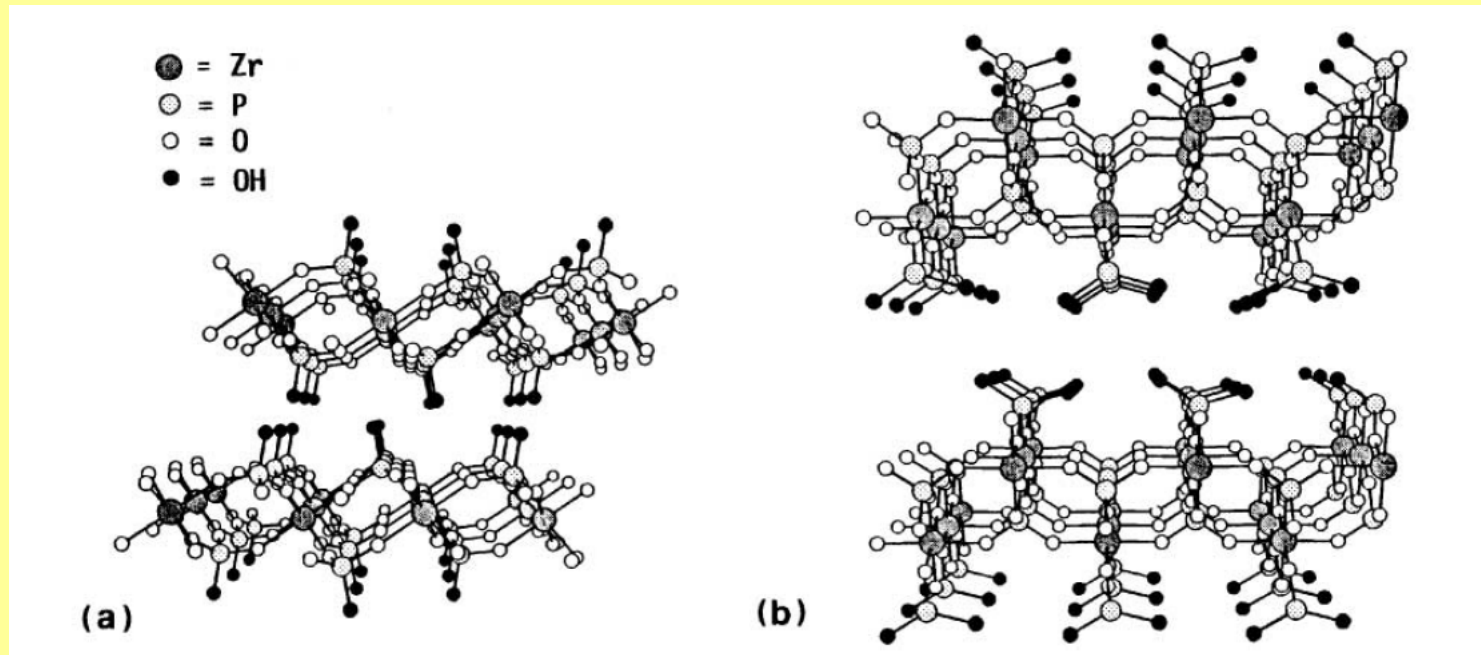
6 Raman active modes

3 vibrational modes A_{1g}^1 , B_{2g} , and A_{2g}^2 can be detected when the incident laser is perpendicular to the layered phosphorene plane: 361 cm^{-1} , 438 cm^{-1} , 465 cm^{-1}

As the number of phosphorene layers increases, the three Raman peaks red-shift



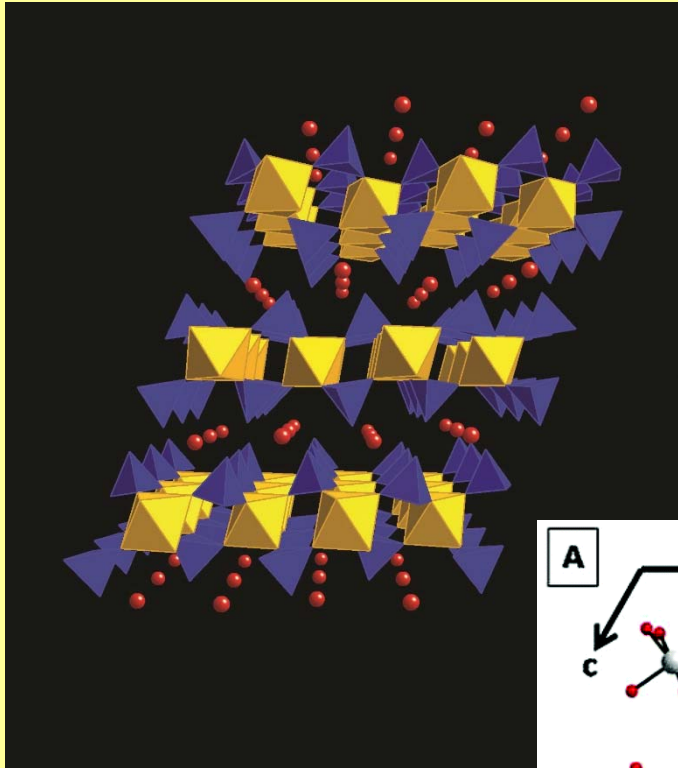
Zirconium Phosphates



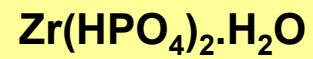
(a) α -zirconium phosphate = $\text{Zr}(\text{HPO}_4)_2 \cdot \text{H}_2\text{O}$
interlayer spacing 7.6 Å

(b) γ -zirconium phosphate = $\text{Zr}(\text{PO}_4)(\text{H}_2\text{PO}_4)_2 \cdot 2\text{H}_2\text{O}$
interlayer spacing 12.2 Å

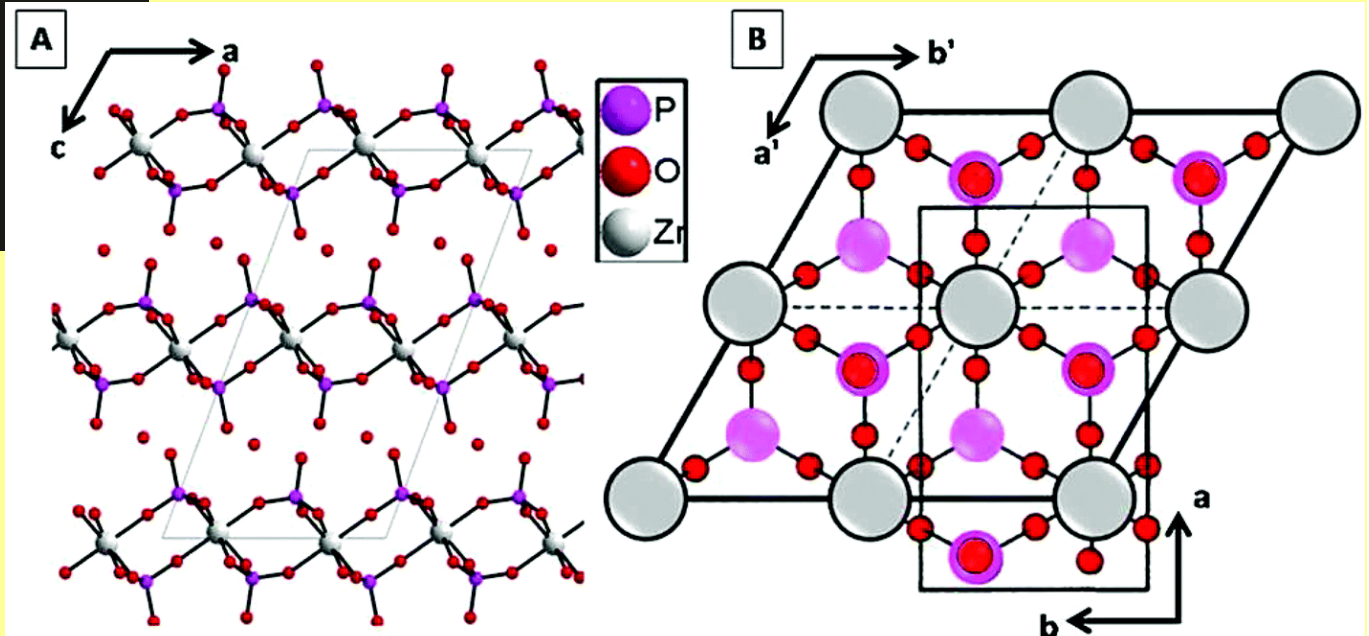
Zirconium Phosphates



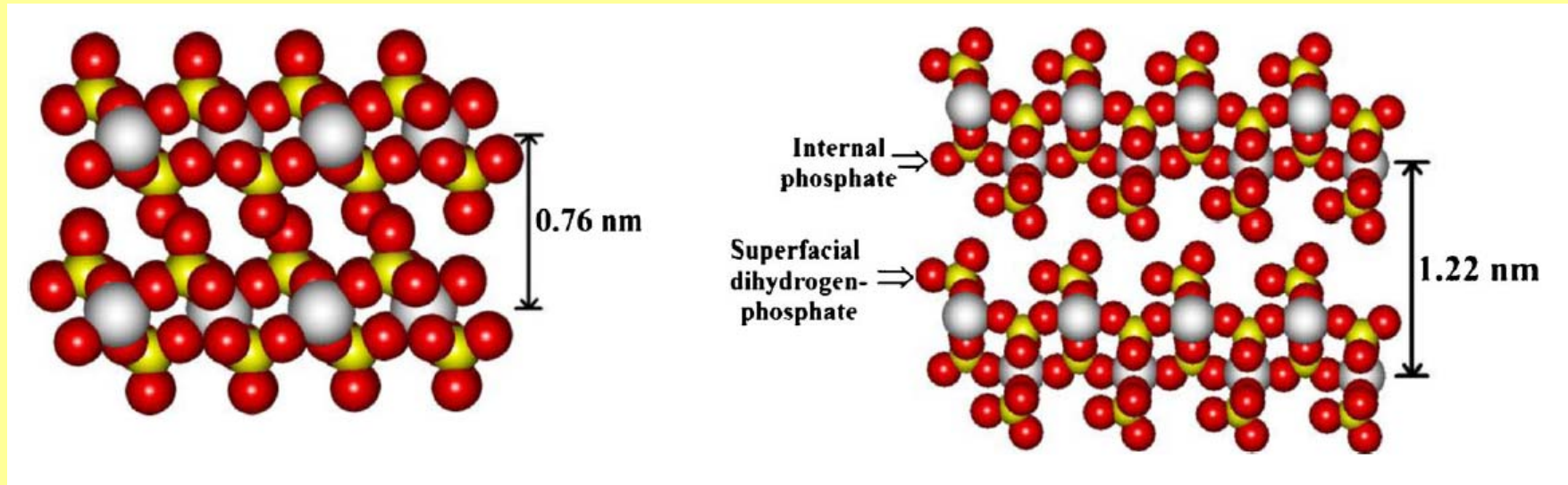
α -zirconium phosphate



interlayer spacing 7.6 Å



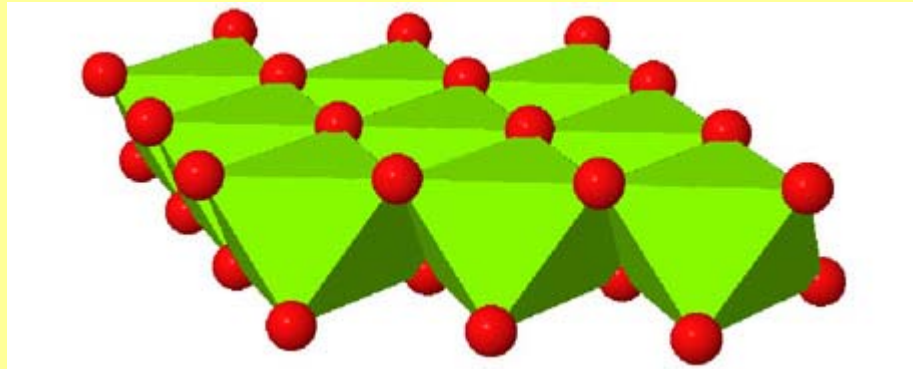
Zirconium Phosphates



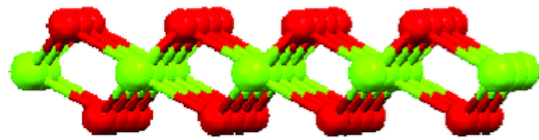
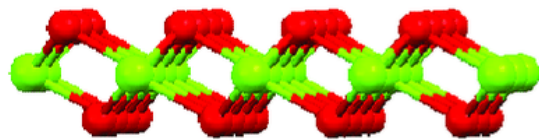
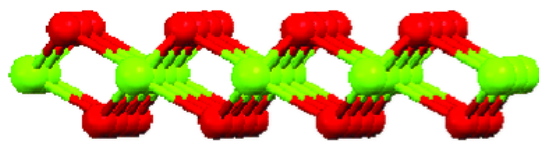
(a) α -zirconium phosphate = $\text{Zr}(\text{HPO}_4)_2 \cdot \text{H}_2\text{O}$
interlayer spacing 7.6 Å

(b) γ -zirconium phosphate = $\text{Zr}(\text{PO}_4)(\text{H}_2\text{PO}_4)2\text{H}_2\text{O}$
interlayer spacing 12.2 Å

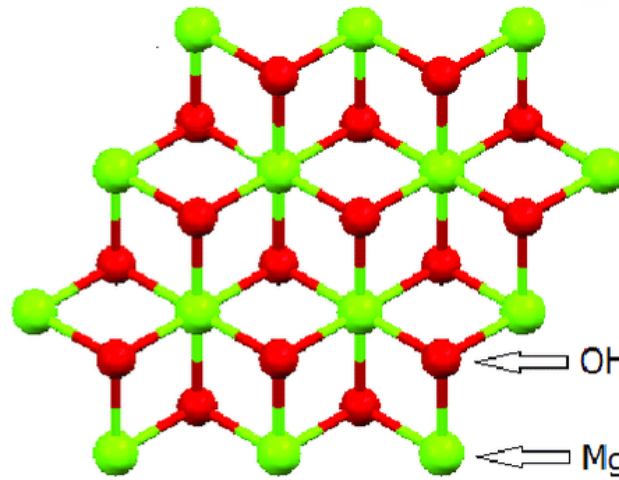
Brucite - $Mg(OH)_2$



CdI_2 hexagonal

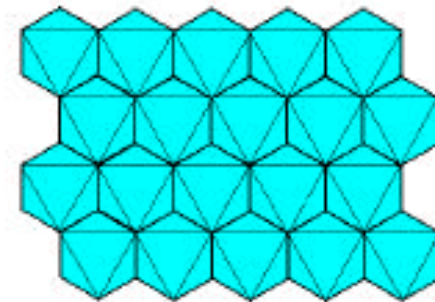


Side view

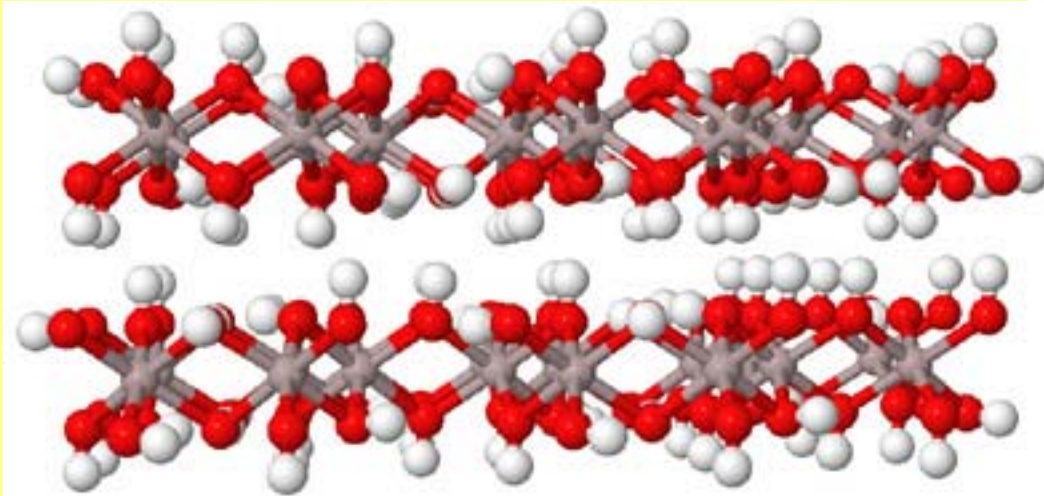
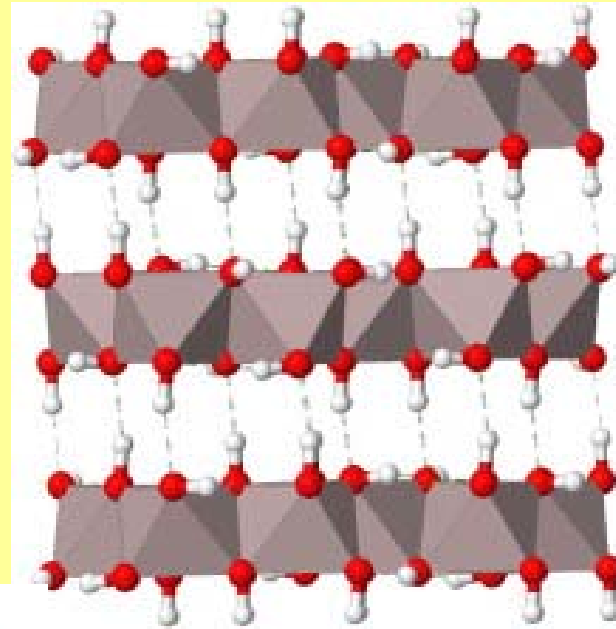
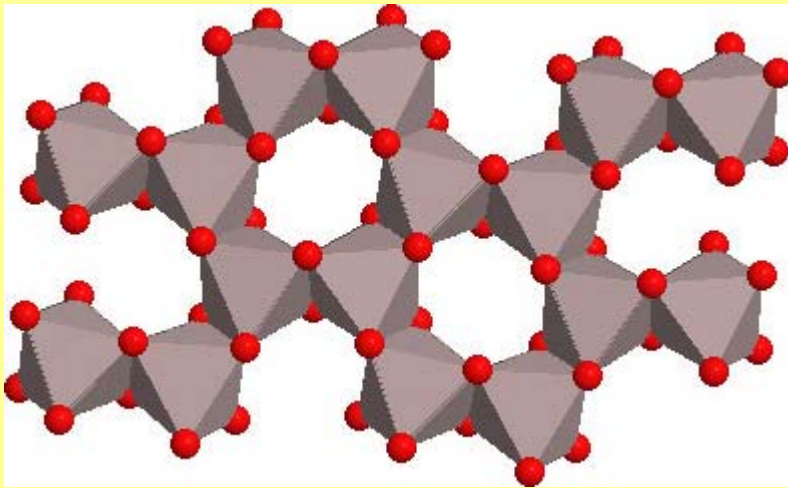


Top view

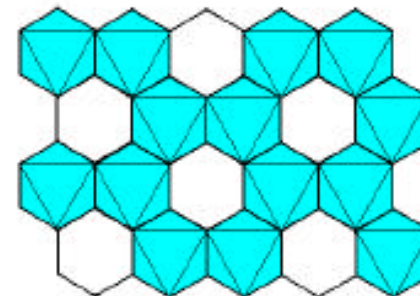
trioctahedral



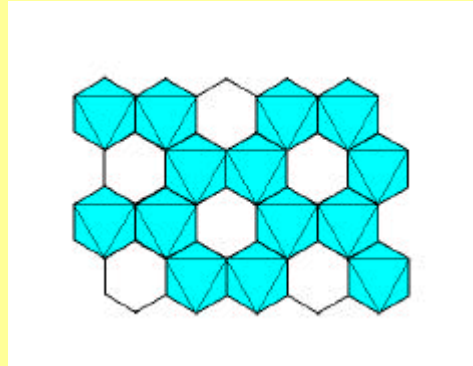
Bayerite and Gibbsite - $\text{Al}(\text{OH})_3$



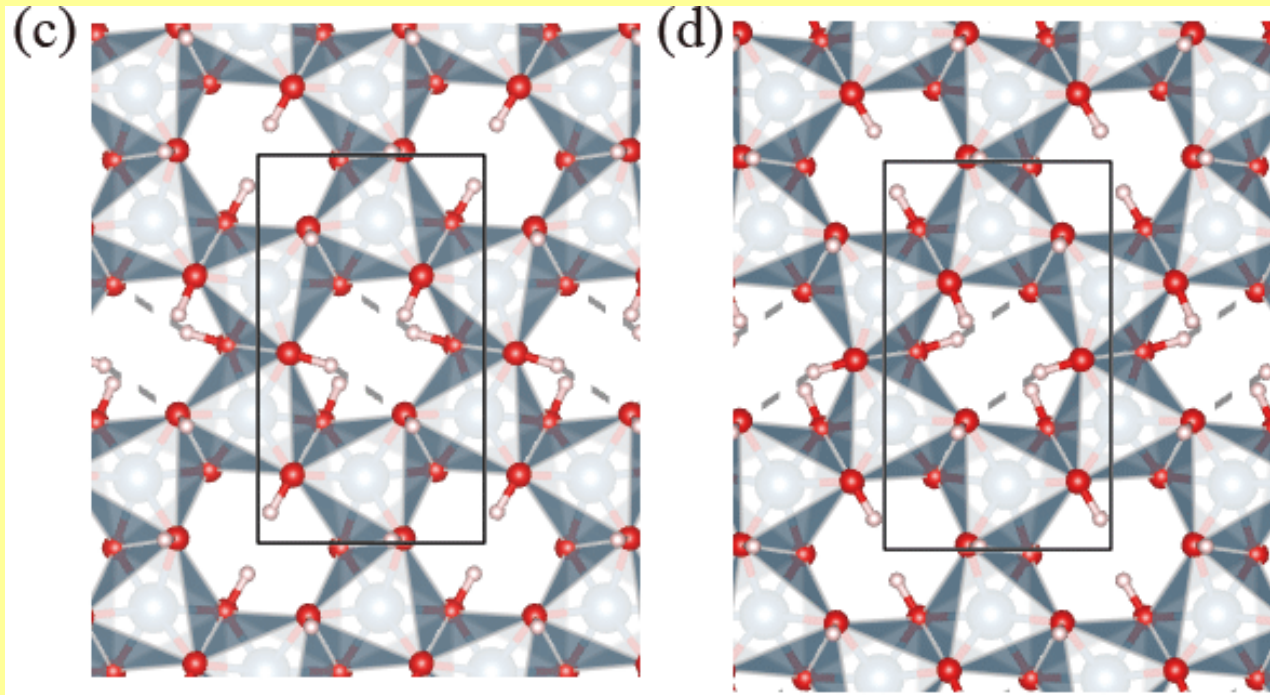
dioctahedral



Bayerite and Gibbsite - $\text{Al}(\text{OH})_3$



Opposite faces of a single layer $\text{Al}(\text{OH})_3$ (A and B sides, respectively)

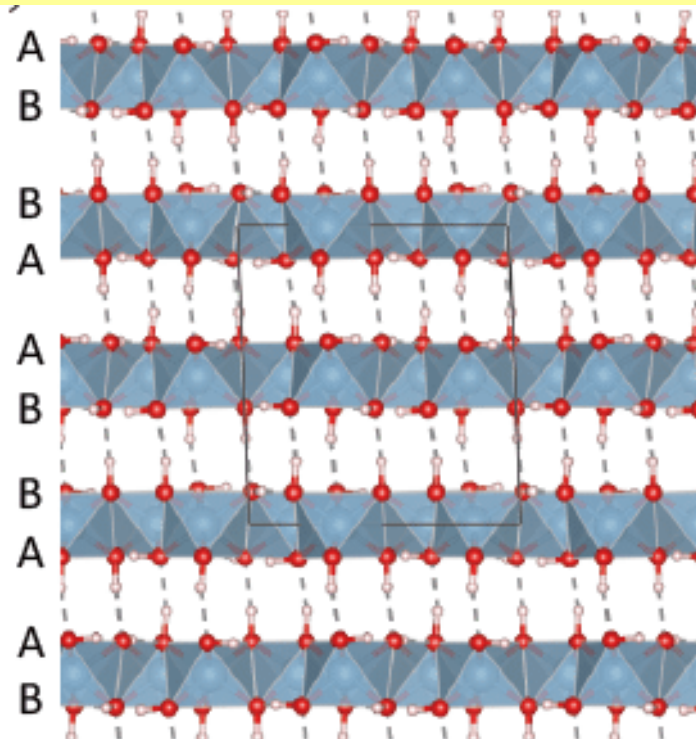
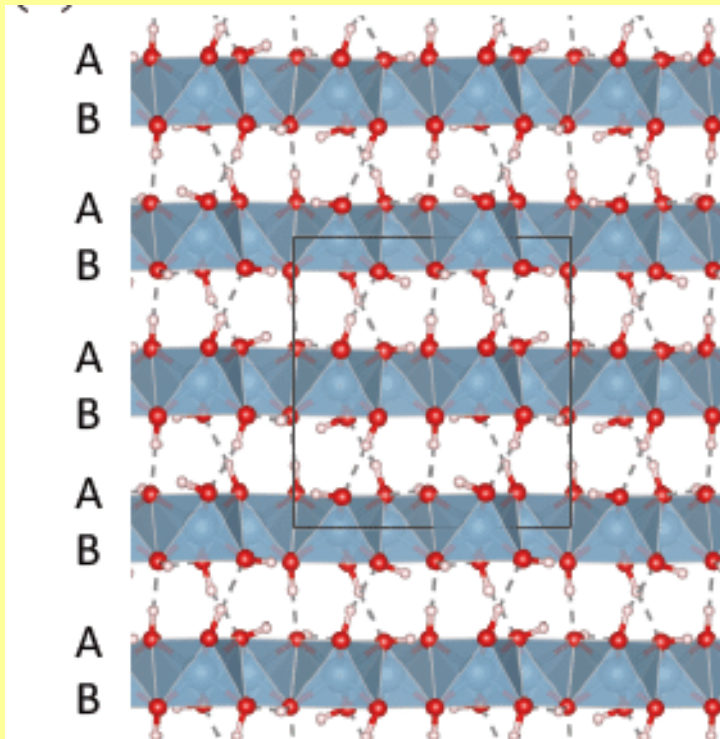


Bayerite and Gibbsite - $\text{Al}(\text{OH})_3$

Bayerite and Gibbsite phases have an identical single layer as the building block

Bayerite is stacked
by AB-AB sequence
HCP of oxides

Gibbsite is stacked
by AB-BA sequence
CCP of oxides

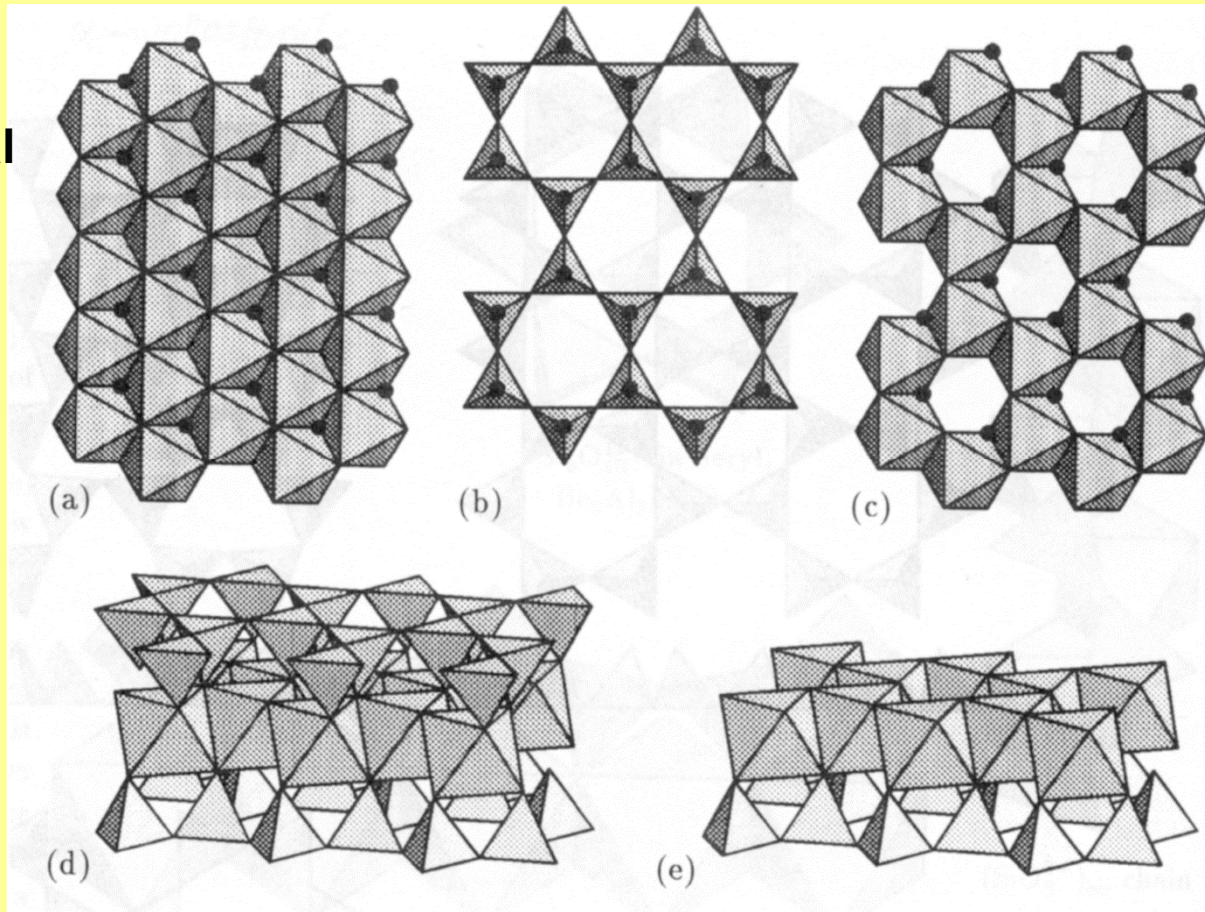


Clay Minerals

$[\text{Si}_4\text{O}_{10}]^{4-}$ tetrahedral sheet

$[\text{Mg}_6\text{O}_{12}]^{12-}$
trioctahedral
sheet of
octahedral
units

$[\text{Al}_4\text{O}_{12}]^{12-}$
dioctahedral
sheet



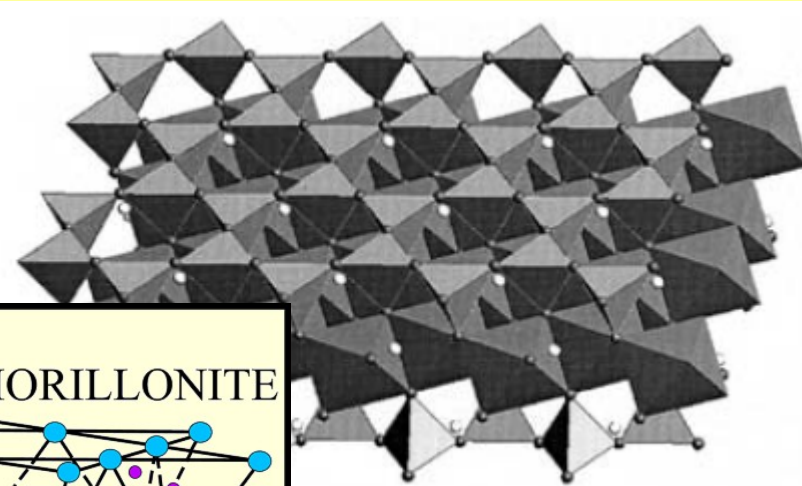
2:1

montmorillonite

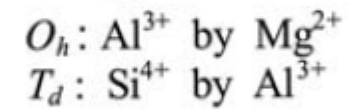
1:1

kaolinite

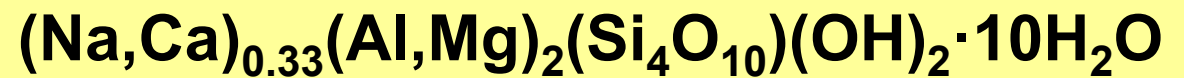
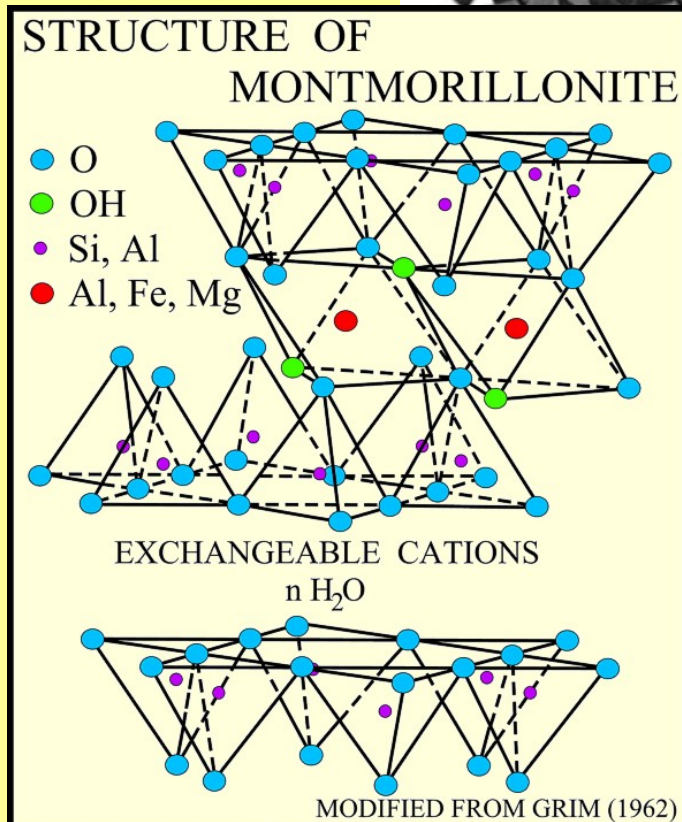
Montmorillonite



- Dioctahedral clay mineral
- $T_d-O_h-T_d$ sandwich
- Isomorphous substitution

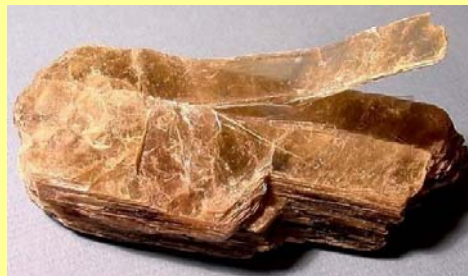


- Net negative charge
- Interlayer cations



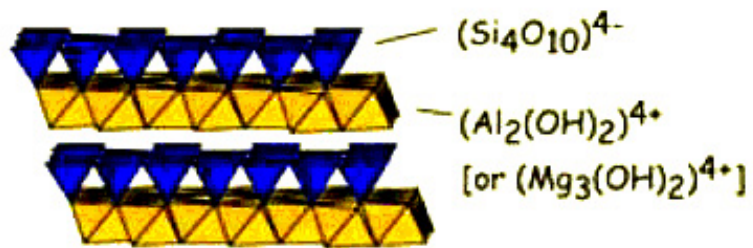
Phyllosilicate Minerals

Structure	Interlayer Charge	Trioctahedral (Y ²⁺)	Diocahedral (Y ³⁺)
O	~0	Brucite	Gibbsite
TO	~0	Serpentine	Kaolinite
TOT	~0	Talc	Pyrophyllite
TOT O TOT	~0	Chlorite	
TOT (X ⁺ , X ²⁺ , H ₂ O) TOT expandable clay	~0.2-0.6	Saponite (smectite)	Montmorillonite (smectite)
	~0.6-0.9	Vermiculite	
TOT (X ⁺ , X ²⁺) TOT non-expandable clay	~0.5-0.75	-	Illite
TOT X ⁺ TOT true mica	1	Phlogopite, Biotite	Muscovite, Paragonite
TOT X ²⁺ TOT brittle mica	2	Clintonite	Margarite

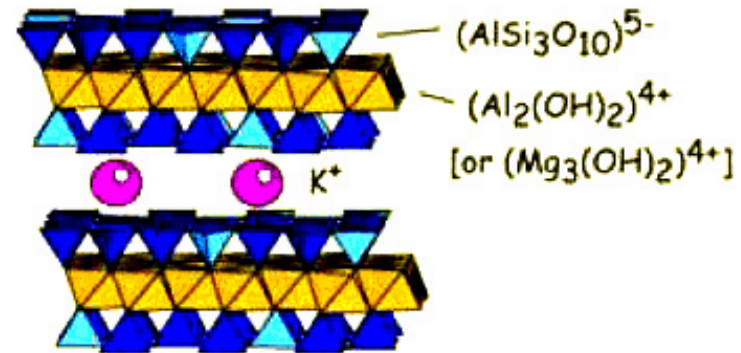


Phyllosilicate Minerals

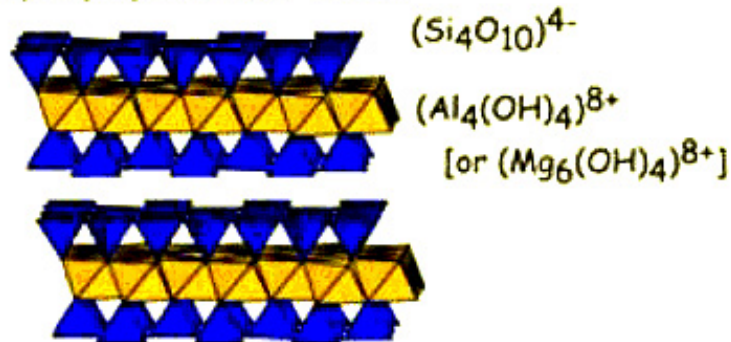
Kaolinite (or Antigorite)



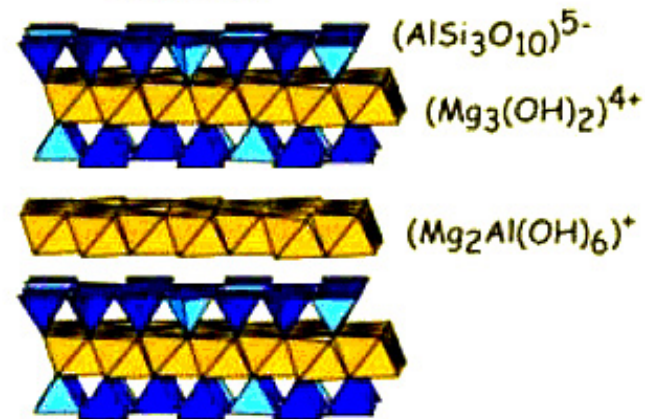
Muscovite (or Phlogopite)



Pyrophyllite (or Talc)



Chlorite



Clay Minerals

N₂ sorption isotherms

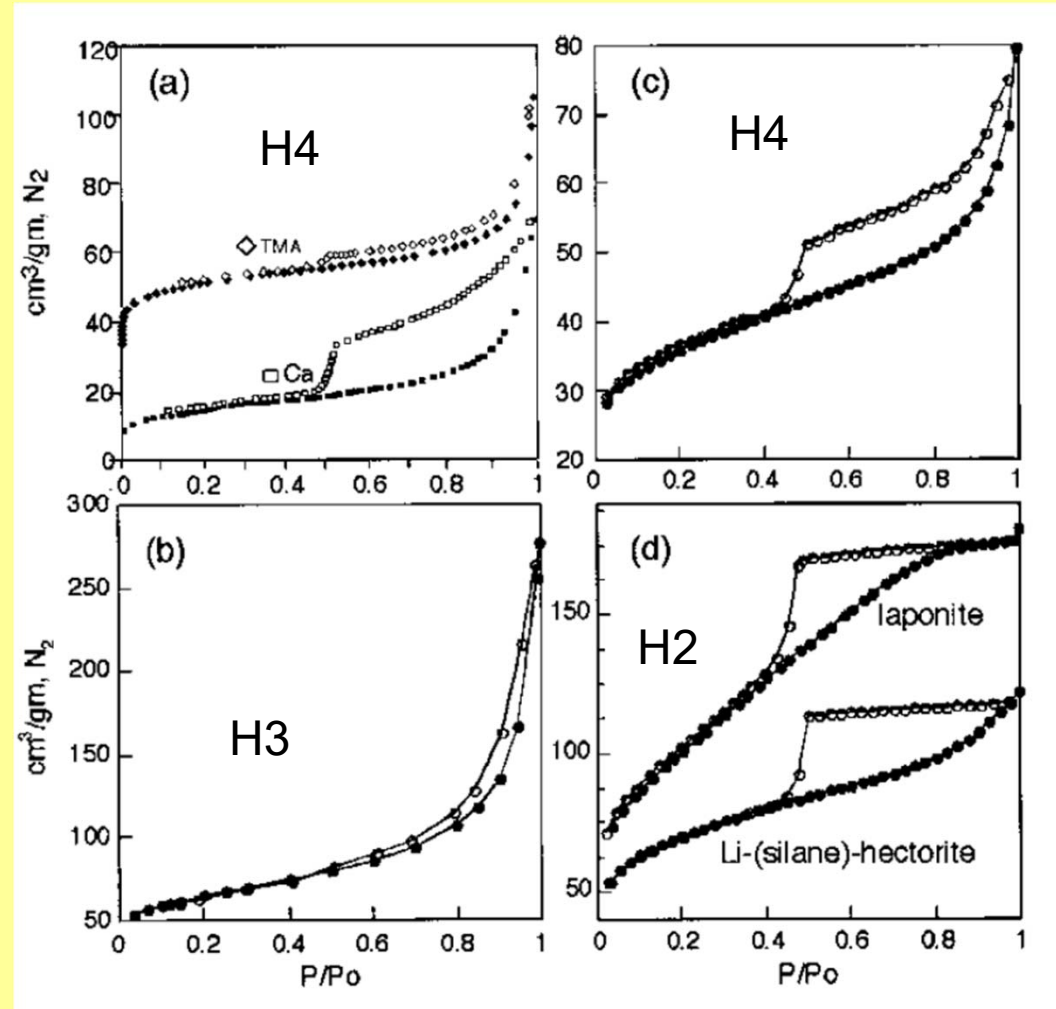
(a) TMA- and Ca-montmorillonite

(b) An Italian sepiolite

(c) Natural SHCa-1 Na-hectorite

(d) synthetic laponite and Li-(silane)-hectorites

Closed symbols = adsorption
Open symbols = desorption



Surface Area

The most important parameters of clays with respect to catalytic applications

TABLE 3 N₂ BET Surface Areas of Various Clay Minerals

Clay	Outgassing conditions	S. A., m ² /g
Kaolinite ^{a,b}	200 °C, overnight, <10 ⁻² torr	8.75
Na,Ca-montmorillonite ^{a,c}	same	31.0
Ca-montmorillonite ^{a,d}	same	80.2
Ca-montmorillonite ^{a,e}	same	93.9
Na-hectorite ^{a,f}	same	64.3
Laponite ^g	105 °C, overnight, 10 ⁻³ torr	360
Sepiolite ^h	96 °C, 3 h	378
Palygorskite ^h	95 °C, <70 h	192

nonpolar guest molecules N₂ do not penetrate the interlayer regions

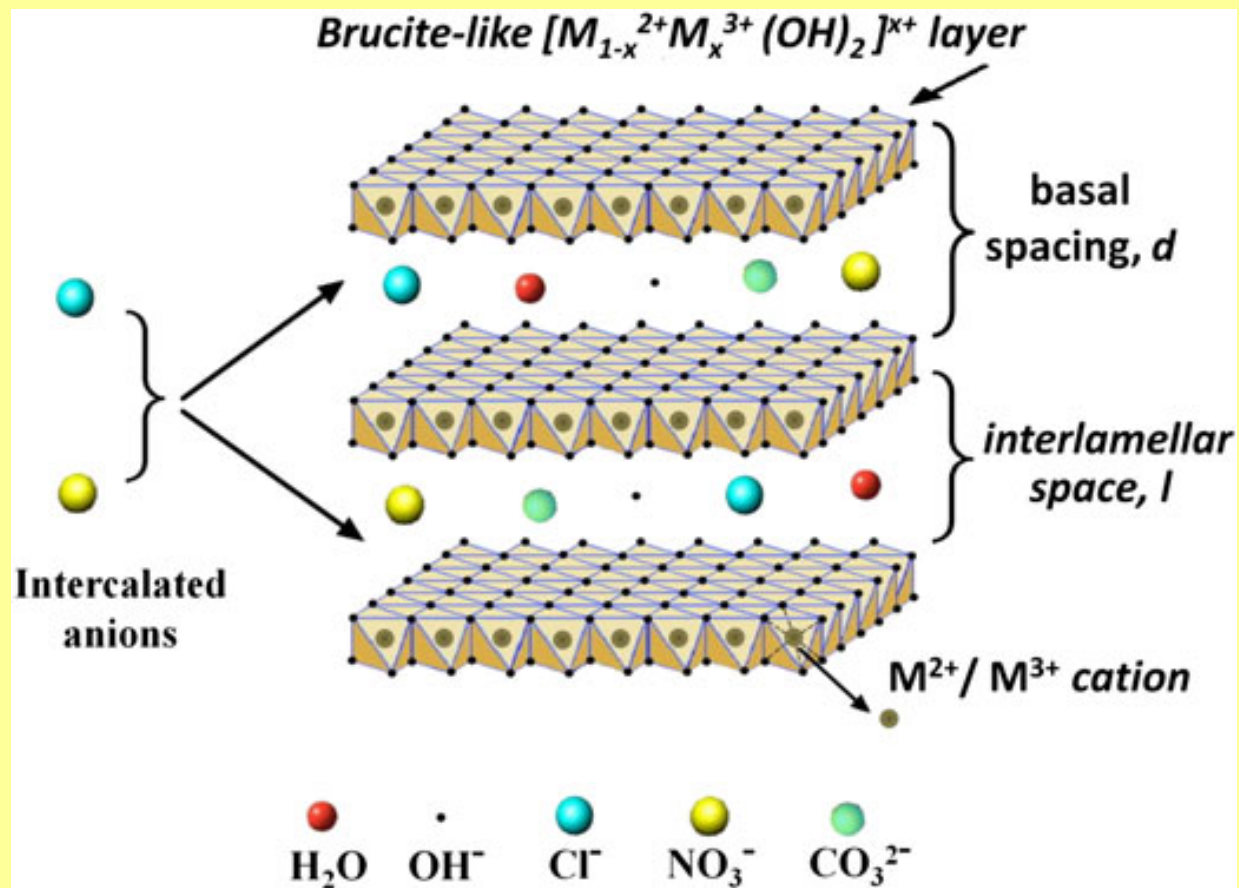
Na⁺ forms of smectites and vermiculites – no penetration

larger ions (Cs⁺ and NH₄⁺ keep the basal planes far enough) - limited penetration

Layered Double Hydroxides

LDH = layered double hydroxides

HT = hydrotalcites



Layered Double Hydroxides

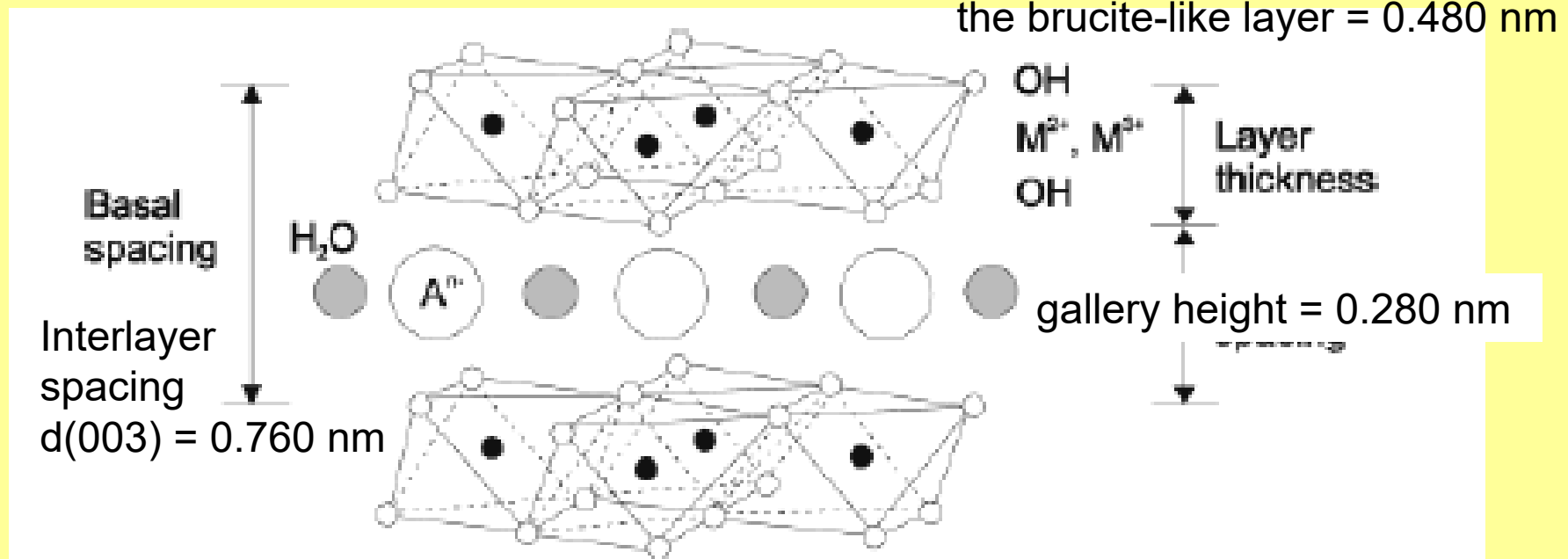
LDH = layered double hydroxides

HT = hydrotalcites

Natural mineral hydrotalcite $\text{Mg}_6\text{Al}_2(\text{OH})_{16}\text{CO}_3 \cdot 4\text{H}_2\text{O}$

Brucite layers, Mg^{2+} substituted partially by Al^{3+}

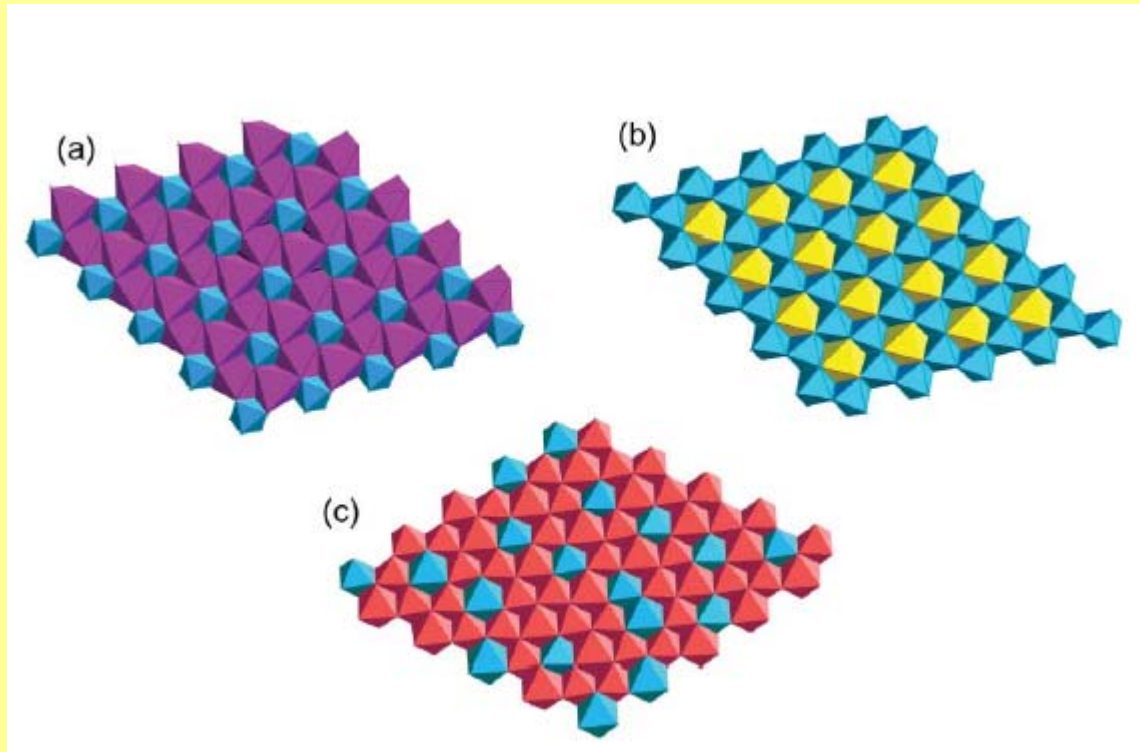
Layers have positive charge



Hydrotalcite $\text{Mg}_6\text{Al}_2(\text{OH})_{16}\text{CO}_3 \cdot 4\text{H}_2\text{O}$

Hydrotalcites

Brucite layers, Mg^{2+} substituted partially by Al^{3+}
Layers have positive charge



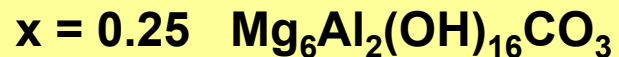
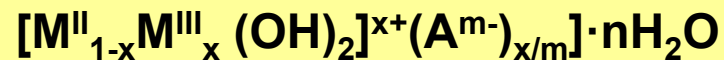
(a) $[\text{Ca}_2\text{Al}(\text{OH})_6]_2\text{SO}_4 \cdot 6\text{H}_2\text{O}$ (b) $[\text{LiAl}_2(\text{OH})_6]\text{Cl}$ (c) $[\text{Mg}_{2.25}\text{Al}_{0.75}(\text{OH})_6]\text{OH}$

Hydrotalcite

The layered structure of LDH is closely related to brucite $\text{Mg}(\text{OH})_2$

a brucite layer, Mg^{2+} ions octahedrally surrounded by six OH^-
the octahedra share edges and form an infinite two-dimensional layer
the brucite-like layers stack on top of one another
either rhombohedral (3R) or hexagonal (2H) sequence

Hydrotalcite $\text{Mg}_6\text{Al}_2(\text{OH})_{16}\text{CO}_3 \cdot 4\text{H}_2\text{O}$ - 3R stacking



Hydrotalcite

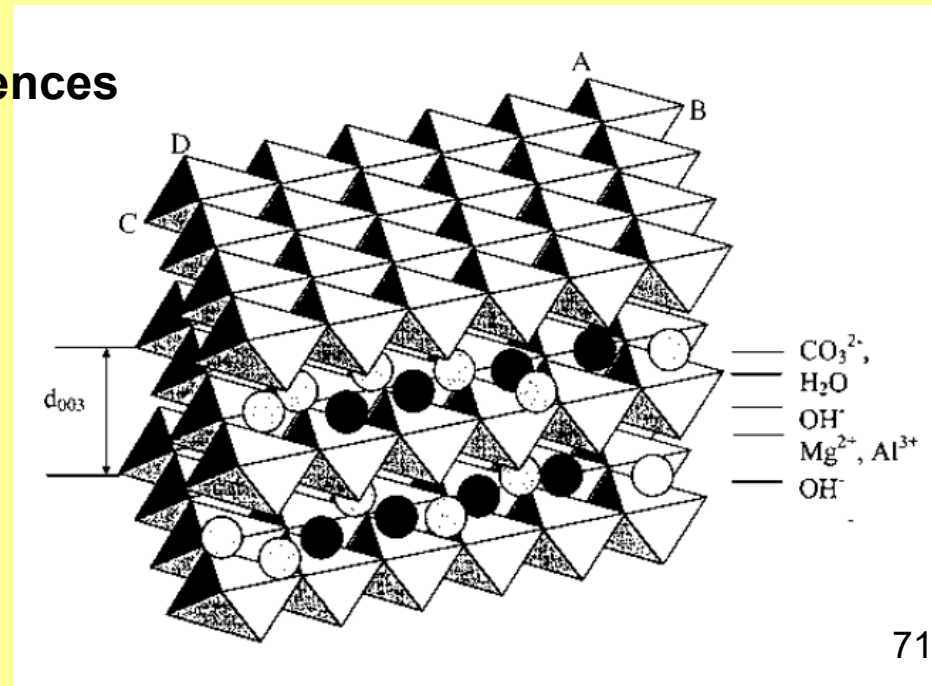
The interlayer spacing c' is equal to d_{003} , $2d_{006}$, $3d_{009}$, etc.;

$$c' = (d_{003} + 2d_{006} + \dots + nd_{00(3n)}) / n$$

The cell parameter c is a multiple of the interlayer spacing c'

$c = 3c'$ for rhombohedral (3R)

$c = 2c'$ for hexagonal (2H) sequences



Hydrotalcite

Hydrotalcite $\text{Mg}_6\text{Al}_2(\text{OH})_{16}\text{CO}_3 \cdot 4\text{H}_2\text{O}$ - 3R stacking

unit cell parameters

$$a = 0.305 \text{ nm} \quad c = 3d(003) = 2.281 \text{ nm}$$

the interlayer spacing: $d(003) = 0.760 \text{ nm}$

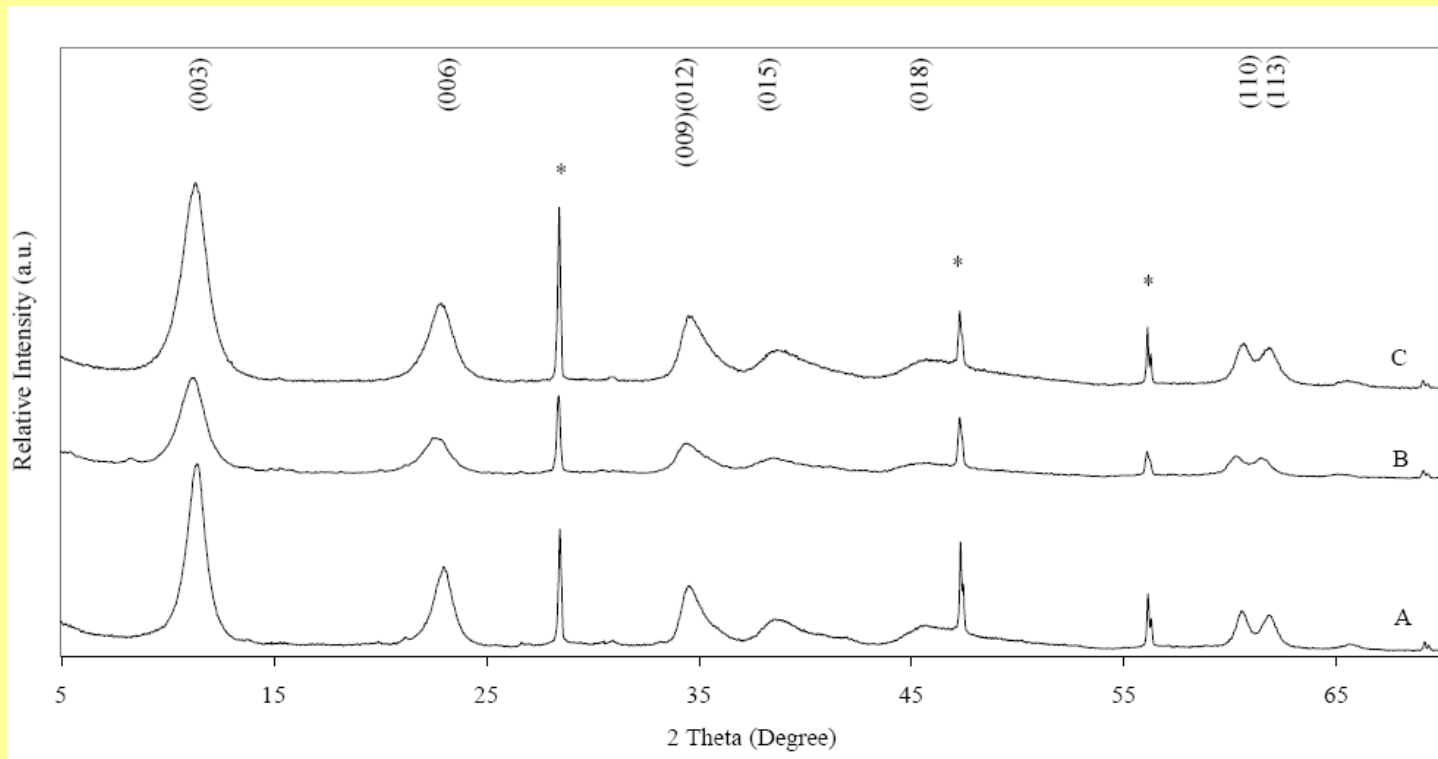
the spacing occupied by the anion (gallery height) = 0.280 nm

a thickness of the brucite-like layer = 0.480 nm

the average M—O bond = 0.203 nm

the distance between two nearest OH^- ions in the two opposite side layers = 0.267 nm shorter than a (0.305 nm) and indicative of some contraction along the c -axis

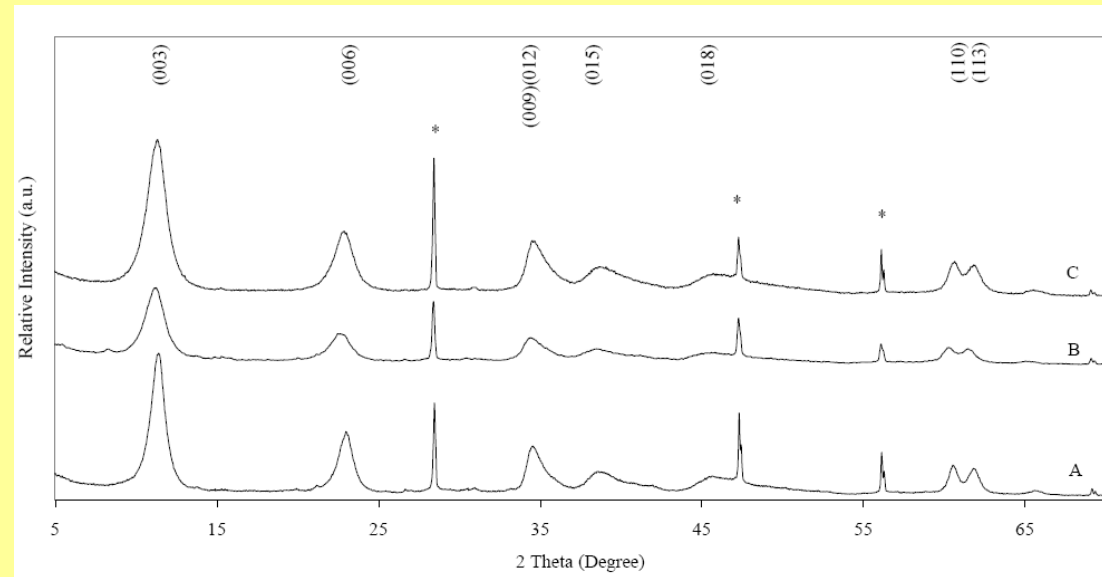
XRD Patterns of LDH



**XRD patterns of layered double hydroxides synthesized by coprecipitation method with various cations composition:
A – Mg/Al; B- Mg/Co/Al; C- Mg/Ni/Al**

*** = Reflections from Si crystal used as a reference**

XRD Patterns of LDH



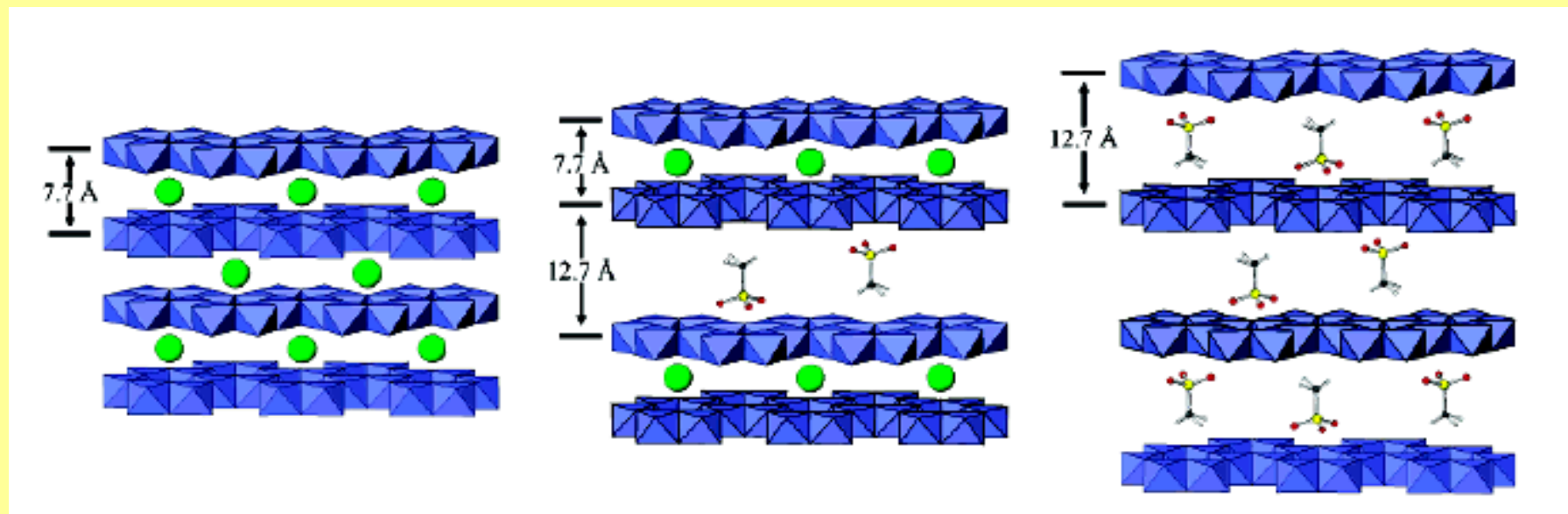
rhombohedral structure
the cell parameters c and a

The lattice parameter $a = 2d(110)$ corresponds to an average cation-cation distance

The c parameter corresponds to three times the thickness of d_{003}

$$c = 3/2 [d_{003} + 2d_{006}]$$

Intercalation to LDH



The intercalation of methylphosphonic acid into Li/Al LDH

(a) $[\text{LiAl}_2(\text{OH})_6]\text{Cl}\cdot\text{H}_2\text{O}$

(b) second-stage intermediate, alternate layers occupied by Cl and MPA anions

(c) first-stage product with all interlayer regions occupied by MPA

Intercalation to LDH

LDH = layered double hydroxides

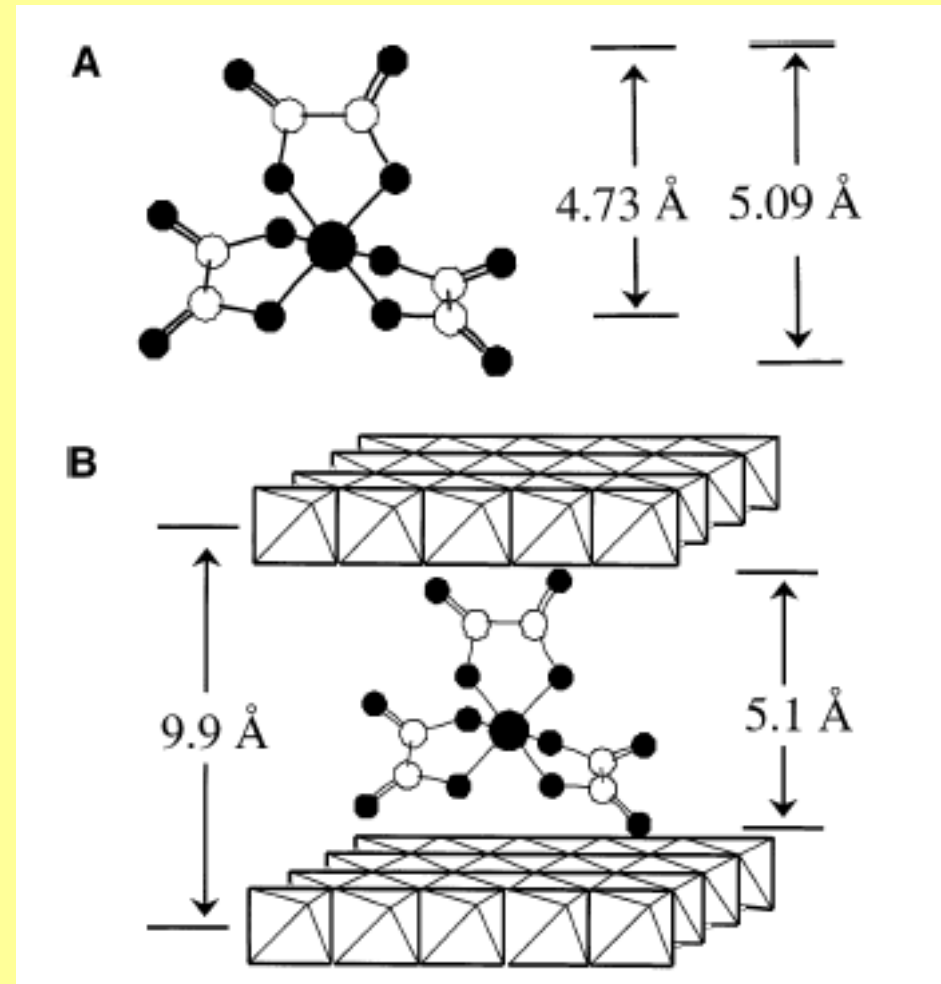
hydrotalcites

mineral $\text{Mg}_6\text{Al}_2(\text{OH})_{16}\text{CO}_3 \cdot 4\text{H}_2\text{O}$

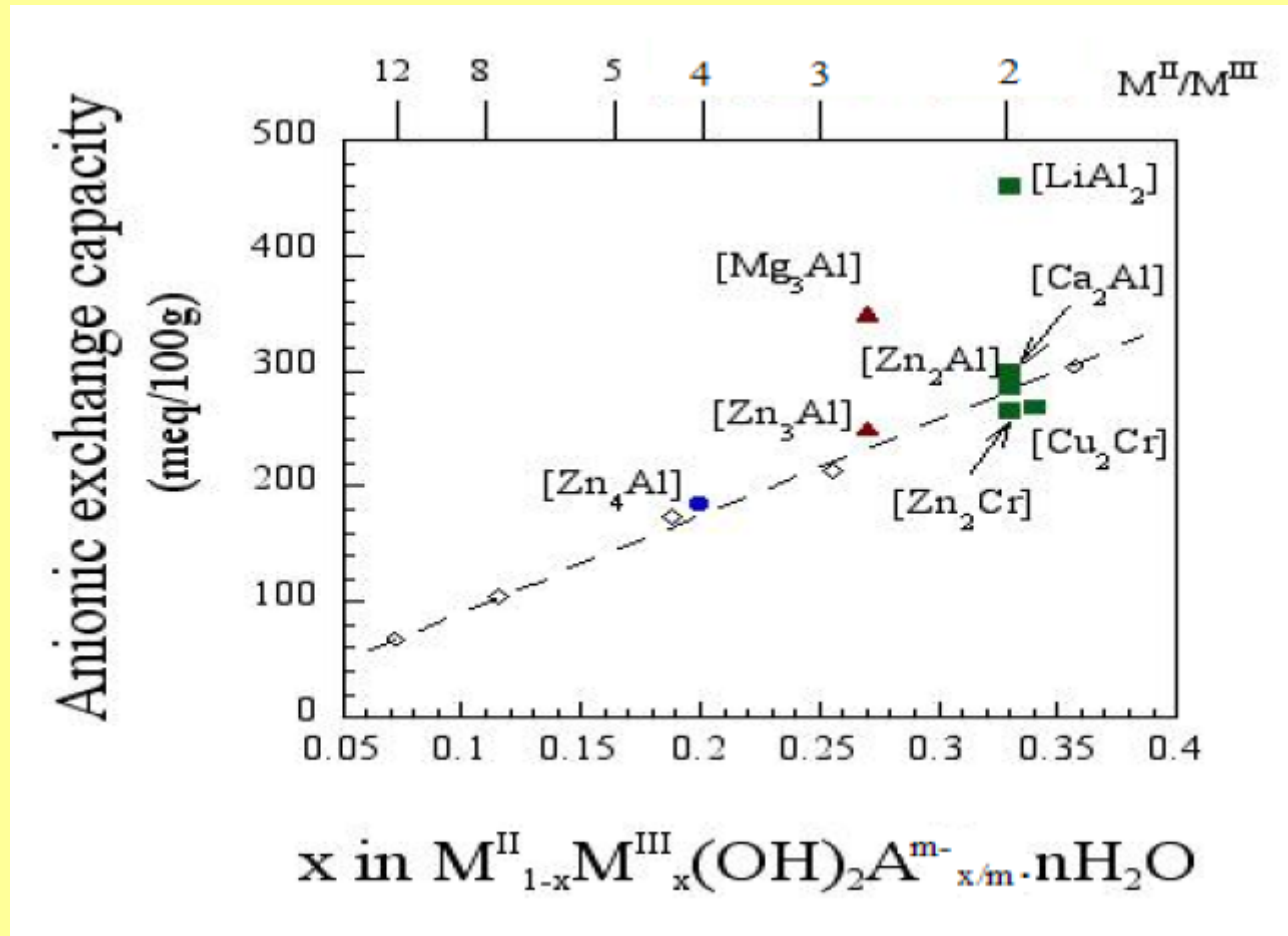
Brucite layers, Mg^{2+} substituted partially by Al^{3+}

Layers have positive charge

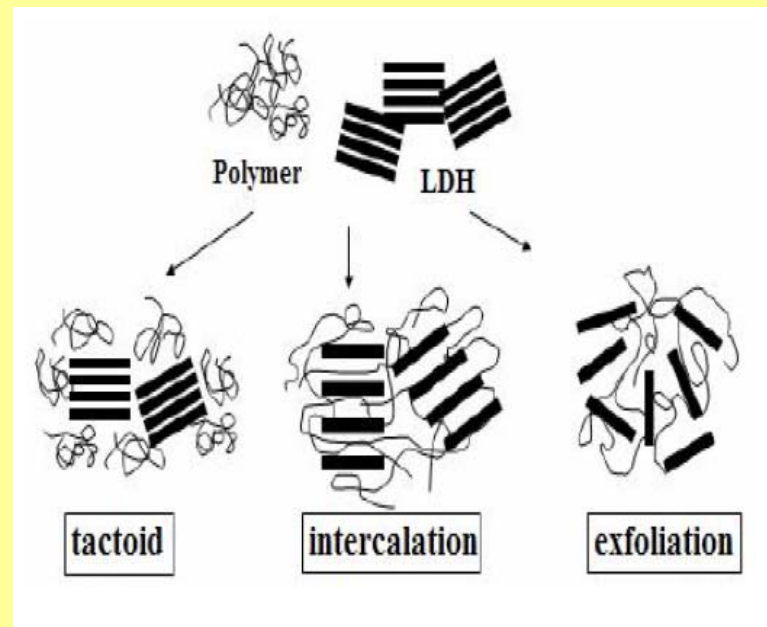
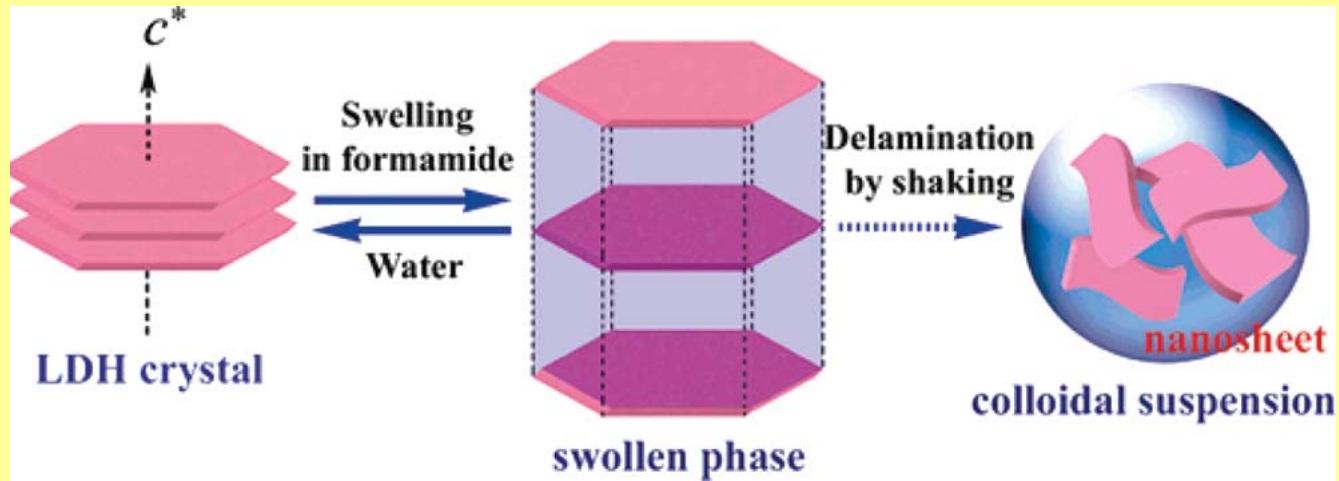
Intercalate anions $[\text{Cr}(\text{C}_2\text{O}_4)_3]^{3-}$



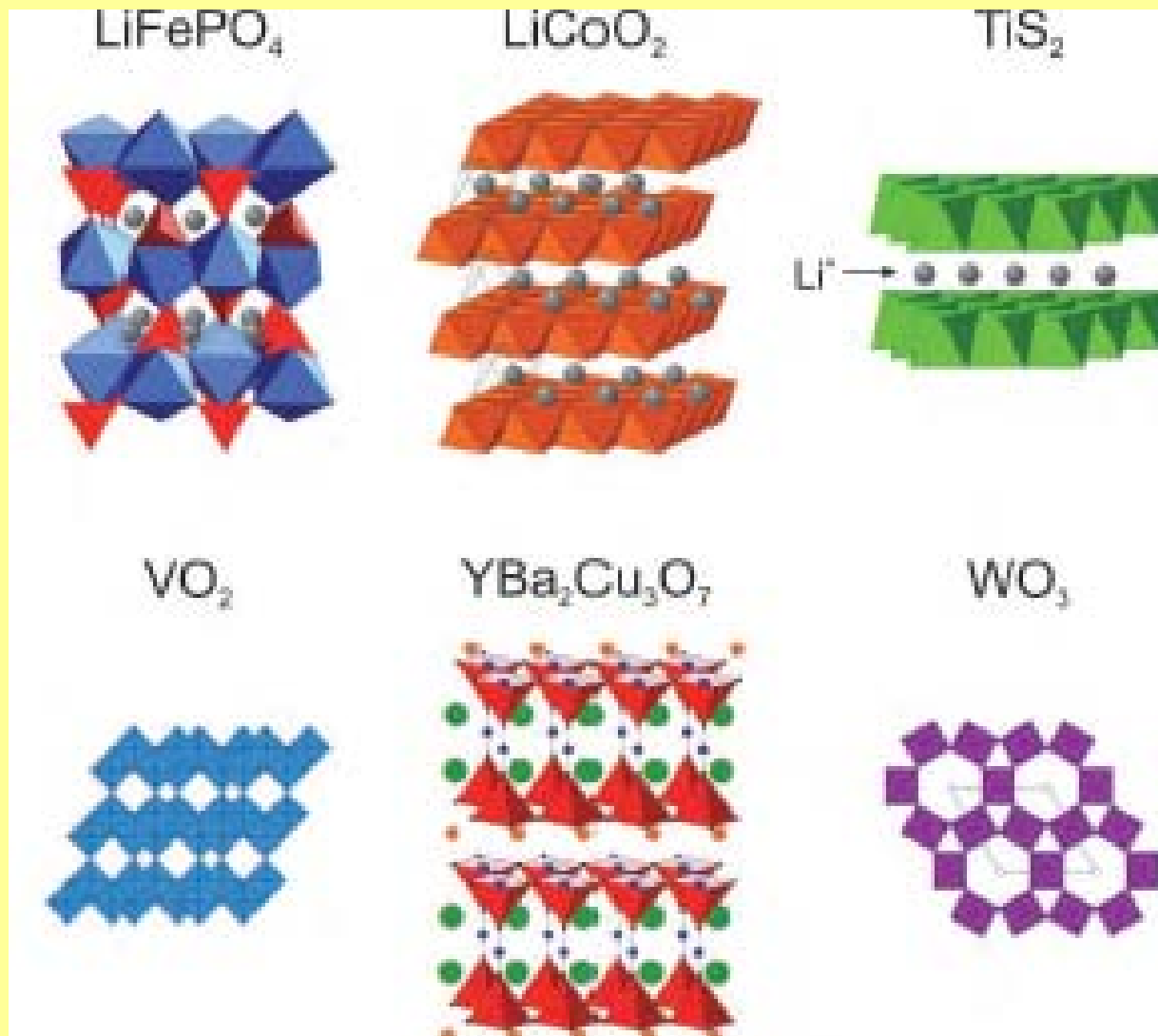
The Anionic Exchange Capacity (AEC)



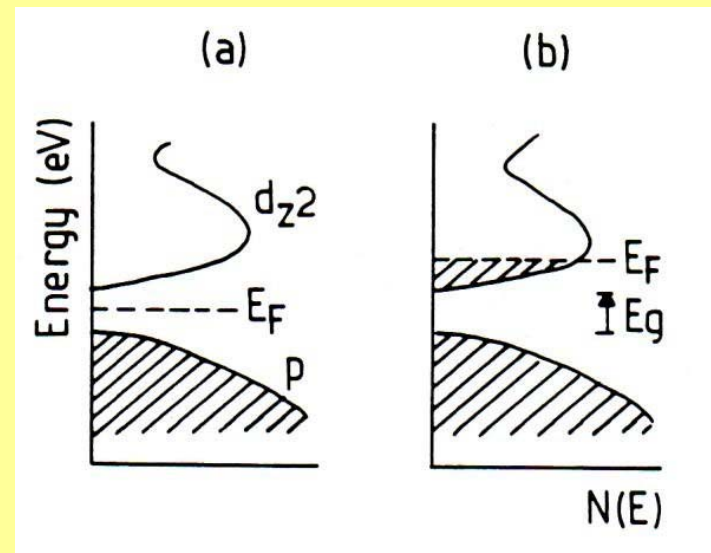
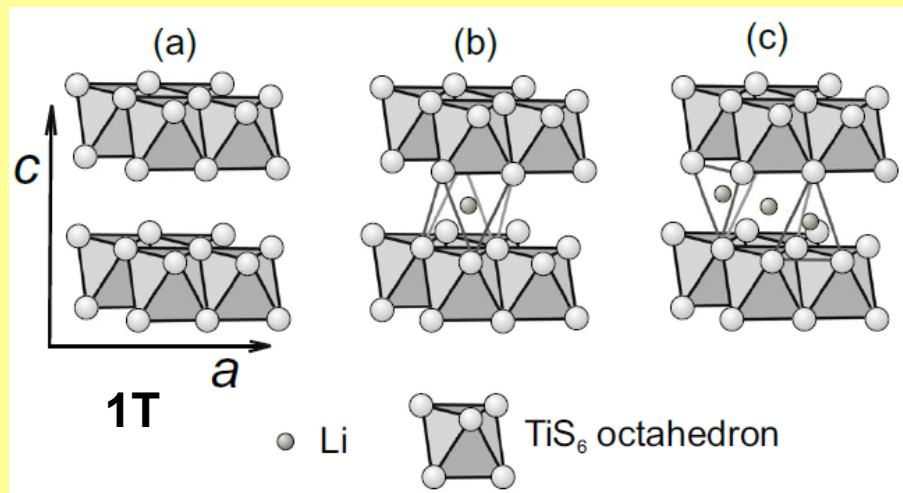
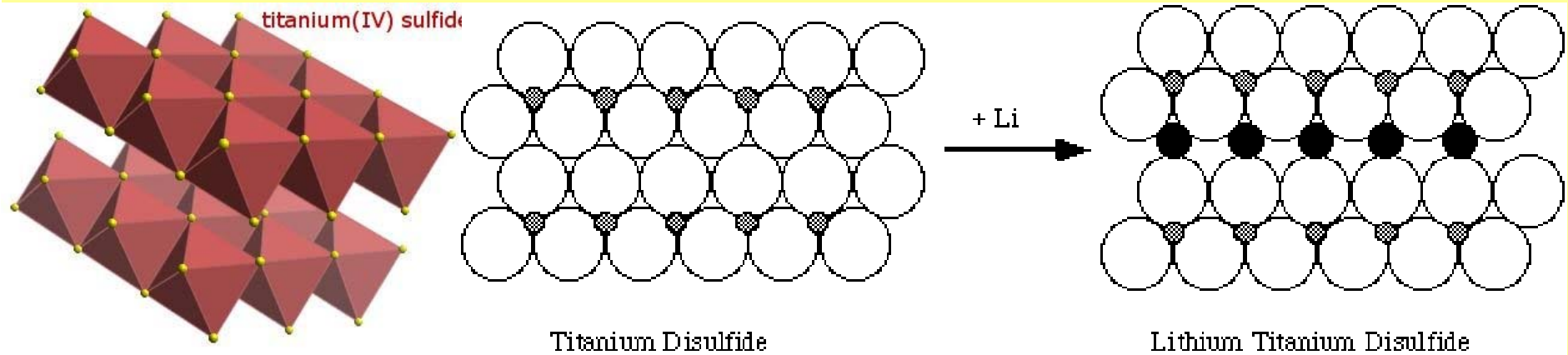
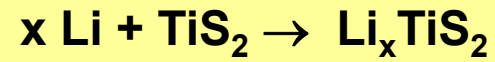
LDH Composite Structures



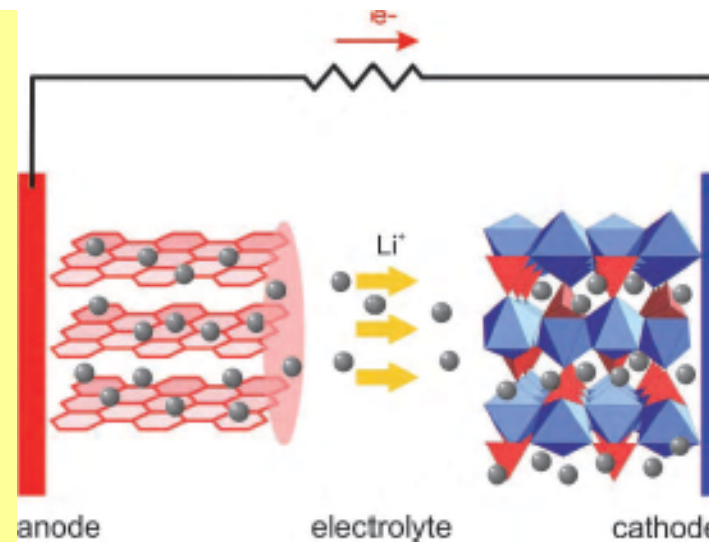
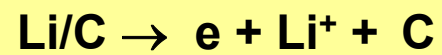
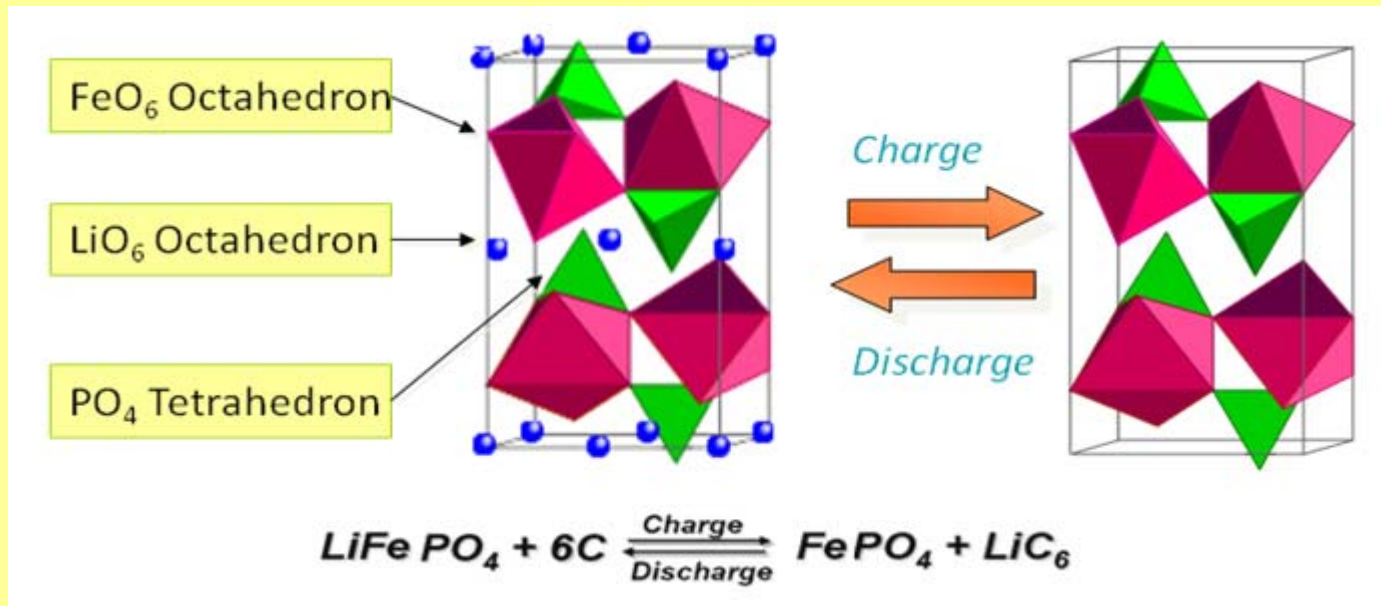
Li Intercalation Compounds



Li Intercalation



Li Intercalation

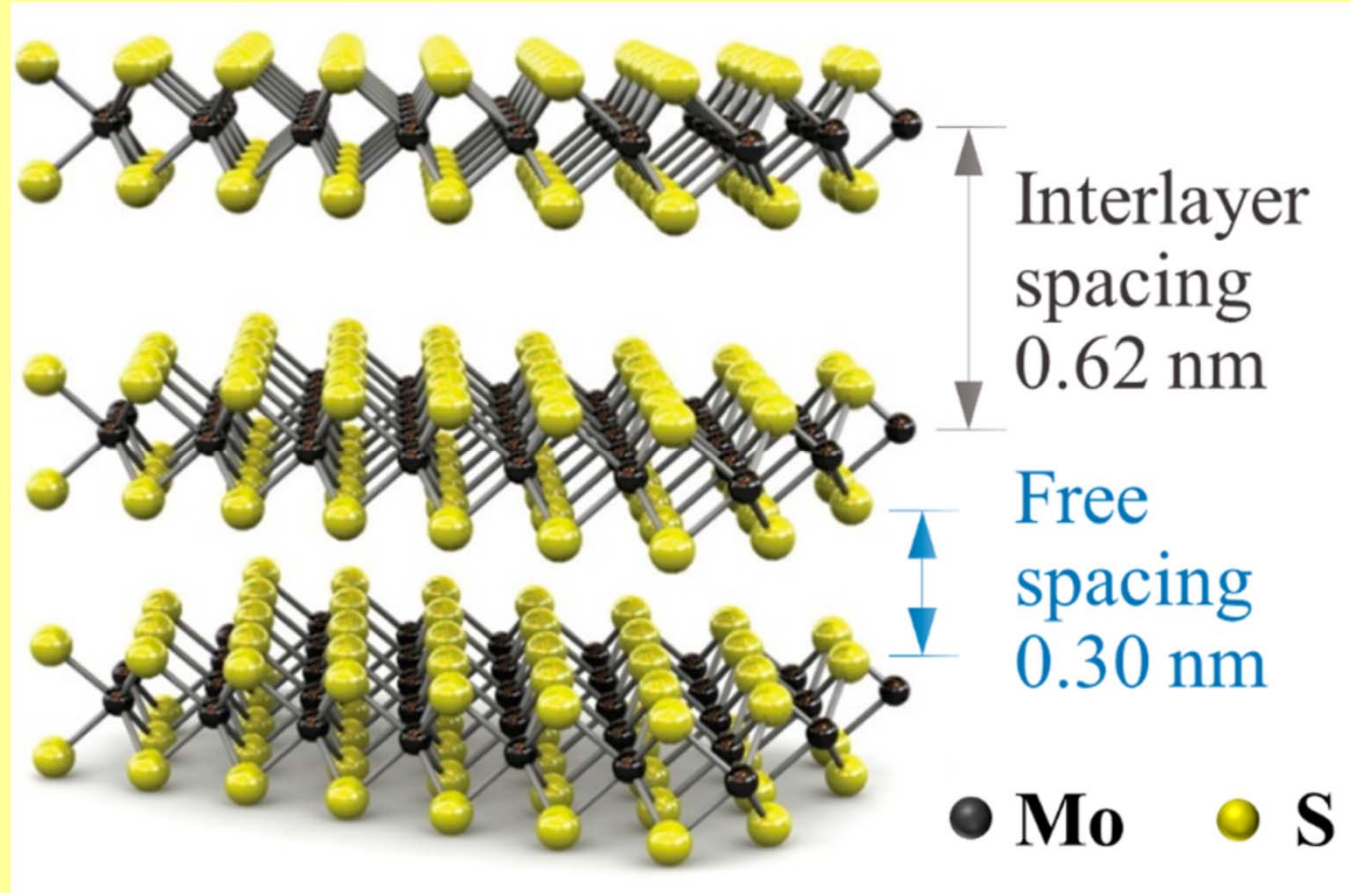


Molybdenum Disulfide (MoS_2)

Mineral molybdenite

Hydrodesulfurization catalyst (at edges)

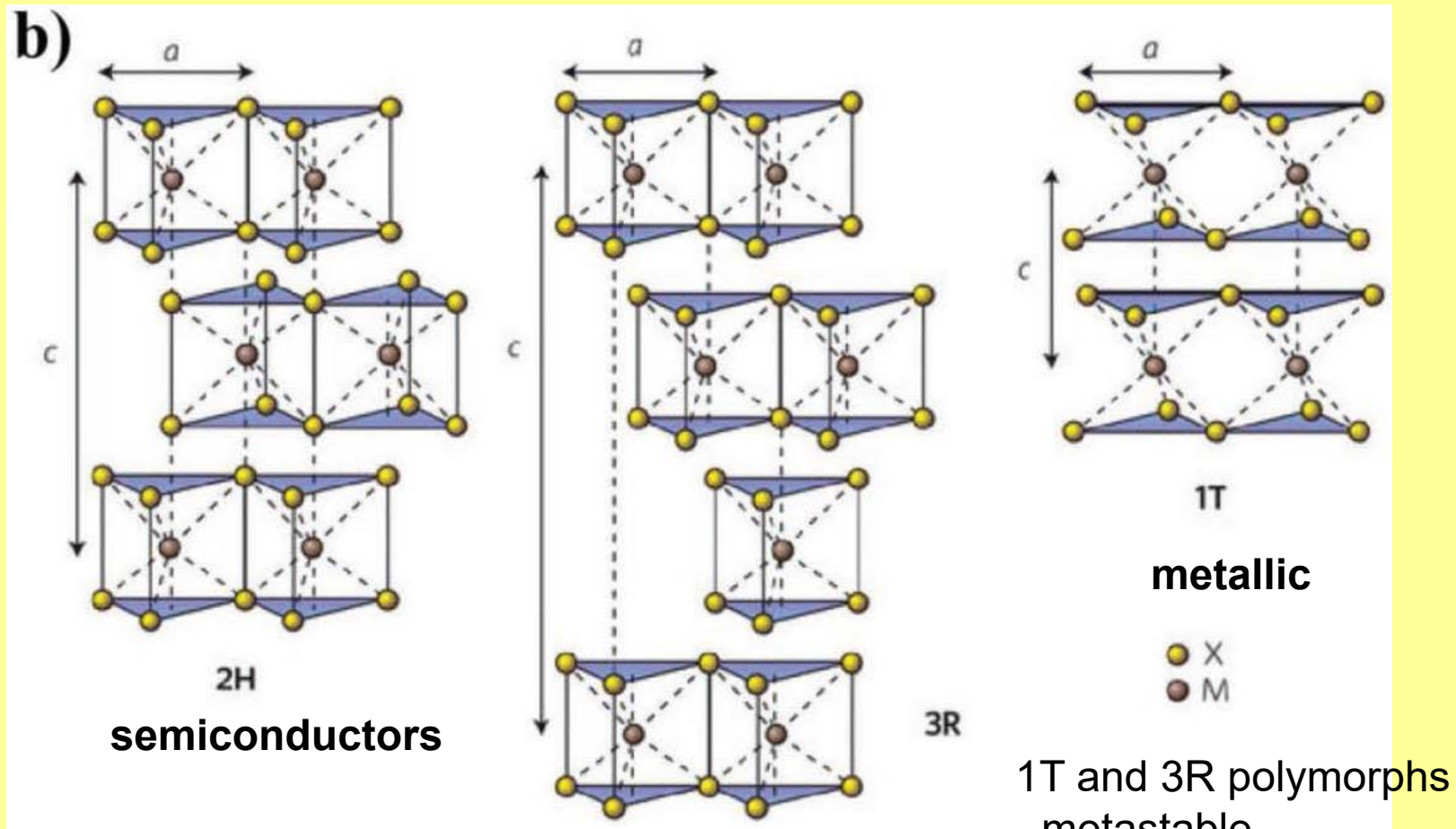
Lubricant



Polymorphs of MoS₂

MoO₆ trigonal prismatic

MoO₆ octahedral

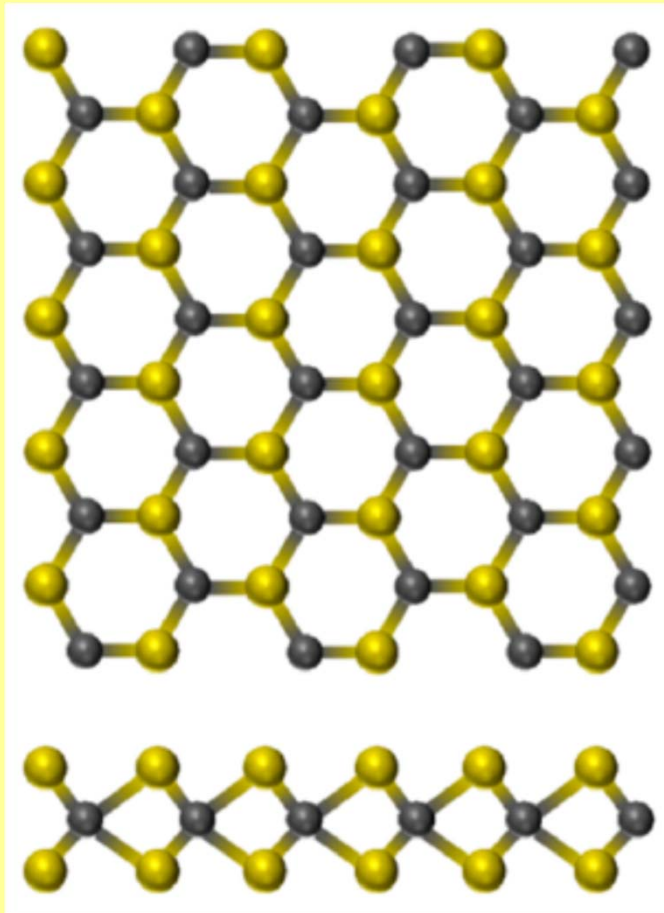


2H phase - thermodynamically stable

Polymorphs of MoS₂

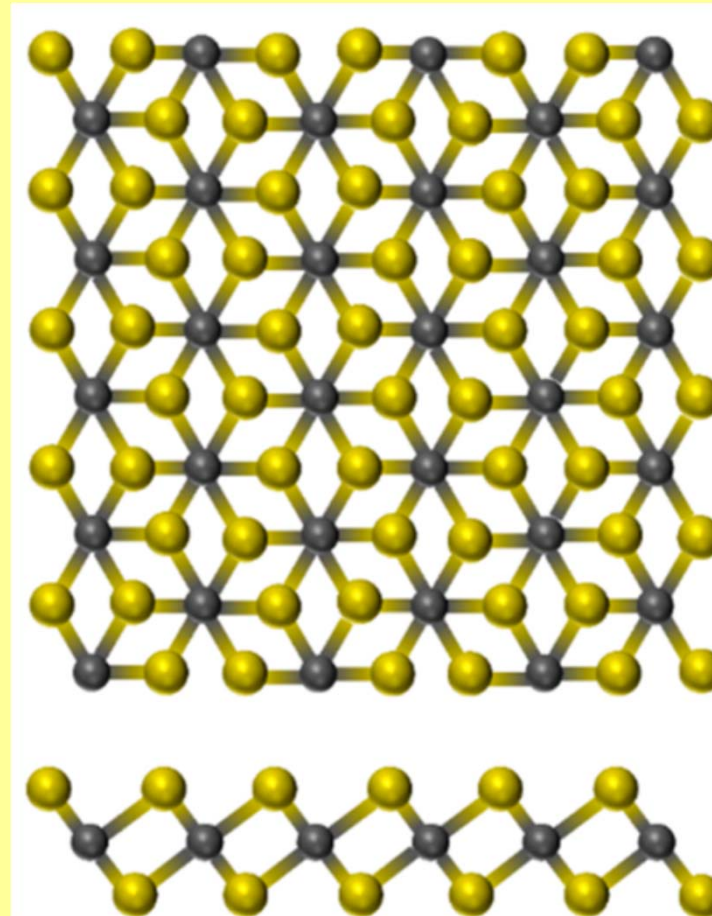
2H - MoO₆ trigonal prismatic

semiconductors



1T - MoO₆ octahedral

metallic



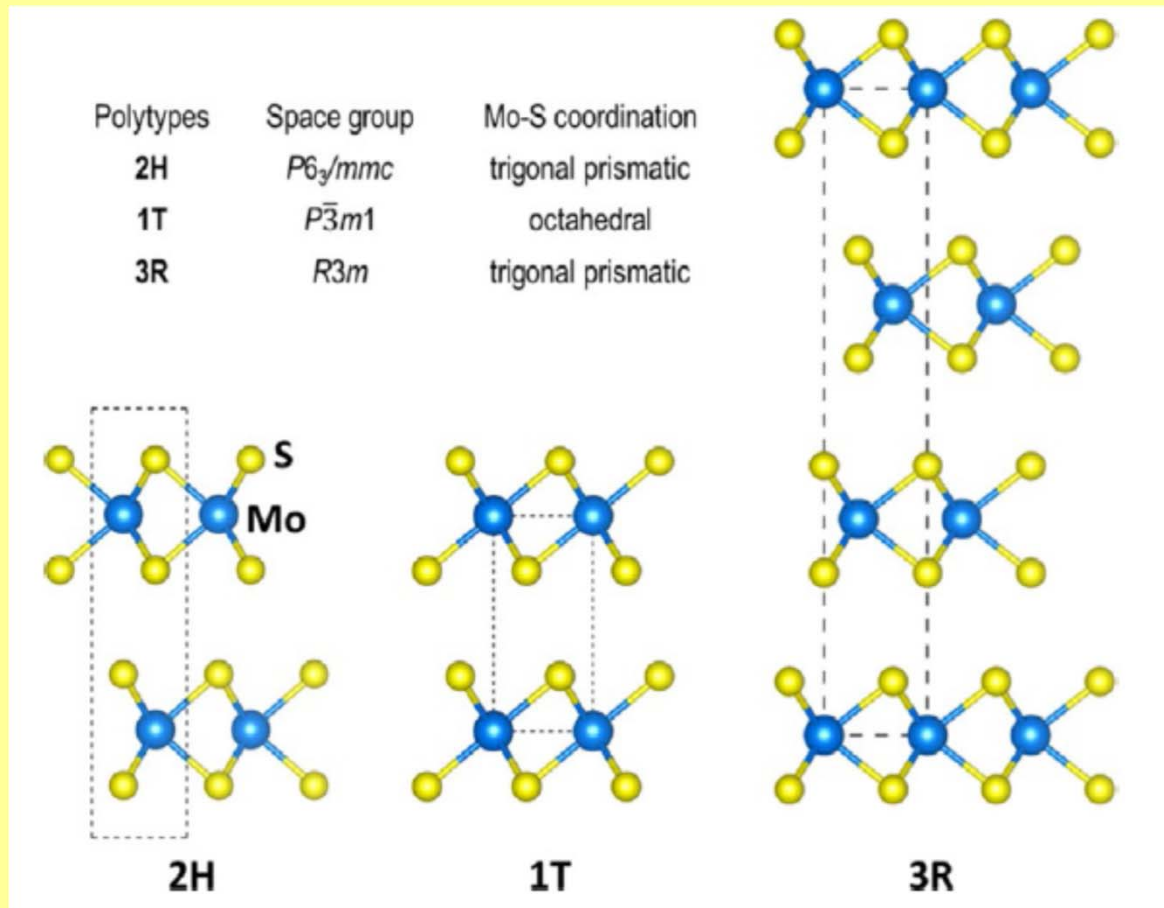
Li intercalation (2H to 1T), annealing (1T to 2H)

Polymorphs of MoS₂

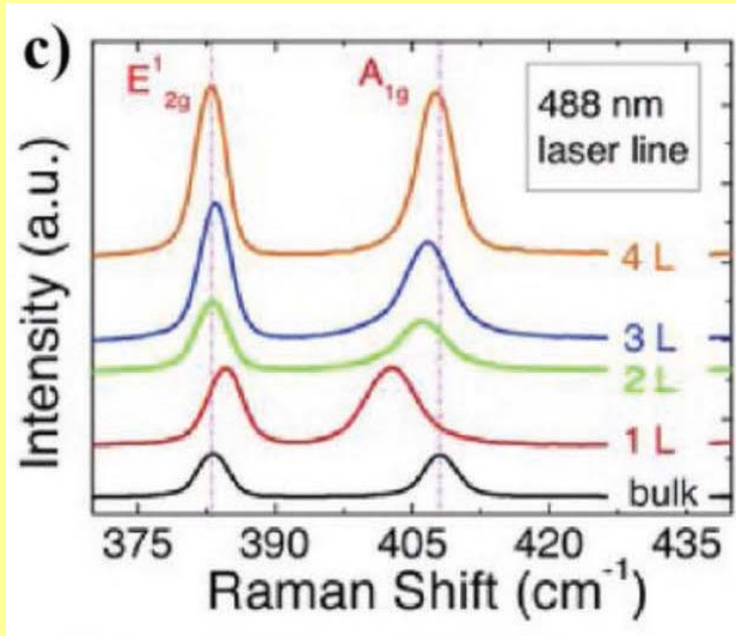
2H, 3R - MoO₆ trigonal prismatic

1T - MoO₆ octahedral

Digit = number of monolayers in the unit cell
 the letters T = trigonal, H = hexagonal, R = rhombohedral

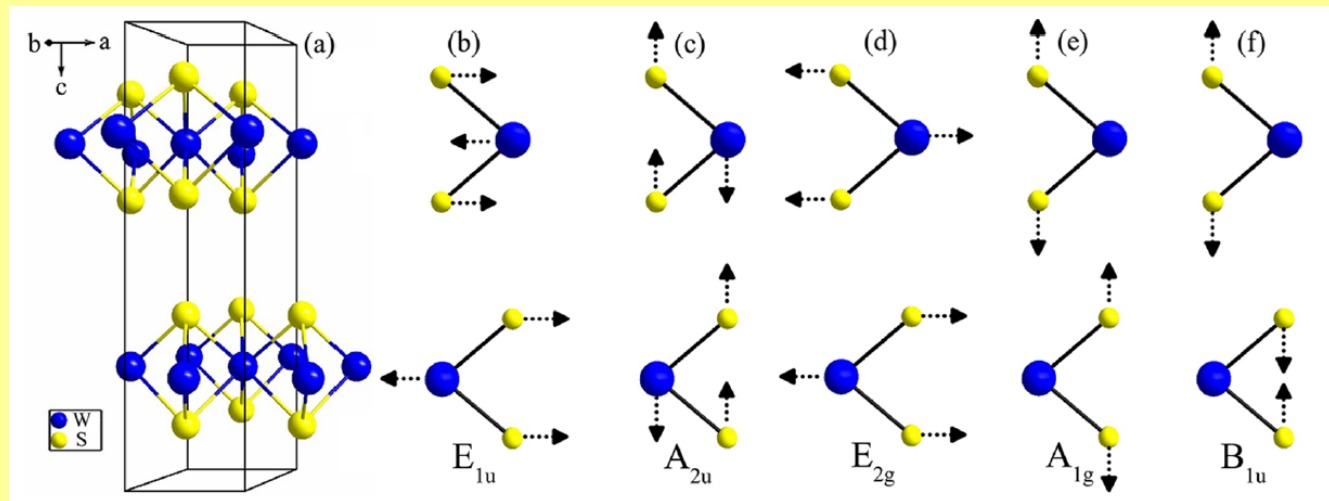


Molybdenum Disulfide (MoS₂)

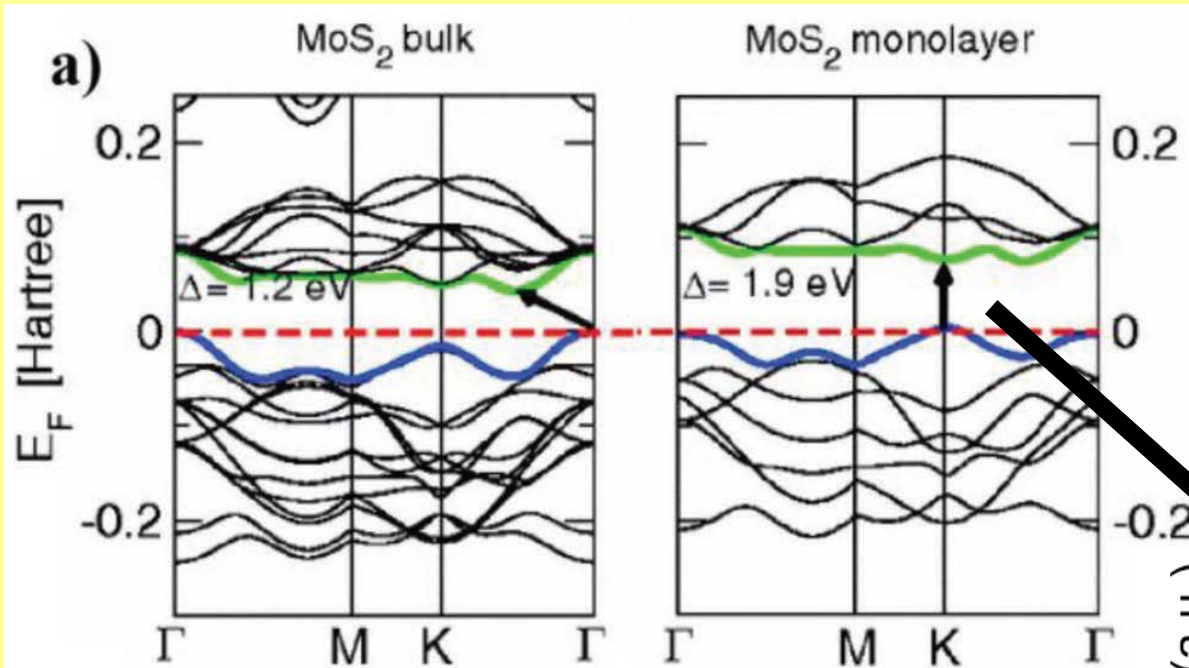


Frequency of A_{1g} band is increasing while that of E_{2g}¹ is decreasing with increase in number of layers

(b,c) infrared and (d-f) Raman-active



Molybdenum Disulfide (MoS₂)



An indirect band gap
1.29 eV

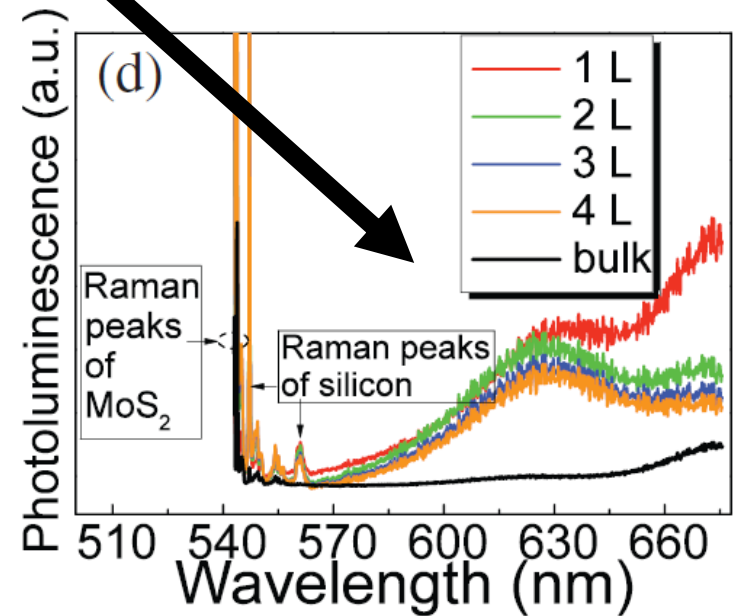
A direct band gap
1.9 eV (2H)

Conduction band

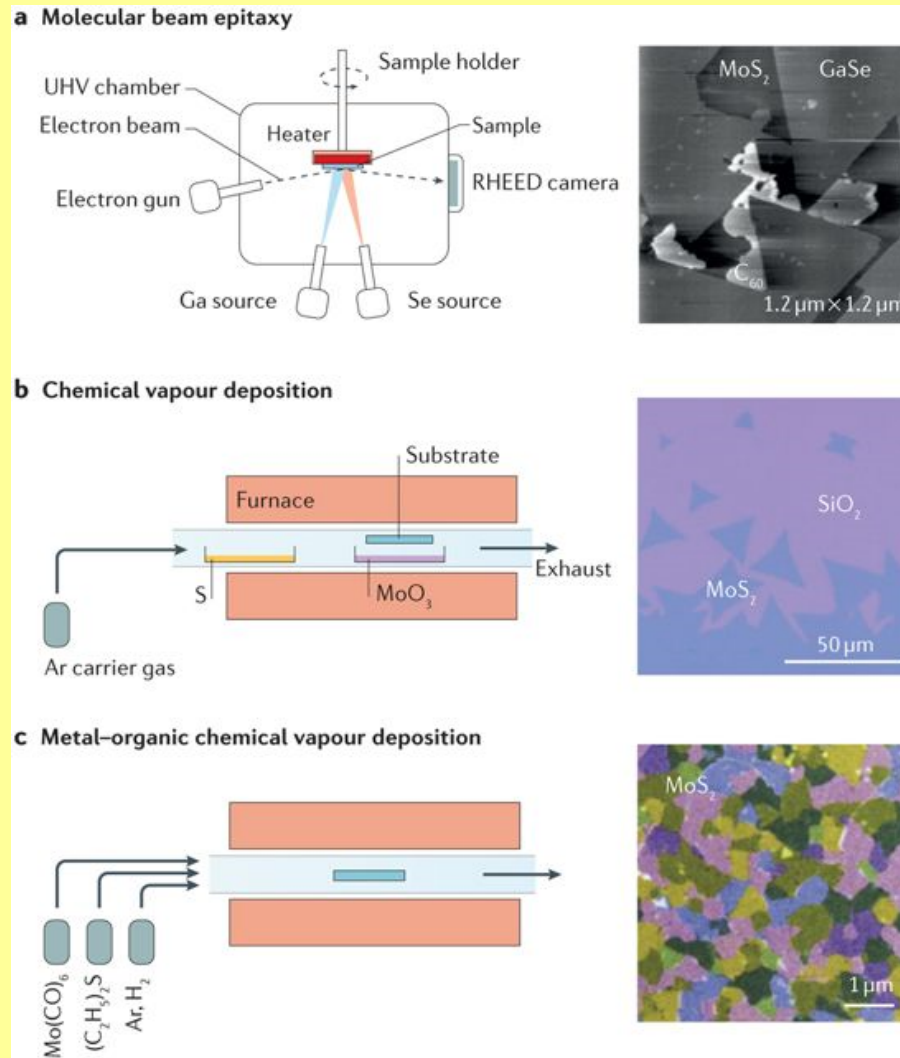
Fermi level

Valence band

photoluminescence



Molybdenum Disulfide (MoS₂)



Molybdenum Disulfide (MoS₂)

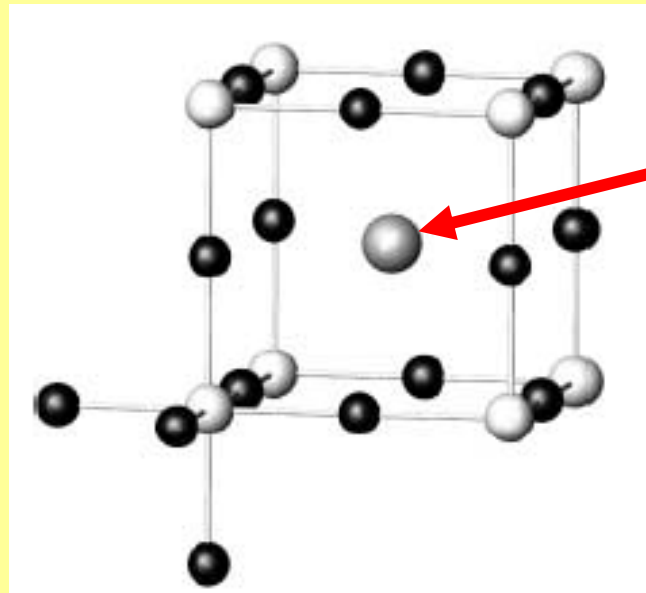
MoS₂ nanosheets - all sulfur atoms exposed on surfaces
S = a soft Lewis base - a high affinity for heavy metal ions
(e.g., Hg²⁺ and Ag⁺) = soft Lewis acids

MoS₂ nanosheets

- **high adsorption capacity - abundant sulfur adsorption sites**
- **fast kinetics - easy access to adsorption sites**

3D Intercalation Compounds

Cu_3N and Mn_3N crystallize in the (anti-) ReO_3 -type structure



the large cuboctahedral void in the structure can be filled

By Pd to yield (anti-) perovskite-type PdCu_3N

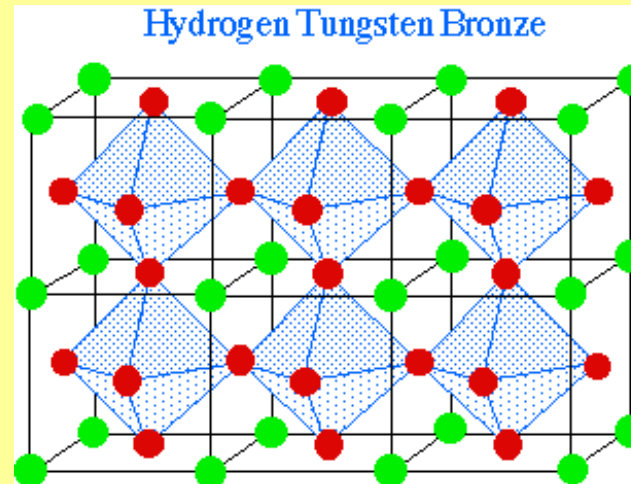
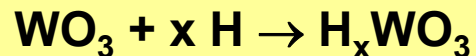
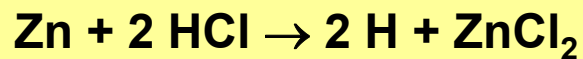
By $M = \text{Ga}, \text{Ag}, \text{Cu}$ leading to MMn_3N

3D Intercalation Compounds

Tungsten trioxide structure

= WO_6 octahedra joined at their corners

= the perovskite structure of CaTiO_3 with all the calcium sites vacant

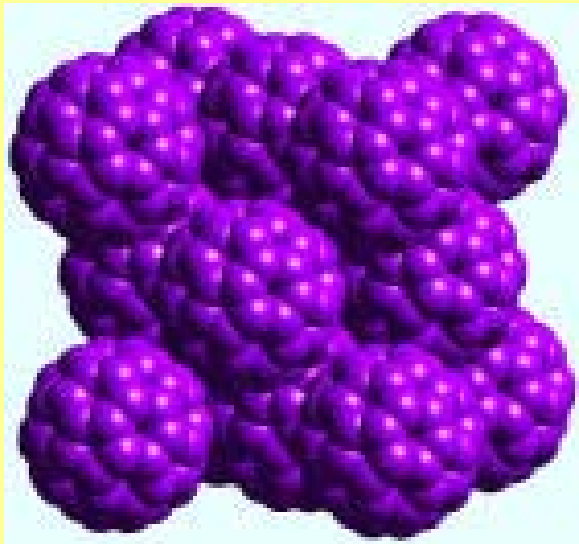
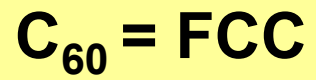


The color and conductivity changes are due to the intercalation of protons into the cavities in the WO_3 structure, and the donation of their electrons to the conduction band of the WO_3 matrix

The material behaves like a metal, with both its conductivity and color being derived from free electron behavior

The coloration reaction used in electrochromic displays for sun glasses, rear view mirrors in cars

0D Intercalation Compounds



Octahedral voids (N)
Tetrahedral voids (2N)

K

